NUCLEATION OF THE ISOTHERMAL MARTENSITIC TRANSFORMATION IN IRON-NICKEL-MANGANESE ALLOYS

by

SATYA RANJAN PATI

B.E. (Met.) University of Calcutta (1961)
S.M. Massachusetts Institute of Technology (1964)

Submitted in partial fulfillment of the requirements

for the degree of

DOCTOR OF SCIENCE

at the

Massachusetts Institute of Technology

1967

Signature of Author
Department of Metallurgy _____

Signature of Professor
in Charge of Research _____

Signature of Chairman of
Departmental Committee on
Graduate Students _____

ABSTRACT

NUCLEATION OF THE ISOTHERMAL MARTENSITIC TRANSFORMATION IN IRON-NICKEL-MANGANESE ALLOYS

by

SATYA RANJAN PATI

Submitted to the Department of Metallurgy on May 12, 1967 in partial fulfillment of the requirements for the degree of Doctor of Science.

By means of quantitative metallography and electrical resistance measurements, the incubation period (time to form a detectable amount of martensite) and the initial nucleation rate have been determined as a function of subzero reaction temperature and austenitic grain size in three iron-nickel-manganese alloys containing 23-25 percent nickel, 2-3 percent manganese and 0.02-0.04 percent carbon. The isothermal martensitic transformation in these alloys has been found to occur over a wide temperature range of at least -196° to -20°C, and the martensitic structure over the entire range is body-centered cubic. The incubation period and nucleation rate as a function of reaction temperature at various austenitic grain sizes show typical C-curve kinetics.

The true initial nucleation rate (not the apparent initial nucleation rate during the incubation period) is independent of grain size, and so the effect of grain size on the incubation period arises merely because of the size of the first-formed plates. Accordingly, it may be concluded that grain boundaries do not predominate as preferred nucleation sites for the martensitic transformation in the alloys studied.

Calculations of the relevant thermodynamic functions indicate that 1 atomic percent manganese is thermodynamically equivalent to 1.6 atomic percent nickel in the driving force for the martensitic transformation. However, alloys of equivalent thermodynamic driving force exhibit striking differences in kinetic behavior due to slight differences in their manganese and carbon contents, suggesting that these elements reduce the potency of the embryos.

The observed activation energies of the isothermal martensitic transformation are in very good agreement with the calculated activation energies based on a nucleation model. Moreover, in these alloys, the potency of the active embryos

remains almost constant during the course of the isothermal transformation, notwithstanding the progressive generation of new embryos due to autocatalytic factors.

The best fit between theory and experiment is obtained on the assumption that the number of pre-existing embryos in the parent austenite is 10^7 per cm^3. The probability of detecting such embryos by transmission electron microscopy is less than 1 in 10^5.

The increase in the rate of isothermal martensitic transformation as a function of time has been shown to be due to the formation of new plates by autocatalysis, while the subsequent retardation is attributable to the partitioning of the austenite by the martensitic plates. The model used provides quantitative agreement with the course of the isothermal transformation up to 12 percent martensite.

Thesis Supervisor: Morris Cohen
Ford Professor of Materials
Science and Engineering

TABLE OF CONTENTS

Chapter Number		Page Number
	Abstract	ii
	List of Figures	vii
	List of Tables	xi
	Acknowledgements	xii
1	Introduction	1
2	Literature Review	3
	2.1 Early Isothermal Studies and nucleation.. and Growth Description of the Martensitic Transformation	3
	2.2 Reaction Path Theory and Isothermal Transformation	5
	2.3 Classical Homogeneous Nucleation Theory and Isothermal Transformation	8
	2.4 Classical Heterogeneous Nucleation Theory	12
	2.5 Incubation Period in Isothermal Transformation	13
	2.5.1 Calculation of Nucleation Rate and Activation Energy of the Isothermal Martensitic Transformation	15
	2.6 Isothermal Formation of Martensite at Preferred Nucleation Sites Using Cataclysmic Model (Kaufman and Cohen's Treatment)	17
	2.7 Recent Studies of Isothermal Martensite	21
3	Plan and Outline of Work	23
4	Experimental Procedure and Development of Quantitative Metallographic Methods	26

Chapter Number		Page Number
	4.1 Specimen Preparation	26
	4.2 Resistance Measurements	31
	4.3 Specimen Examination	34
	4.3.1 Optical Microscopic Examination	34
	4.3.2 Transmission Electron Microscopic Examination	34
	4.4 Quantitative Metallography	36
	4.4.1 Grain Size Measurement	36
	4.4.2 Determination of Volume Fraction of Martensite and Number of Plates per Unit Area and per Unit Length.	36
	4.4.3 Measurement of Radius to Semi-thickness Ratio of Martensitic Plates	38
	4.5 Measurement of Nucleation Rate	43
5	C-Curve Kinetics of Isothermal Martensitic Transformation	53
	5.1 Results	53
	5.2 Discussion of Results	56
6	Effect of Grain Size on Incubation Period and Nucleation Rate	63
	6.1 Results	63
	6.1.1 Incubation Period versus Grain Size	64
	6.1.2 Nucleation Rate versus Grain Size	68
	6.2 Discussion of Results	72

Chapter Number		Page Number
7	Thermodynamic Calculations on Martensitic Transformations	86
	7.1 Introduction	86
	7.2 The Free-Energy Change and Kinetics of Nucleation	87
	7.3 Activation Energy	93
	7.4 The absence of Athermal Martensitic Transformation Below the Temperature Range of Isothermal Transformation	97
	7.5 Attempts at Direct Observation of Embryos	100
8	Progress of the Isothermal Martensitic Transformation	105
	8.1 The Nature of the Transformation Curve	105
	8.2 Calculation of Fraction Transformed as a Function of Time, Taking into Account Partitioning of Austenite and the Autocatalytic Effect	108
	8.3 Discussion of Calculated and Experimental. Curves	112
9	Conclusions	127
10	Suggestions for Further Work	130
11	Bibliography	131
	Appendices	135
	A. Compositional Variations in Specimens as a Function of Austenitizing Temperature	135
	B. Transmission Electron Microscopic Observations	137
	C. Calculation of Total Number of Embryos Including the Correction Due to Embryos Being Swept Up by the Martensitic Plates	139
	Biographical Note	141

LIST OF FIGURES

Figure Number		Page Number
1	24Ni3Mn Alloy, Having a Grain Size of 0.012 mm, Reacted at -115°C to 0.9 percent Martensite Showing a low $(\overline{r/c})$. Etched with 25 percent Sodium Bisulphite in Water. 500X.....	39
2	24Ni3Mn Alloy, Having a Grain Size of 0.025 mm, Reacted at -115°C to 0.9 percent Transformation. Etched with 25 percent Sodium Bisulphite in Water. 500X.....	39
3	24Ni3Mn Alloy, Having a Grain Size of 0.099 mm, Reacted at -115°C to 1 percent Transformation Showing High $(\overline{r/c})$. Etched with 25 percent Sodium Bisulphite in Water. 500X.....	40
4	Average Radius to Semithickness Ratio of Martensitic Plates as a Function of Grain Size in 23Ni3Mn, 24Ni3Mn, and 25Ni2Mn Alloys..	42
5	Mean Volume per Martensite Plate, Calculated from Equation (15) and (16) as a Function of Grain Size for 23Ni3Mn, 24Ni3Mn, and 25Ni2Mn Alloys.....	45
6	N_V for 0.2 percent Transformation for Martensitic Plates of Uniform Size as a Function of Austenitic Grain Size in 23Ni3Mn, 24Ni3Mn, and 25Ni2Mn Alloys.....	49
7	N_V for 0.2 percent Transformation Taking into Account Variation in Martensitic Plate Sizes as a Function of Austenitic Grain Size in 23Ni3Mn, 24Ni3Mn, and 25Ni2Mn Alloys.....	51
8	24Ni3Mn Alloy, Having a Grain Size of 0.025 mm, Reacted at -115°C to 1 percent Transformation Showing a Small Cluster. Etched with 25 percent Sodium Bisulphite in Water. 500X.....	52

Figure Number		Page Number
9	24Ni3Mn Alloy, Having a Grain Size of 0.025 mm, Reacted at -115°C to 1 percent Transformation Showing a Long Dense Cluster. Etched with 25 percent Sodium Bisulphite in Water. 200X.....	52
10	Incubation Period as a Function of Reaction Temperature for the 24Ni3Mn Alloy.....	54
11	Incubation Period as a Function of Reaction Temperature for the 25Ni2Mn Alloy.....	55
12	Nucleation Rate as a Function of Reaction Temperature for the Alloys of 24Ni3Mn and 25Ni2Mn.....	57
13	Grain Size as a Function of Austenitizing Temperature (1 hour) for 23Ni3Mn, 24Ni3Mn, and 25Ni2Mn Alloys.....	65
14	The Incubation Period as a Function of Grain Size for the 24Ni3Mn Alloy, Reacted at the Indicated Temperatures.....	66
15	Incubation Period as a Function of Grain Size for the 23Ni3Mn and 25Ni2Mn Alloys Reacted at the Indicated Temperatures.....	67
16	The Initial Nucleation Rate as a Function of Grain Size for the 24Ni3Mn Alloy Reacted at the Indicated Temperatures.....	70
17	The Initial Nucleation Rate as a Function of Grain Size for 23Ni3Mn and 25Ni2Mn Alloys Reacted at the Indicated Temperatures.....	71
18	Incubation Period as a Function of $\bar{d}^{-3}$ for the 24Ni3Mn Alloy Reacted at the Indicated Temperatures.....	74
19	Incubation Period as a Function of $\bar{v}^{-1}$ for the 24Ni3Mn Alloy Reacted at the Indicated Temperatures.....	76
20	Incubation Period as a Function of $\bar{d}^{-3}$ for the 25Ni2MnA Alloy Reacted at -20°C.....	83

Figure Number		Page Number
21	The Change in Free Energy Accompanying Martensitic Transformation in Iron-Nickel-Manganese Alloys as a Function of Temperature From Equation (31).....	88
22	The Free Energy Change Accompanying the Martensitic Transformation in Iron-Nickel-Manganese and Iron-Nickel Alloys as a Function of Temperature from Equation (31)...	91
23	Calculated and Measured Values of Activation Energy as a Function of Temperature for Isothermal Nucleation of Martensite in 24Ni3Mn Alloy.....	94
24	Calculated and Measured Values of Activation Energy as a Function of Temperature for Isothermal Nucleation of Martensite in 23.2%Ni - 3.62%Mn Alloy of Shih et al.[16] ...	96
25	Measured Activation Energy for the Isothermal Martensitic Transformation in Iron-Nickel-Manganese Alloys as a Function of the Free Energy Change Accompanying the Transformation.	98
26	Calculated Time for 0.2 percent Transformation as a Function of Reaction Temperature for Indicated Embryo Radii in 24Ni3Mn Alloy.....	101
27	Comparison of Experimental and Calculated Transformation Curve for the 24Ni3Mn Alloy Reacted at the Indicated Temperatures. The Values of P used in the Calculations are Indicated for Each Curve.....	113
28	Comparison of Experimental and Calculated Transformation Curve for the 24Ni3Mn Alloy Reacted at the Indicated Temperatures. The Values of P used in the Calculations are Indicated for Each Curve.....	114
29	Number of Plates Formed per cm^3 of the 24Ni3Mn Alloy, as a Function of Time of Transformation at -115°C.	120

Figure Number		Page Number
30	Total Number of Embryos as a Function of Fraction of Transformation, Considering Autocatalysis and Partitioning. Correction Due to Embryos Being Swept up by the Formation of Martensitic Plates is also Included.....	125
31	Fine Structure of Isothermally Formed Martensite in the 24Ni3Mn Alloy, Reacted at -105°C. 31,000X.....	138
32	Fine Structure of Isothermal Martensite in the 24Ni3Mn Alloy, Reacted at -105°C. 95,000X.....	138

LIST OF TABLES

Table Number		Page Number
I	Composition of Alloys in Weight Percentages.....	28
II	Activation Energies for Isothermal Martensitic Transformations in 24Ni3Mn and 25Ni2Mn Alloys....	61
III	Grain Size Effect in 25Ni2MnA Alloy.....	69
IV	Calculation of Nucleation Rate as a Function of Number of Plates Formed in 24Ni3Mn Alloy for a Reaction Temperature of -115°C, Taking into Account Autocatalysis.....	80
V	Calculation of Activation Energy for the 24Ni3Mn Alloy from the Progress of Transformation and from the Initial Nucleation Rate at 0.2 percent Transformation Taking Autocatalysis into Account within 0.2 percent Transformation.....	116
VI	Calculation of Nucleation Rate as a Function of Number of Plates Formed from (1) the Measured Number of Plates as a Function of Time and (2) Equation (27), for the 24Ni3Mn Alloy Reacted at -115°C.....	121
VII	Number of Martensitic Plates per Unit Volume, N_V, Required to Give Different Amounts of Transformation for A Grain Size of 0.025 mm ($q=9.28 \times 10^{-9}$ cm^3) and for Constant and Varying m, Calculated from Equation (36).....	123

ACKNOWLEDGEMENTS

The author expresses his sincere appreciation to the following people for thieir assistance in conducting the work reported in this thesis:

Professor Morris Cohen for suggesting this investigation and for his continued help and guidance throughout the course of this investigation and for his assistance in writing the manuscript.

Professor John F. Breedis for his invaluable help in carrying out the electron microscopic investigation and frequent valuable suggestions.

Professor J.W. Cahn for helpful discussions; Miss M. Yoffa for her able technical assistance and help in preparation of the manuscript; Mrs. J. Operacz for her help in experimental work.

Office of Naval Research, for providing the financial support under contract number Nonr-1841(35),NR 031-142. The work was performed in part at the MIT Computation Center.

The author is especially indebted to Miss Marguerite Meyer to whom he has repeatedly turned for general counsel, special favours, and for help in preparing the manuscript.

Finally, the author wishes to thank his wife, Hiru, for her invaluable assistance in computations and preparation of the manuscript.

1. INTRODUCTION

Studies of the isothermal mode of the martensitic transformation can make an important contribution to the understanding of the martensitic transformation kinetics. The slow initial rate of transformation during the incubation period, which is the time taken to form a detectable amount of martensite before any pronounced acceleration of the rate occurs due to autocatalytic effects, can be taken as a measure of the initial nucleation rate. In fact, the initial nucleation rate and activation energy for martensitic reaction can be derived in this way. In the present investigation, these quantities are measured for a series of iron-nickel-manganese alloys which happen to undergo isothermal transformation to martensite without the presence of prior athermal martensite.

The effect of grain size on the nucleation kinetics and the autocatalytic nature of the martensitic transformation can also be uniquely examined in the isothermal mode of transformation. Most of the previous studies on the effect of grain size have dealt with the raising of M_s with increasing grain size. However, this approach complicates any quantitative understanding of the basic effect of grain size, since a change in M_s is accompanied by a change in the driving force for the reaction. A change in the magnitude of the autocatalytic

factor in the transformation might also be associated with a change in M_s. Another complication arises, especially when M_s is close to room temperature, due to the possible entree of the stabilization phenomenon. On the other hand, by utilizing the isothermal martensitic transformation at subzero reaction temperatures, the effect of the grain size may be studied more quantitatively by eliminating the effect of temperature differences on the above-mentioned factors. By the same token, it becomes possible to deduce the nature and magnitude of the autocatalytic effects through an analysis of the course of the isothermal transformation.

In the present investigation, an attempt has been made to carry out direct measurements of the nucleation rate of the isothermal martensitic transformation, from which the activation energy for the nucleation of martensitic transformation has been obtained. The measured activation energies have been interpreted in terms of a nucleation model of the martensitic transformation. The effect of grain size and the autocatalytic nature of the transformation on the nucleation rate have also been studied. Finally, the isothermal transformation curve has been derived quantitatively, considering the autocatalytic nature of the nucleation process and the partitioning of the austenite by the martensitic plates.

2. LITERATURE REVIEW

In this section only a brief discussion is presented on various theories of isothermal martensitic transformation; the emphasis is centered on the work which is pertinent to the present investigation. For a more detailed description of the theories and experimental results, the reader is referred to the reviews of Kaufman and Cohen[1], and Reed and Breedis[2].

2.1 Early Isothermal Studies and Nucleation and Growth Descriptions of the Martensitic Transformation

Kurdjumov and Maksimova[3] first reported the existence of isothermal martensitic transformation in a number of steels and iron-base alloys. They found that in a 1.6 percent carbon steel, isothermal transformation first started around -100°C; and at temperatures above -100°C, the transformation ceased after only a small fraction of martensite being formed. At temperatures below -100°C, the rate of transformation was slower, the lower the temperature.

In a 0.60 percent carbon - 6 percent manganese - 2 percent copper steel[3], and in an iron - 23 percent nickel - 3.4 percent manganese alloy[4], the isothermal transformation exhibited a C-curve behavior with the nose occurring at -133°C and -47°C respectively.

In order to explain the C-curve behavior of the isothermal kinetics, the above authors assumed that isothermal nucleation is controlled by the activation energy of nucleation, W, and activation energy of growth, Q. Thus, the nucleation rate $\dot{N}$ is:

$$\dot{N} = K \exp(-Q/RT) \exp(-W/RT) \qquad (1)$$

where K is a temperature-independent constant, R is the gas constant, and T is the temperature in °K.

At temperatures above the nose of the C-curve, the nucleation step is considered to be the rate-controlling process, while at temperatures below the nose the growth of the plate is supposed to control the rate of transformation. The main difficulty with this treatment lies in its high temperature dependence of the growth rate of the martensitic plate. The value of Q derived by the authors predicts a ten-fold increase in the rate of martensite propagation at -20°C over that at -196°C. However, Bunshah and Mehl[5] found that the rate of propagation of martensite is essentially independent of temperature over this range, implying that Q is about zero. Also, the nucleation rate derived from the initial transformation rate by Kurdjumov and Maksimova does not represent the initial nucleation rate since the alloys contained different amounts of athermal martensite at different temperatures of isothermal runs; thus, no incubation period was observed in

these instances. Furthermore, the nucleation rate was considered to remain constant up to 50 percent transformation, and this is also in contradiction to the presently established view that after the initial slow rate of nucleation the rate increases appreciably due to autocatalysis.

The existence of isothermal martensite was soon confirmed by Das Gupta and Lement[6] in a 0.7 percent carbon - 15 percent chromium steel and by Kulin and Speich[7] in an iron - 14 percent chromium - 9 percent nickel alloy. Subsequently, authors found that the plot of logarithm of the initial nucleation rate (for temperatures below the nose of the C-curve) against the reciprocal of temperature showed a marked deviation from linearity, thus contradicting the findings of Kurdjumov and Maksimova[3].

However, in these cases as well, the true nature of the initial isothermal transformation was overshadowed by complications arising from different amounts of athermal martensite being present at the start of isothermal transformation at various temperatures.

2.2 Reaction Path Theory and Isothermal Transformation

Cohen et al.[8] originally proposed the reaction path theory to describe the athermal martensitic transformation. Subsequently, Machlin and Cohen[9] presented the reaction

path description of the isothermal mode of martensitic transformation. In classical nucleation, an embryo is assumed to reach the status of a nucleus when it achieves the critical size at any given temperature, whereas in the reaction path description, it is assumed that within the tiny volume where the nucleus forms, the lattice passes through a succession of states as the atoms go through their primitive motion to convert the austenite into martensite. The succession of states is regarded as a reaction path which contains a free energy barrier between the initial and final states. Thus, in the reaction path theory the activation is achieved by fluctuations in the structural configuration of embryos, rather than in their size.

Cohen et al.[8] suggested that embryos for this process are strain centers comprising non-equilibrium lattice defects. These strain embryos are thought to be sheared partway along the reaction path, constituting local regions of high free energy. Hence, the required free energy of activation is reduced by the amount of free energy associated with the most potent embryos, i.e., the barrier for these high-energy sites is lower than that which would be faced by an embryo originating in a perfect lattice.

A distribution of embryos of different energies is assumed. When the temperature drops and the energy associated

with the most potent embryos exceeds the activation energy barrier for the corresponding temperature, then they spontaneously move the rest of the way to become martensite. The athermal nature of the transformation is accounted for by embryos of decreasing potency becoming operative as the nucleation barrier diminishes with lowering of temperature. For isothermal nucleation above M_s, the energy barrier at the temperature concerned is overcome by the superimposition of thermal fluctuations on the most potent embryos.

Machlin and Cohen[9] studied the isothermal martensitic transformation in an iron - 30 percent nickel alloy at a series of reaction temperatures. The amount of athermal martensite present at the beginning of the isothermal run was kept constant by prequenching the specimens in liquid nitrogen. This converted all embryos with free energies above the activation energy corresponding to 77°K, $\{W_a(77°K)\}$, to athermal martensite, and then the specimens were upquenched to predetermined temperatures for isothermal transformation. It was shown by the authors that the relative activation free energy of nucleation can be calculated from the measurements of initial transformation rates by using the expression:

$$\ln \left[\frac{\text{Initial transformation rate at T°K}}{\text{Initial transformation rate at 77°K}}\right]\frac{77}{T} = \frac{[W_a(T)-W_a(77°K)]}{RT} \qquad (2)$$

where the free energy difference $[W_a(T) - W_a(77°K)]$ is referred to here as the relative activation free energy of nucleation. In the reaction path terminology, $[W_a(T) - W_a(77°K)]$ is the increment of free energy that must arise from thermal fluctuations at T in order to activate embryos of free energy $W_a(77°K)$, which are the most potent ones remaining after the prequench into liquid nitrogen. The isothermal transformation of an iron - 30 percent nickel alloy showed a C-curve behavior with the maximum rate occurring between 77°K and 203°K. From a plot of $[W_a(T) - W_a(77°K)]$ against temperature, the temperature for maximum initial rate was determined as 150°K. Thus, the reaction path treatment could explain the C-curve kinetics of isothermal transformation.

Though this theory has been useful for calculating the relative activation free energy of nucleation, and its temperature dependence has been found to agree with the generally accepted form, this approach provides no way of calculating the true activation energy barrier for the reaction path, since it would then be necessary to know the free energies of all the intermediate states, and this complex information is unobtainable.

2.3 Classical Homogeneous Nucleation Theory and Isothermal Transformation

Cech and Hollomon[10] studied the isothermal martensitic

transformation in an iron - 23 percent nickel -3.7 percent manganese alloy between -79°C and -196°C. This also showed a C-curve behavior with the nose around -130°C. These investigators failed to obtain any incubation period since up to 3 percent athermal martensite (depending on temperature) was present in their specimens at the beginning of isothermal runs. The specimens also contained a surface layer of higher martensite content due to depletion of manganese content at the surface.

Fisher[11] has quantitatively treated the isothermal data of Cech and Hollomon, on the basis of classical homogeneous nucleation theory. The total energy change accompanying the formation of a lenticular nucleus of radius r and semi-thickness c is given by:

$$\Delta W = \pi r^2 c \Delta f + 2\pi r^2 \sigma + 4\pi\theta r c^2 \qquad (3)$$

where Δf is the chemical free energy change accompanying the formation of unit volume of martensite, σ is the interfacial energy per unit area, and $4\theta(\frac{c}{r})$ is the strain energy per unit volume.

The critical energy of activation, ΔW^*, is obtained by differentiating equation (3) with respect to r and c and

equating to zero. Finally, one obtains

$$\Delta W^* = 8192\pi\theta^2\sigma^3/27\Delta f^4 \tag{4}$$

The homogeneous nucleation rate $\dot{N}$ is given then by:

$$\dot{N} = \left(\frac{N}{V}\right) \nu \exp\left(-\Delta W^*/RT\right) \tag{5}$$

Where N is the Avogadro's number, V is the molar volume, and ν is the lattice vibration frequency.

The temperature for the maximum nucleation rate is then derived by setting $\frac{d\dot{N}}{dT} = 0$, whence

$$(4T/\Delta f)\ \frac{d\Delta f}{dT} + 1 = 0 \tag{6}$$

Using Jones and Pumphrey's[12] data on iron-nickel alloys, Fisher[11] found good agreement with the experimental results.

Fisher derived a relation between the fraction of martensite formed f and time t assuming a constant rate of nucleation $\dot{N}$, and the partitioning of austenite into smaller and smaller pockets as the transformation progresses. The nth plate to form is assumed to transform a constant fraction m, of $\left(\frac{1}{n}\right)^{th}$ of the remaining untransformed volume. Finally, the fraction transformed as a function of time is given by:

$$f = 1 - \left[1+(1+m)\dot{N}t/n_o\right]^{-m/1+m} \tag{7}$$

where n_o is the number of grains per unit volume. By fitting this equation to the experimental curves of Cech and Hollomon,[10] values of m and $\dot{N}/n_o$ was obtained. Unfortunately, m had to be varied by a factor of 5 to account for the various transformation curves. Also, when $\theta^2\sigma^3$ obtained from the $\dot{N}$ values derived from the best fit was used to compute the nucleation rates as a function of temperature, using equations (4) and (5), the agreement was not satisfactory.

There are a few other severe objections to the homogeneous nucleation theory. First, Fisher[13] tried to explain athermal transformation characteristics in iron-nickel alloys by this approach, but the $\theta^2\sigma^3$ value had to be reduced to $\frac{1}{6}$th of that used for iron-nickel-manganese alloys. For the athermal transformation in 3 percent chromium steels[14], $\theta^2\sigma^3$ comes out to be 5 times larger than that of the iron-nickel manganese alloys. Second, according to this treatment, no transformation to martensite should occur in alloys with more than 30.1 atomic percent nickel, whereas Kaufman and Cohen[15] have found the M_s to extend down to 50°K for an alloy of iron - 33 atomic percent nickel. Third, from the $\theta^2\sigma^3$ values derived for the iron-nickel alloys[13], a very low value for interfacial energy (σ = 4.6 ergs/cm^2) is obtained which is not consistent with the crystallographic description of the austenite-martensite interface.

2.4 Classical Heterogeneous Nucleation Theory

There is abundant evidence in the literature to indicate that the martensitic reaction is heterogeneous in character. Failure of the homogeneous nucleation theory to account for the M_s approaching absolute 0°K led to the development of this heterogeneous theory. In a purely formal way, localized variations in free energy are considered to be frozen in during the cooling of the parent phase. These embryos may become critical in size without requiring thermal fluctuations when a suitably low temperature is reached, thus accounting for the athermal nature of transformation. However, if the energy associated with these regions is not high enough, thermal fluctuations may help them to overcome the nucleation barrier and thereby account for the isothermal transformation.

Fisher et al.[14] suggested that in dilute iron-base solid solutions compositional fluctuations in the matrix might provide the preferential sites for nucleation. However, there are two limitations in regarding compositional fluctuations as the basis for martensitic nucleation. First, martensitic transformations occur in many substitutional solid solution systems where the compositional fluctuations of the type considered are hard to visualize. Second, since these fluctuations are regarded as statistical distributions of compositional variations, the nucleation should be random; on the

contrary, the nucleation is definitely heterogeneous.

Cohen et al.[15] tried to overcome the latter difficulty by postulating the existence of structural heterogeneities, consisting of non-equilibrium structural imperfections. The parent phase is presumed to contain a spectrum of these high free energy sites which in turn become active nuclei without thermal fluctuations when the temperature is lowered sufficiently. The M_s is thus determined by the local free energy of the most potent embryos. Thermal fluctuations may also help the embryos of less than critical energy of activation to overcome the activation barrier.

Classical nucleation can be included in the heterogeneous concept[1] to calculate the activation energy. The activation energy so calculated is found to be too strongly dependent on temperature, and this treatment fails to explain the isothermal kinetics when put to a quantitative test.

2.5 Incubation Period in Isothermal Transformation

Ground work was first laid for the quantitative treatment of the isothermal martensitic transformation when Shih, Averbach and Cohen[16] reported for the first time the existence of an incubation period in isothermal transformation. The incubation period was defined as the time required to form a detectable amount of martensite which was 0.2 percent in this case.

They studied the isothermal formation of martensite in an iron - 23.2 percent nickel - 3.62 percent manganese alloy, and in an iron - 5.24 percent manganese - 1.10 percent carbon alloy at a series of reaction temperatures in the range of -196°C to -90°C. In both cases athermal martensite was completely avoided. Their results showed that the reaction rate at the beginning of the strictly isothermal reaction was very slow, but as soon as some detectable amount of martensite was produced the transformation rate increased rapidly. Eventually, the transformation rate died away. They also demonstrated that the incubation period and the slow initial rate of transformation are lost when 1 - 2 percent athermal martensite is present at the beginning. In the latter case, the transformation rate was at a maximum at the beginning and gradually decreased with time.

This explained why the previous investigators[3,4,10] reported a maximum at the beginning, since their specimens had some athermal martensite present prior to the isothermal run. It also became clear that the true characteristics of the isothermal transformation are best studied in the absence of any prior-formed martensite, and that only the initial rates are relevant to the nucleation theories. The complete course of the isothermal curve also indicated that autocatalysis was responsible for increasing the rate of transformation after

formation of some martensite and that the transformation rate, finally decreased due to partitioning of austenite into smaller and smaller pockets.

2.5.1 Calculation of Nucleation Rate and Activation Energy of the Isothermal Martensitic Transformation

Since the martensitic transformation is nucleation-controlled, Shih et al.[16] calculated the initial nucleation rate for the isothermal martensitic transformation using the expression:

$$0.002 = \dot{N}\bar{v}\tau_i \qquad (8)$$

where τ_i is the incubation period, defined as the time for the formation of the first 0.2 percent of martensite, $\bar{v}$ is the average volume of the initially-formed martensitic plates, and $\dot{N}$ is the nucleation rate defined as the number of plates formed per second per cm^3 of the parent phase. The volume was calculated from the measurements of radii and thicknesses of initially formed martensitic plate, and finally the nucleation rate was obtained assuming it was constant during the incubation period. In order to obtain the activation energy, these investigators used the strain embryo concept, wherein the nucleation is regarded as occurring only at preferred sites

but still is under the impetus of thermal fluctuations. The preferred sites are considered as regions of local strain or imperfections in the lattice, having a distribution of free energies above that of the unstrained matrix. If W_a is the free energy of nucleation required to form a nucleus from the perfect lattice, then a strain embryo of free energy W could be activated by the increment of free energy $\Delta W_a = W_a - W$.

In the isothermal transformation, the most potent embryos nucleate in the early stages of the transformation. According to Shih et al., the activation energy is given by:

$$\dot{N} = n_i \nu \exp(-\Delta W_a / RT) \qquad (9)$$

where n_i is the number of most potent embryos per cm^3 of the alloy, ν is the lattice vibration frequency, taken as 10^{13} sec^{-1}, ΔW_a is the increment of free energy required to activate the most potent embryos. To estimate a value of n_i, Shih et al. arbitrarily assumed that only one most potent embryo was present per grain of austenite, so that n_i could be calculated from grain size. The resulting activation energies varied from 13,900 calories/mole at -90°C to 6,150 cal./mole at -196°C. Further discussion of these activation energies is reserved for later Sections (5.2 and 7.3).

2.6 Isothermal Formation of Martensite at Preferred Nucleation Sites Using Cataclysmic Model (Kaufman and Cohen's Treatment)

Knapp and Dehlinger[17] have treated the athermal martensitic transformation in steel by adopting Frank's[18] model of the austenite-martensite interface. In this treatment the embryo is considered as a thin oblate spheroid surrounded by loops of dislocations lying in the interface. Knapp and Dehlinger assume that an embryo will trigger spontaneously into full size plate on cooling as soon as the chemical driving force exceeds the required interfacial and strain energies. In other words, initiation of the athermal transformation is determined by a free energy balance, rather than by the maximum or saddle point in the free energy. For a given pre-existing embryo size, one visualizes that the driving force increases as the temperature drops; then the chemical force overbalances the non-chemical restraining force and a net driving force arises. This can be likened to a mechanical stress on the dislocation interface, which is thereby moved outward to generate martensite from the existing embryo. At a temperature where this event takes place, the propogation can be quite rapid because, not only is the interface mobile, but the net force on it increases as the particle expands. This leads to cataclysmic growth because, the chemical driving force remains constant at a given

temperature, while the non-chemical restraining force decreases with an increase in particle size[1].

According to the above hypothesis for the athermal transformation, no thermal fluctuations are necessary. Later, Kaufman and Cohen[1] extended this treatment to account for the isothermal mode of transformation. Their theory is outlined below in some detail, since this model has been found to explain the isothermal kinetic data of the present investigation.

To facilitate the calculation of the net stress on the dislocation loops of the embryo, Kaufman and Cohen[1] considered the embryo as a thin ellipsoid, and replaced the array of interface dislocation loops by a single giant loop at the periphery of the embryo, which was geometrically equivalent to the array. The radius of this circumferential loop is r, and its Burger's vector λ turns out to be cb/d where b is the Burger's vector of a single interface dislocation loop, c is the semi-thickness of the embryo, and d is the mean distance between the individual dislocation loops.

The energy of the giant loop, W^{ℓ} is then calculated and is found to go through a maximum as a function of r. This occurs when $r = r_c = \frac{9}{4} r^*$, where r^* is the radius of the embryo corresponding to the maximum in overall free-energy barrier. The embryo with radius r_c grows cataclysmically since

the overall free energy (ΔW) decreases with growth of all embryos larger than r*.

For sizes in the range of $r^* \leq r \leq r_c$ the embryo can expand spontaneously and lower its total free energy if thermal fluctuations provide sufficient energy to make each unit step between r and r_c. Considering the activation energy per unit step during the isothermal growth from r to r_c, and taking the unit growth step $\Delta r = \lambda$; the activation energy is found as:

$$\Delta W^{\ell} = \frac{2.5\pi b^2}{d^2}(\sigma/A)^{1/2}\{3\sigma r^{3/2} + \Delta f(\frac{\sigma}{A})^{1/2} r^2\} \text{ergs/unit growth of loop} \quad (10)$$

The activation energy per unit step (ΔW^{ℓ}) has a maximum value, (ΔW^{ℓ}_{+}) at $r = r_{+}$. Thus, for embryos with $r^* \leq r \leq r_{+}$ the activation energy will be equal to ΔW^{ℓ}_{+}. For an embryo radius above r_{+}, the activation energy per unit growth step decreases as a function of increasing r and becomes zero at r_c.

Therefore, in those cases where $r_{+} \leq r \leq r_c$, the activation energy is obtained by direct substitution into equation (10).

Thus, the activation energy for the isothermal martensitic transformation is given by equation (10). This presupposes that autocatalytic effects are absent, i.e., subcritical embryos are not activated. Hence, the equation is applicable to the initial nucleation process during the incubation period.

If ΔW_a is the observed activation energy for the initial rate of isothermal formation, then ΔW_a must reflect the spontaneous thermal growth of the most potent or largest embryos present, having a radius r_e, where $r_* \leq r_e \leq r_c$. Inserting some of the numerical constants in equation (10), the activation energy for embryos of size r_e is expressed as:

$$\Delta W_e^{\ell} = 4 \times 10^{-2} (\sigma/A)^{1/2} \{3\sigma (r_e)^{3/2} + \Delta f (\sigma/A)^{1/2} r_e^{\,2}\} \text{ ergs/unit growth of loop} \qquad (11)$$

Kaufman and Cohen[1] compared the calculated values of ΔW_e^{ℓ} with the experimentally-observed activation energy values ΔW_a of Shih et al.[16], by assuming different values of r_e and using computed values of σ[17] and A[15,17]. The iron - 23.2 percent nickel - 3.62 percent manganese alloy of Shih et al. was assumed thermodynamically equivalent to an iron - 25 atomic percent nickel alloy in order to obtain Δf. Good agreement was obtained between the calculated and experimental values of activation energy, assuming an embryo radius of 180A°. Some aspects of the application of this theory to experimental results will be discussed in Section 7.3.

However, it should be mentioned that this is the only theory to date which has been able to interpret quantitatively the isothermal transformation kinetics, and hence, has been used in this investigation.

2.7 Recent Studies of Isothermal Martensite

After the work of Shih et al.[16], Philibert and Crussard[19] also observed the presence of an incubation period in the isothermal transformation. Later, Entwisle[20] extended the isothermal studies in three iron-nickel-manganese alloys mainly in an effort to check the findings of Shih et al.[16]

Assuming that the first-formed martensitic plates are limited by grain or twin boundaries, Entwisle derived an expression for the mean volume $\bar{v}$ of initially-formed martensitic plates, and showed it to be proportional to the cube power of the austenitic grain diameter $\bar{d}$. Combining equations (8) and (9),

$$0.002 = n_i \bar{v} \tau_i \nu \exp(-\Delta W_a/RT) \tag{12}$$

Then for a particular alloy and at a particular reaction temperature,

$$\tau_i \propto \frac{\bar{d}^{-3}}{n_i} \tag{13}$$

Thus, Entwisle suggested that a study of the incubation period versus grain size would indicate whether n_i is independent of grain size or not.

The most recent comprehensive work on the isothermal martensitic transformation is of Raghavan and Entwisle[21] and of Raghavan[22]. These authors have shown that the incubation period is dependent on austenitic grain size according to equation (18), so that n_i essentially remains constant for different grain sizes. They have also devised a method of calculating the fraction of martensite formed isothermally as a function of time by taking into account the autocatalytic effects and partitioning of the austenite. By assuming a single average potency for the embryos (both initial and autocatalytic) and an autocatalytic parameter which is proportional to the amount of martensite formed, and using the partitioning model of Fisher[11], they have been able to match the calculated curve of fraction transformed versus time with the experimental transformation curve in the early stages of the transformation.

Some other aspects of the work of these authors will be discussed in conjunction with the results of the present investigation.

3. PLAN AND OUTLINE OF WORK

The main objective of the present investigation is to measure the nucleation rate of the isothermal martensitic transformation. It is evident from the literature survey that no direct measurement of nucleation rate has been made up to the present time. The isothermal nucleation rate can be obtained only when the athermal martensitic transformation is avoided before the isothermal reaction, so that an incubation period can be detected. In order to meet this criterion, three alloys were chosen which would undergo substantial isothermal transformation to martensite over a wide range of temperatures. Their nominal compositions were in the vicinity of 23-25 percent nickel, 2-3 percent manganese, 0.02-0.04 percent carbon, and balance iron.

The temperature of isothermal transformation was investigated in considerable detail; the effect of grain size on the incubation period and nucleation rate was also carefully studied. A range of grain sizes was obtained by two different methods: (1) by varying the austenitizing temperatures of specimens having a constant amount of cold work, and (2) by varying the previous thermal and mechanical history of specimens, but keeping the final austenitizing temperature constant.

The following experimental steps were adopted:

Resistance measurements were carried out at the temperature of isothermal transformation to ascertain the initiation as well as the progress of the martensitic reaction. These resistance changes were related to the extent of transformation by quantitative metallography.

Quantitative metallographic techniques were used extensively to determine (1) the number of martensitic plates per unit volume for deriving the nucleation rates, (2) the length-to-thickness ratio and volume of martensitic plates, and (3) the grain size.

Transmission electron microscopy was carried out to study the morphology of the isothermally-formed martensite and to discover if embryos could be observed in the thin foils.

Since information is now available in the literature for calculations of different thermodynamic functions related to the martensitic transformations in ternary alloys of iron-nickel-manganese, computer calculations were undertaken for the chemical free-energy change and activation energy of the martensitic transformation in the alloys under study. The purpose was to compare more realistically the theoretically calculated quantities with the experimental values, because in the previous work along these lines[1] it had to be assumed

that iron-nickel-manganese alloys were thermodynamically equivalent to iron-nickel alloys due to lack of information concerning the iron-manganese system. It has been shown in this thesis that the above assumption is not true.

The volume fraction of martensite has also been calculated as a function of time in the isothermal transformation by taking into account the autocatalytic nature of the reaction and the partitioning of austenite. The limitations of the models adopted are revealed through comparisons between the calculated and experimental curves.

4. EXPERIMENTAL PROCEDURE AND DEVELOPMENT OF QUANTITATIVE METALLOGRAPHIC METHODS

4.1 Specimen Preparation

The alloys used in this investigation were received in the form of 0.500 inches diameter forged rods, five feet long. They were supplied by the Ford Scientific Laboratory of Dearborn, Michigan. The ends of the rods were discarded to remove pipes and cracks existing therein. The remainder of each rod was then cut up into six-inch lengths for swaging into test specimens, taking one-half inch specimens inbetween for macroscopic examination. The latter specimens were polished mechanically and then immersed in an acid solution of 50 cc hydrochloric acid, 7 cc sulphuric acid and 18 cc of water for at least 12 hours. Flaws on the surface became obvious after this treatment. Such flaws, as well as the inhomogeneous surface layer on the rods, were removed by machining down to 0.480 inches in diameter.

For preparing the specimens in which the grain size was altered by varying the austenitizing temperature, the rods were sealed in evacuated quartz tubes and homogenized at 1250°C for 10 days. The quartz tubing collapsed during this long anneal, but the vacuum remained intact. Upon air cooling to room temperature, the surface layer had become somewhat depleted of carbon and manganese,and this was removed by machining

from 0.48 to 0.41 inches in diameter. Chips were then taken from the ends of the homogenized rods for chemical analysis. The compositions of the alloys are listed in Table I. Throughout the text the alloys are referred to by their nominal nickel and manganese contents in weight percent.

The homogenized rods were then cold swaged to 0.090 inches in diameter with intermediate anneals at 800°C for 30 minutes after each 70 percent reduction in area. The rods were sealed in evacuated vycor tubes prior to the softening anneals. The vycor tubes containing the specimens were air cooled after each anneal. After the final anneal, an additional 51 percent cold reduction in area was given to the specimens, which was sufficient to recrystallize the material during the subsequent austenitizing treatment of 1 hour, even at the lowest austenitizing temperature used in this investigation. The rods were then centerless ground to a diameter of 0.060 inches.

For preparation of the specimens whose grain size had to be altered without varying the final austenitizing treatment, the as-received rods (with surface defects removed) were swaged directly to 0.225 inches in diameter before the homogenization treatment. The swaged rods were then sealed in evacuated vycor tubes and homogenized at 1200°C for 3 days. The vycor tubes containing the rods were air cooled to room

TABLE I

Composition of Alloys in Weight Percentages

Referred in the Text as	Manufacturer's Designation	Nickel	Manganese	Carbon	Nitrogen	Iron
23Ni3Mn	2550	23.45	2.88	0.043	0.01	Balance
24Ni3Mn	2551	24.2	2.98	0.017	0.001	Balance
25Ni2Mn	2552	25.15	1.96	0.024	0.001	Balance
25Ni2MnA	2552A*	25.14	1.91	0.015	0.001	Balance

Impurities	Weight Percentages
Phosphorus	<0.001
Sulphur	0.003
Silicon	<0.002

* Used only for varying the grain size of the specimens without altering the final austenitizing treatment.

temperature after the anneal. The surface layer of the rods was removed by machining from 0.225 inches to 0.190 inches in diameter, and then the rods were swaged to 0.125 inches in diameter. From this stage, different rods were given different thermal and mechanical treatments (as reported in the results) so as to obtain various grain sizes without altering the final austenitizing treatment. During this process of adjusting the prior thermal and mechanical histories of the specimen, the anneals were followed by electropolishing to remove about 0.004 inches of the specimen diameter. The electropolishing was carried out in a cooled and stirred solution of 95 percent glacial acetic acid and 5 percent of a 60 percent strength perchloric acid solution with an applied potential of 90 volts. A sheet of pure nickel, in the form of a hollow cylinder, was used as a cathode, and completely surrounded the sample in order to obtain uniform removal of material from the sample. The final diameter of the specimens of this group was 0.0535 inches but different groups received different amounts of cold work, depending upon the final size desired.

All the resistance measurements for the isothermal transformations were carried out with 2.5-inch specimens. Pure 0.020-inch nickel wire 8 inches in length was used for the electrical leads. The two current leads were spot welded to the ends of the sample, and the two potential leads were

positioned 0.25 inches in from each end. The specimen was then electropolished for 30 seconds at 105 to 110 volts as previously described, rinsed in water and alcohol, and dried in a forced hot-air stream. The specimen was then plated with 0.001 to 0.002 inch thick pure nickel for reasons discussed in Appendix A. The resistivity leads were then folded and the sample was sealed in an evacuated 9 mm vycor tube. The specimen was then ready for the final austenitizing treatment.

In the procedure for altering the grain size by varying the austenitizing temperature, temperatures higher than 900°C could not be used for the reasons discussed in Appendix A. The results presented herein were obtained by using austenitizing temperatures no higher than 900°C to prevent surface compositional variations. In Section 4.4 the results for higher austenitizing temperatures are included just to emphasize the differences obtained using different methods of calculations. However, this problem of compositional variation at the surface due to high austenitizing temperature does not arise at all when the grain size is varied by varying the prior thermal and mechanical history of specimens, but the final austenitizing treatment is kept low.

The temperature control in the austenitizing furnace was ± 3°C. After austenitizing, the vycor tube containing the specimen was cooled in air, this cooling rate being fast enough to maintain the fully austenitic state of the alloys at room temperature without introducing residual stresses. The vycor tube was then carefully broken away from the sample to prevent any scratching. After straightening the nickel leads, the specimen was electropolished as before. The time of electropolishing was selected to remove the nickel plating and further to reduce the specimen diameter by 0.002 to 0.003 inches. The specimen was now ready for the isothermal transformation.

4.2 Resistance Measurements

The course of the isothermal transformation was followed with a Kelvin double bridge by observing the change in the resistance of the specimen maintained at a constant subzero reaction temperature. The resistance of the sample was also measured at 20°C in a waterbath, both before and after isothermal transformation at the reaction temperature. This yielded the resistance change at 20°C, ΔR, due to the transformation. The ratio of $\Delta R/R$ at 20°C was taken as a measure of the extent of transformation.

The volume fraction of martensite was measured by point-counting several specimens of the alloys under investigation after different extents of transformation in order to determine the $\Delta R/R$ ratio per percent of martensite formed. The resistance ratio per 1 percent martensite for the alloys used in this investigation was found to be:

$$\frac{\Delta R}{R} \text{ at } 20°C = 4.5 \times 10^{-3} \text{ per 1 percent martensite}$$

This $\Delta R/R$ factor could easily be converted by measurement to the corresponding value at each reaction temperature, and hence the fraction of martensite formed could be obtained as a function of time by in-situ resistivity measurements. Thus the incubation period, defined as the time required to form 0.2 percent martensite (the smallest reliably detectable amount), could also be determined.

The resistance of a typical specimen 2.5 inches long and 0.058 inches in diameter was approximately 0.023 ohms. For this value the minimum change in resistance that could be measured corresponded to 0.1 percent transformation, but the time for 0.2 percent was chosen for the "start of the transformation". The isothermal runs were begun in all cases within 1½ hours after the austenitizing treatment by immersing the specimen into a low-temperature reaction bath.

It took about 5 seconds for the specimen to reach within 1°C of the bath temperature. Thus, no correction was necessary for the reaction time.

The first reading of resistance could be taken in about 10-15 seconds after the time of immersion; the specimen was then exactly at the bath temperature. In following the resistance as a function of time at the isothermal transformation temperature, readings were taken as often as possible, usually at intervals of 0.30 minutes when short incubation periods were expected. For samples with long incubations, readings were taken at intervals of one minute until a definite indication of resistance drop due to the transformation had been noticed. However, these intervals were reduced as the specimen approached the incubation period. This was necessary in order to be able (1) to detect the initiation of transformation as closely as possible and (2) to stop the run for metallographic measurements after only a very small fraction of martensite had been formed.

The isothermal transformations were conducted at a series of reaction temperatures from -196° to -20°C. Methylene chloride was used for the isothermal baths at reaction temperatures above -60°C. A mixture of 75 percent petroleum ether and 25 percent methyl-cyclohexane was adopted for the isothermal baths in the temperature interval of -196° to -70°C.

The bath temperature was maintained by additions of small amounts of liquid nitrogen or dry ice powder, and was monitored constantly with a calibrated copper-constantan thermocouple. The temperature of the bath was maintained within ± 0.2 °C of the stated temperature during the course of an isothermal run, and resistance readings were taken when the galvanometer was exactly at the null point. The bath was stirred vigorously to maintain uniformity of temperature.

4.3 Specimen Examination

4.3.1 Optical Microscopic Examination

After the isothermal transformation run, the resistance specimen was mounted in a cold-setting compound and ground longitudinally to the plane of maximum cross section. Following mechanical polishing, the specimen was electropolished at 90 volts for 60 seconds, in the set-up described before. The specimen was then etched in a solution of 25 grams of sodium bisulphite in 100 cc of water.

4.3.2 Transmission Electron Microscopic Examination

Specimens for transmission electron microscopy were prepared from 0.016 inch thick sheets which had the same amount

of cold reduction in area as the swaged specimens for transformation runs. Discs of 2.2 mm diameter were punched out of these sheets, and were austenitized for one hour at a number of austenitizing temperatures within the range investigated in the transformation kinetics studied. Thin foils were prepared from these discs to observe the austenitic structure. To examine the isothermally-transformed structures, austenitic discs were first isothermally transformed (to approximately 5-10 percent martensite) and were then used for the preparation of thin foils.

In either case, a crater was formed in the center of the specimen by applying a 1 mm diameter nitric acid jet at 36 volts for 8-9 minutes, leaving about one-third of the original thickness of the specimen at the base of the crater. The edges of the specimen were then lacquered, and electropolishing was carried out in a chromic-acetic acid solution (133 cc of glacial acetic acid - 7 cc of distilled water - 25 gm of CrO_3), at 14 volts, using a stainless steel cathode. The temperature of the electrolyte was maintained at 16-20°C. The specimen was finally examined with a Siemens Elmiskop-1, operated at 100Kv.

4.4 Quantitative Metallography

4.4.1 Grain-Size Measurement

Grain-size determinations were carried out on specimens which were transformed to a small amount of martensite so that grain boundaries could be easily observed. They were etched deeply to bring out the austenitic grain boundaries. The grain-size measurements were made by the linear intercept method, counting the number of grain boundary intersections during a traverse. Since the twin boundaries, as well as the grain boundaries, can restrict the size of martensitic plate, they were also taken into account. Counts of 200 to 300 intersections were repeated in at least two different areas of the specimen.

The grain sizes reported in the results are stated in terms of the equivalent spherical grain diameter, which is derived from the relation:

$$\bar{d} = 1.6485L^{(23)},$$

where L is the mean linear intercept.

4.4.2 Determination of Volume Fraction of Martensite and Number of Plates per Unit Area and per Unit Length

The volume fraction of martensite formed in a sample was determined by point-counting, using a 7 x 7 grid of 10cm x 10cm superimposed on the specimen image. Since the martensitic

transformation was not uniform across the section of the specimen, especially in specimens with small fractions transformed, point-counting was done at 200 to 250 grid positions in each sample, to obtain the average value of the fraction of martensite formed over the entire specimen. A magnification of 500 x or 1000 x was adopted, depending on the martensitic plate size. To relate the resistance changes to the extent of transformation, at least 1500 to 2000 intersections having martensite were counted in each specimen, and this procedure was repeated on 3 to 4 specimens in each alloy. The average of the results of such determinations was taken for calibration.

The nucleation rate of isothermal martensitic transformation can be related to theory only if it is determined in the early stages of transformation, so that autocatalytic effects are not pronounced. For direct determination of the nucleation rate, the number of martensitic plates formed per unit volume, N_V, as to be obtained. This quantity can be determined from the number of plates per unit area, N_A, and the number of plates per unit length, N_L. However, determination of N_A and N_L on specimens transformed only to a very low fraction of martensite (0.2 to 0.5 percent) poses experimental difficulties, since the transformation is not at all uniform at that early stage of transformation.

Therefore, in order to get an average value of N_A the grid was placed in 5 alternate positions across the cross-section of the specimen at 1000 x, and this was repeated at 50 different positions along the length, at intervals of 1 mm. At each of the grid positions, the number of martensitic plates falling within the area of the grid was counted, from which the average number of plates per unit area of the specimen could be calculated.

The average number of plates per unit length of the specimen was determined by a linear-intercept method. Usually 5 traverses were made along the length of the sample, and their average value was obtained.

4.4.3 Measurement of Radius to Semithickness Ratio of Martensitic Plates

Figs. 1-3 show photomicrographs of specimens of different grain sizes having a small fraction of martensite*. It is evident that even at a very early stage of transformation the martensitic plates are of nonuniform size. Thus, to determine the average radius to semithickness ratio of the martensitic plates, the distribution of sizes has to be taken into account.

* Photographs are shown only for the 24Ni3Mn alloy. Similar behavior is noted in the other alloys.

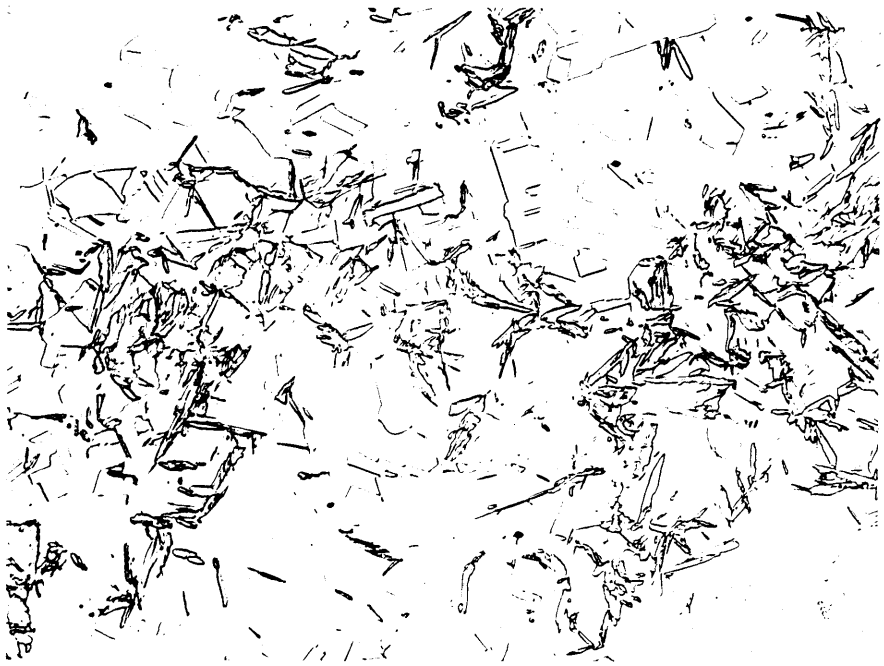

Figure 1. 24Ni3Mn alloy, having a grain size of 0.012 mm, reacted at -115°C to 0.9 percent martensite. Note low $(\overline{r/c})$. Etched with 25 percent Sodium Bisulphite in water. 500X.

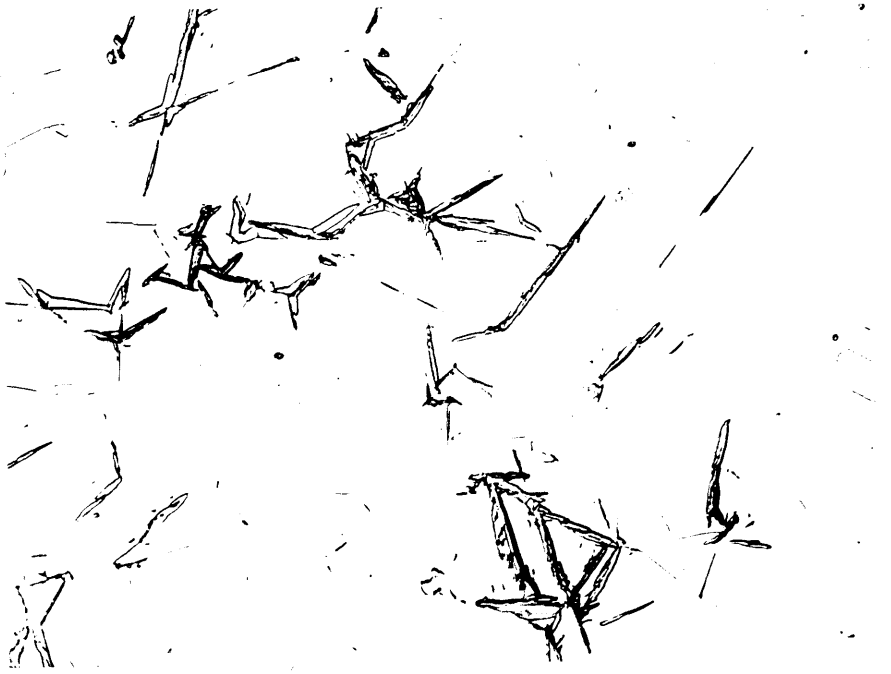

Figure 2. 24Ni3Mn alloy, having a grain size of 0.025 mm, reacted at -115°C to 0.9 percent transformation. Etched with 25 percent Sodium Bisulphite in water. 500X.

Figure 3. 24Ni3Mn alloy, having a grain size of 0.099 mm, reacted at -115°C to 1 percent transformation. Note high $(\overline{r/c})$. Etched with 25 percent Sodium Bisulphite in water. 500X.

If the martensitic plates are considered as circular plates with a distribution of radius r and semithickness c, then according to Fullman,[24] the average radius to semi-thickness ratio, $(\overline{r/c})$, is given by:

$$\overline{r/c} = \frac{3\pi^2}{64} \frac{\bar{F}}{\bar{E}} \tag{14}$$

where $\bar{E}$ is the mean of the reciprocals of the plate lengths as intersected by a cross-sectioning plane, and $\bar{F}$ is the mean of the reciprocals of the plate widths as intersected by a cross-sectioning plane. About 150-200 measurements each of the length and thickness intersections were made to obtain an average value of $\overline{r/c}$ for a particular specimen and this procedure was repeated for specimens of different grain sizes to obtain this ratio as a function of grain sizes. Fig. 4 shows a plot of $\overline{r/c}$ as a function of grain size; clearly this ratio increases with increasing grain size, in contrast to the findings of Raghavan[22] who did not observe a systematic trend of $\overline{r/c}$ as a function of grain size. The increasing trend of this ratio with increasing grain size is also apparent from the photomicrographs of Figs. 1-3. The values of $\bar{r}$ and $\bar{c}$ as a function of grain size for the alloys under investigation are listed in Table 1A. Table 1B shows the $\bar{r}$ and $\bar{c}$ as a function of fraction transformation for the 24Ni3Mn alloy having a grain size of 0.025 mm.

TABLE 1A

Average Radius and Semithickness of Martensitic Plates as a Function of Grain Size for the 23Ni3Mn, 24Ni3Mn and 25Ni2Mn Alloys, Reacted at Different Reaction Temperatures to Small Fractions of Transformation.

Average Grain Diameter $\bar{d}$ mm	Average $\bar{r}$ Radius cm x 10^3	Average Semithickness $\bar{c}$ cm x 10^3
0.012	0.353	0.031
0.013	0.415	0.029
0.020	0.465	0.036
0.025	0.57	0.037
0.033	0.589	0.033
0.074	0.614	0.035
0.099	0.683	0.032
0.14	0.69	0.029
0.19	0.71	0.028

TABLE 1B

Average Radius and Semithickness of Martensitic Plates as a Function of Fraction Transformation for the 24Ni3Mn Alloy having a Grain Size of 0.025 mm.

Fraction Transformation f	Average Radius, $\bar{r}$ cm x 10^3	Average Semithickness $\bar{c}$ cm x 10^3
0.002	0.865	0.048
0.01	0.479	0.039
0.025	0.392	0.034
0.050	0.324	0.03
0.08	0.405	0.034
0.10	0.377	0.023
0.17	0.385	0.030
0.22	0.463	0.029
0.27	0.387	0.031
0.30	0.46	0.027
0.38	0.521	0.042

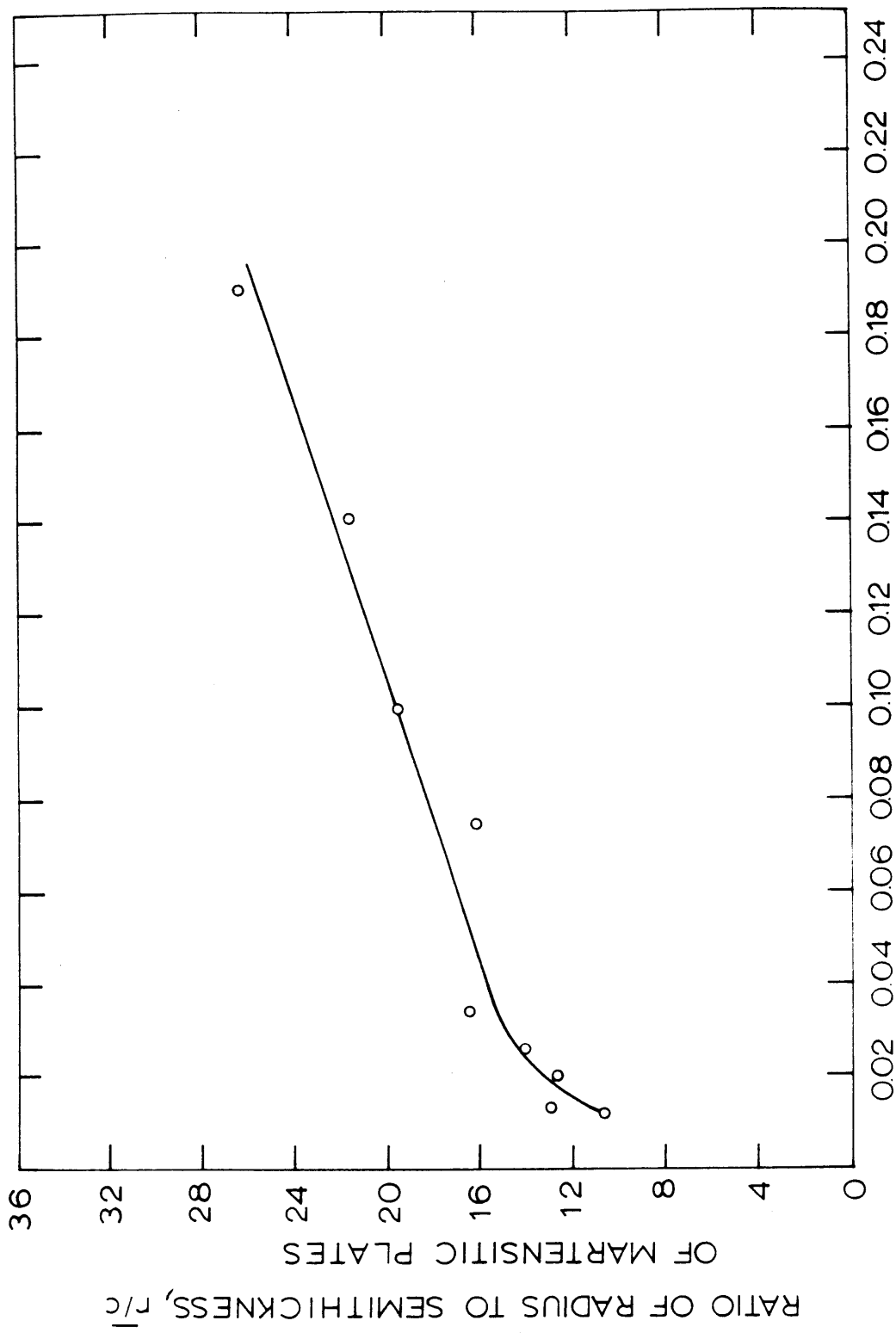

Figure 4. Average Radius to Semithickness Ratio of Martensitic Plates as a Function of Grain Size in 23Ni 3Mn, 24Ni 3Mn, and 25Ni 2Mn Alloys.

4.5 Measurement of Nucleation Rate

The initial nucleation rate for isothermal martensite formation can be obtained experimentally by two different methods as discussed below:

(1) One method is based on the measurement of the incubation period for formation of isothermal martensite, and the mean volume ($\bar{v}$) of the martensitic plates formed within this time. If it is assumed that at each reaction temperature the rate of nucleation is constant during the incubation period, at least up to time (τ_i) for 0.2 percent martensite, then according to the relation proposed by Shih et al.[16]

$$0.002 = \dot{N}\,\bar{v}\,\tau_i \tag{8}$$

Shih et al. assumed the martensitic plates to be lens-shaped and obtained the mean plate volume from metallographic measurements of radii and thicknesses. However, this procedure leads to an inaccurate estimation of the volume because the average volume is given by the average of $\pi r^2 c$, where r is the radius and c is the semithickness of the martensitic plates, and not by the $\pi \bar{r}^2 \bar{c}$, where $\bar{r}$ is the average radius and $\bar{c}$ is the average semithickness. Entwisle[20] considered each initial martensitic plate as an oblate spheroid of volume $v = \frac{4}{3}\pi r^2 c$, where r is the radius and c is

the semithickness of the martensitic plates. The volume per martensitic plate can be obtained as a function of the austenitic grain size on the assumption that the effective plate diameter is controlled by the grain or twin boundaries. Using this assumption Entwisle deduced the average martensitic plate radius $\bar{r}$ in terms of the average spherical grain diameter $\bar{d}$, from which

$$\bar{v} = \frac{4}{3}\pi \frac{(0.4076\bar{d})^3}{(\overline{r/c})} = \frac{0.2837\bar{d}^3}{(\overline{r/c})} \qquad (15)$$

The average volume per martensitic plate then can be calculated using equation (15) from the measurement grain size and $\overline{r/c}$ of the martensitic plates. The result is shown in Fig. 5. However, from the metallographic observations in the present work, it became evident that not all the martensitic plates extend to grain or twin boundaries, even in the early stages of transformation and especially at the larger grain sizes. Thus, equation (15) is likely to over-estimate the average volume per martensitic plate.

In order to check this and to determine the average volume per martensitic plate more realistically, account was taken of the size distribution discussed in Section 4.4.3. The

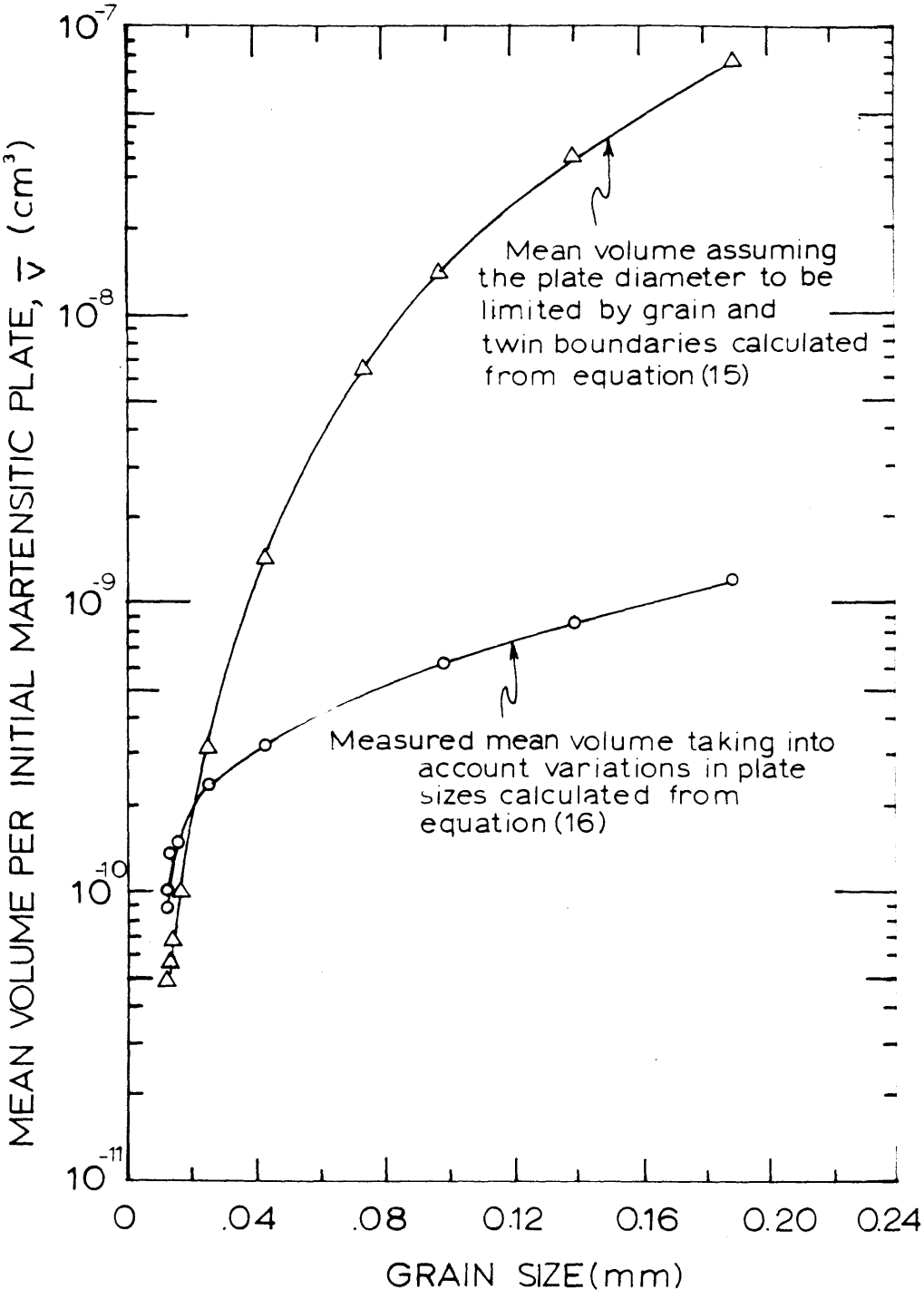

Figure 5. Mean Volume per Martensitic Plate, Calculated from Equation (15) and (16) as a Function of Grain Size for 23Ni 3Mn, 24Ni 3Mn, and 25Ni 2Mn Alloys.

morphology of the plates also indicated that they might very well be considered to be circular plates. For this case, Fullman[24] has shown that the mean martensitic plate volume is given by

$$\bar{v} = \frac{\pi^2 f}{8\bar{E}N_A} \tag{16}$$

where f is the fraction of martensite formed, and the remaining symbols have already been defined. The mean volume per martensitic plate at 0.2 percent transformation, calculated as a function of austenitic grain size using equation (16), is shown in Fig. 5.

It is evident that the assumption of the effective diameter of the martensitic plate being controlled by grain or twin boundaries leads to an overstatement of the volume per plate, especially at the larger grain sizes. The average volume per martensitic plate for 0.2 percent transformation then should be calculated from equation (16), and this average volume can be substituted in equation (8) to obtain the nucleation rate corresponding to 0.2 percent transformation.

(2) The second procedure for measuring the nucleation rate does not depend upon obtaining the mean volume per martensitic plate, but instead assumes plates of uniform size.[25] Although it has just been indicated that the plates are actually not of uniform size, even at the early stages of transformation, nevertheless this procedure is utilized below to show how the nucleation rate obtained in this way might deviate from the rates obtained by the first procedure.

If the first-formed plates can be regarded as uniform circular discs with thicknesses very much smaller than the radius, then according to Fullman[24]

$$N_V = \frac{2}{\pi} \frac{N_A^2}{N_L} \tag{17}$$

where N_A is the number of plates per unit area on a random section, N_L is the number of plates intersected per unit length along a random traverse, and N_V is the number of plates per unit volume.

By definition,

$$\dot{N} = \left(\frac{1}{1-f}\right) \frac{dN_V}{dt} \tag{18}$$

where f is the fraction transformed in time t. In the early stages of transformation, $1-f \simeq 1$, and if autocatalytic effects

are neglected up to the time τ_i of 0.2 percent transformation, then

$$\dot{N} = \frac{N_V}{\tau_i} \tag{19}$$

where $\dot{N}$ and N_V now correspond to 0.2 percent transformation.

Since one of our aims was to determine the nucleation rate as a function of austenitic grain size, N_V for 0.2 percent transformation was calculated from equation (18) using the measured values of N_A and N_L corresponding to 0.2 percent transformation. The result is shown in Fig. 6. It is seen from the graph that the number of plates per unit volume for 0.2 percent transformation decreases with the increase in grain size, which is consistent with the fact that the average volume of the martensitic plates increases with increasing in grain size. However, the actual values of N_V calculated in this way falls somewhat short of what is obtained if one takes into account the variations in plate sizes, as explained below.

Equation (16) expresses the average volume per martensitic plate taking into account the variations in sizes. Now, one can calculate the N_V for 0.2 percent transformation from the relation

$$N_V = \frac{f}{\bar{v}} = \frac{8}{\pi^2} \bar{E} N_A \tag{20}$$

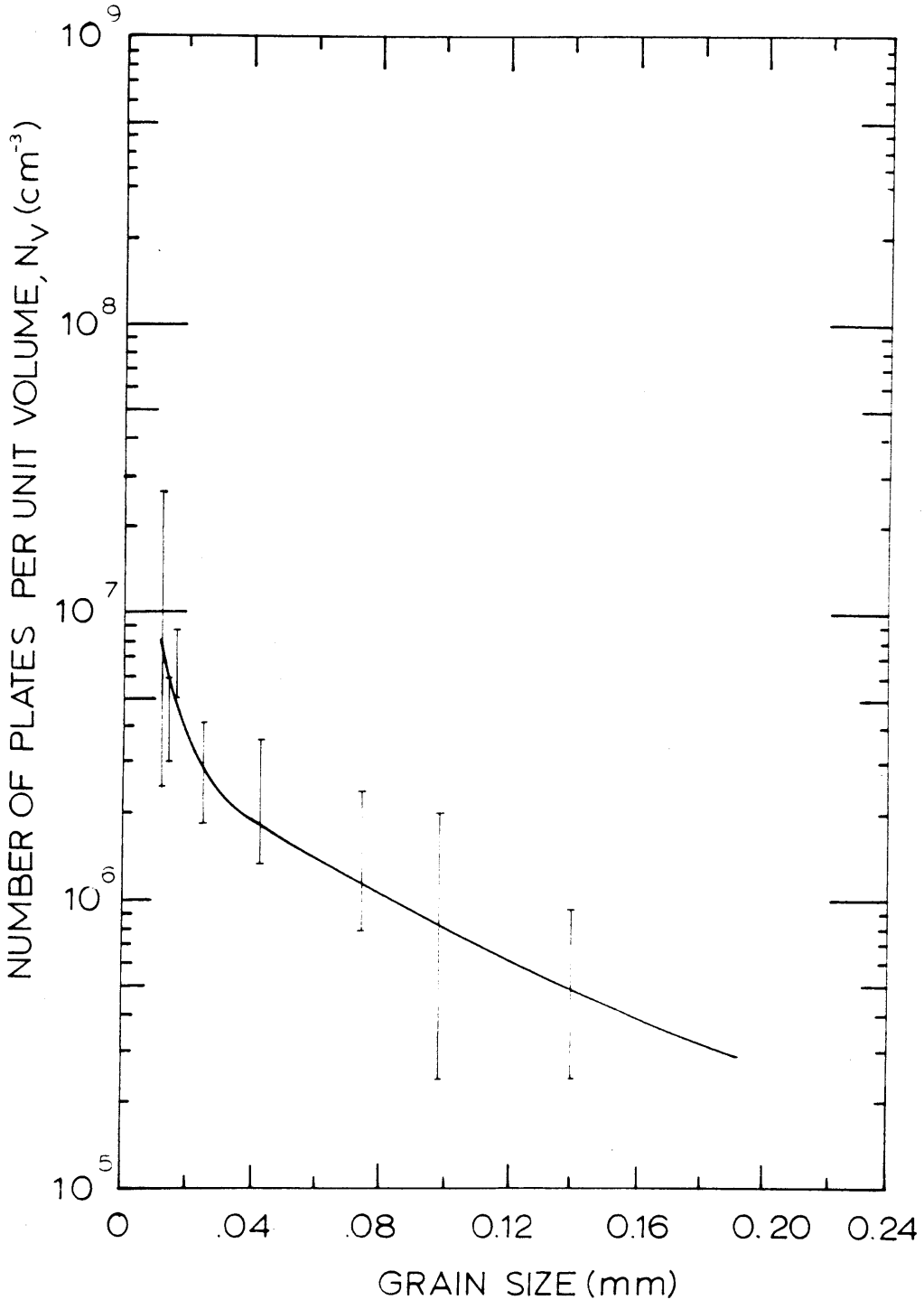

Figure 6. N_V for 0.2 Percent Transformation for Martensitic Plates of Uniform Size as a Function of Austenitic Grain Size in 23Ni 3Mn, 24Ni 3Mn, and 25Ni 2Mn Alloys.

where $\bar{E}$ and N_A corresponds to 0.2 percent transformation. N_V calculated from the above equation is shown in Fig. 7.

From comparison of Figs. 6 and 7, it is evident that N_V for 0.2 percent transformation, calculated from equation (17), is smaller by a factor of 2-5 depending on the grain size than when calculated from equation (20). This discrepancy arises mainly due to experimental difficulties in accurate estimation of N_V at such a small fraction transformation. The occurance of transformation in clusters further complicates the situation and hence cause the observed disparity. Figs. 8-9 demonstrate the occurrence of transformation in clusters. Although, even for a small fraction of transformation, the values of N_V calculated from equation (17) do not differ much (well within an order of magnitude) from the values obtained from equation (20), nevertheless to be consistent with the observed variations in plate sizes, the values of N_V derived from the latter approach have been used in the nucleation-rate calculations reported in this investigation. All the nucleation rates reported in the text correspond to 0.2 percent transformation unless mentioned otherwise.

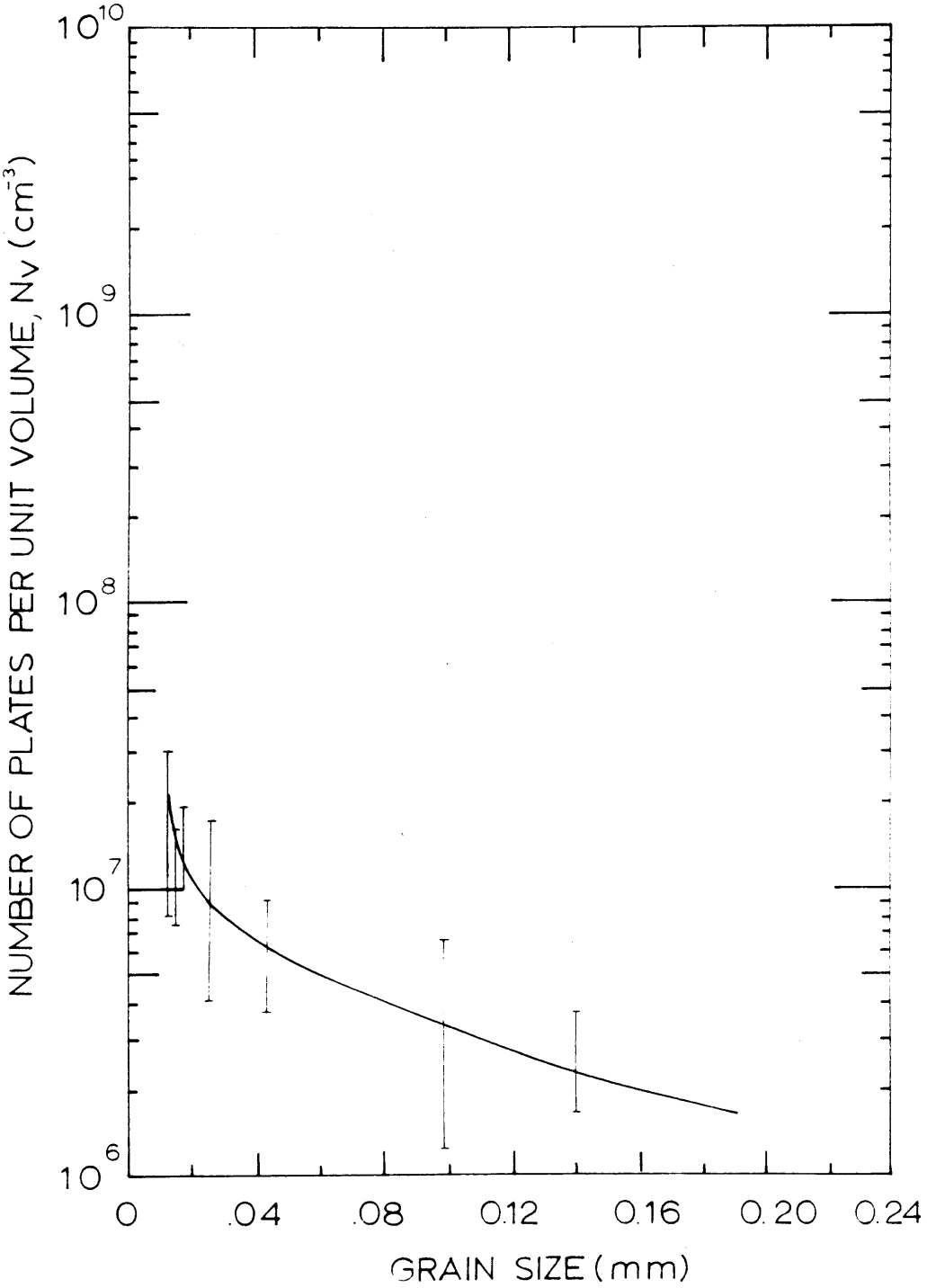

Figure 7. N_V for 0.2 Percent Transformation Taking into Account Variation in Martensitic Plate Size as a Function of Austenitic Grain Size in 23Ni 3Mn, 24Ni 3Mn, and 25Ni 2Mn Alloys.

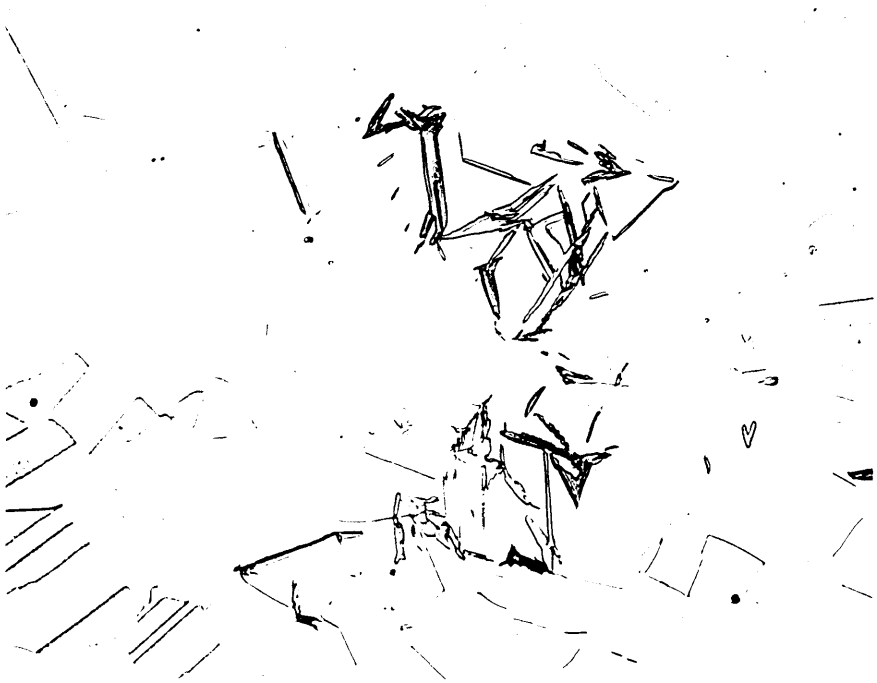

Figure 8. 24Ni3Mn Alloy, having a grain size of 0.025 mm, reacted at -115°C to 1 percent transformation. Note a small cluster. Etched with 25 percent Sodium Bisulphite in Water. 500X.

Figure 9. 24Ni3Mn Alloy, having a grain size of 0.025 mm, reacted at -115°C to 1 percent transformation. Note a long dense cluster. Etched with 25 percent Sodium Bilsulphite in water. 200X.

5. C-CURVE KINETICS OF ISOTHERMAL MARTENSITIC TRANSFORMATION

The kinetics of the isothermal martensitic transformation as a function of reaction temperature have been studied in two alloys, namely, 24Ni3Mn and 25Ni2Mn, which permitted a wide range of temperatures to be investigated. All the results reported in this section are for an austenitizing treatment of 1 hour at 900°C (grain size of 0.025 mm).

5.1 Results

Fig. 10 shows the incubation period τ_i (time required to form 0.2 percent martensite) as a function of reaction temperature for the 24Ni3Mn alloy. The horizontal line at each reaction temperature level indicates the range of values obtained for the incubation period in 3-5 different specimens. The curve has been drawn through the average of the incubation periods. The incubation period had a minimum value at -125°C and increased rapidly with increasing or decreasing reaction temperature.

Fig. 11 shows the incubation period as a function of reaction temperature for the 25Ni2Mn alloy. The arrow at -80°C indicates that the specimen had already begun to transform within that time. Thus, only one-half of the C-curve is observed here because the incubation period below -60°C is

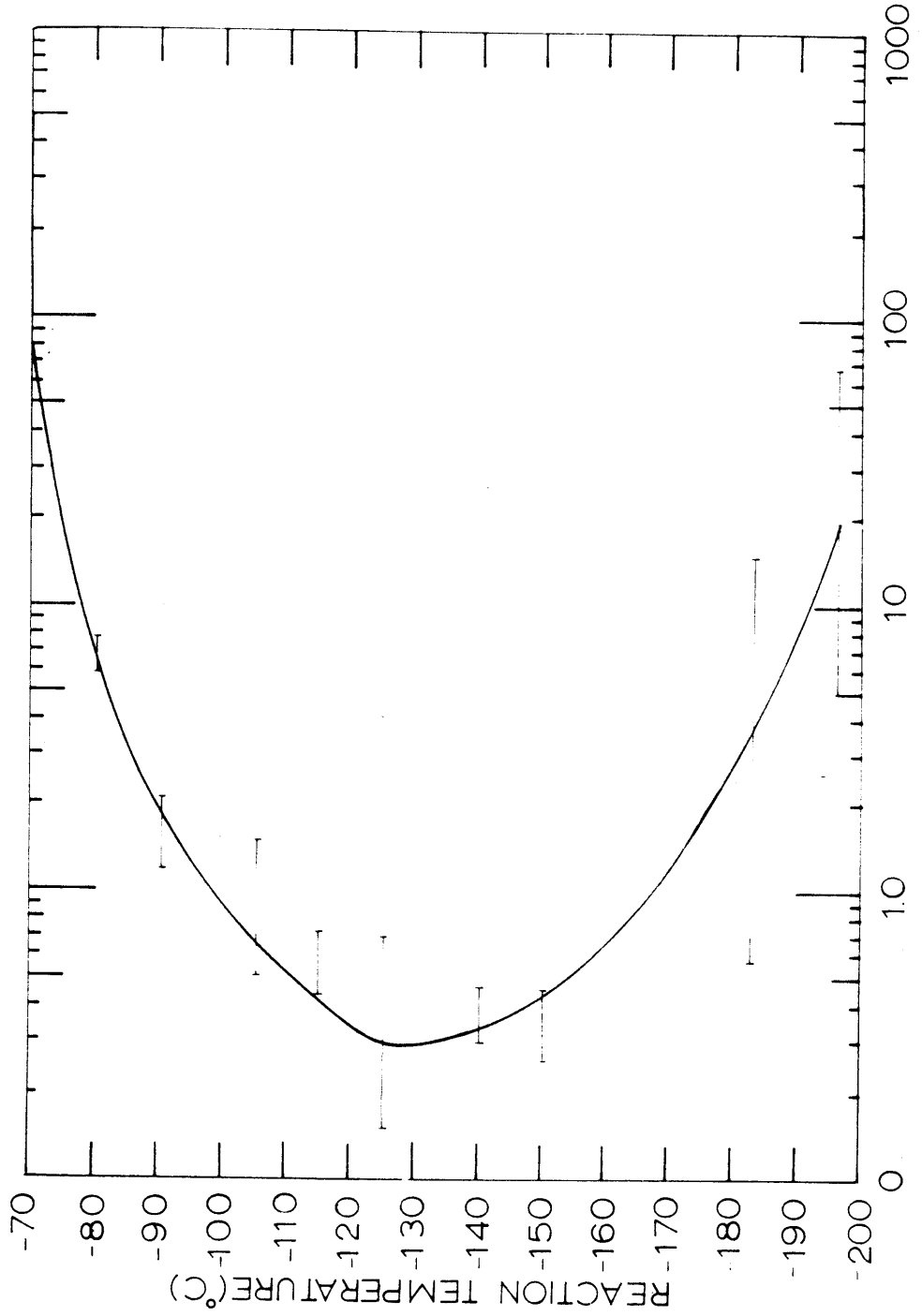

Figure 10. Incubation Period as a Function of Reaction Temperature for the 24Ni 3Mn Alloy.

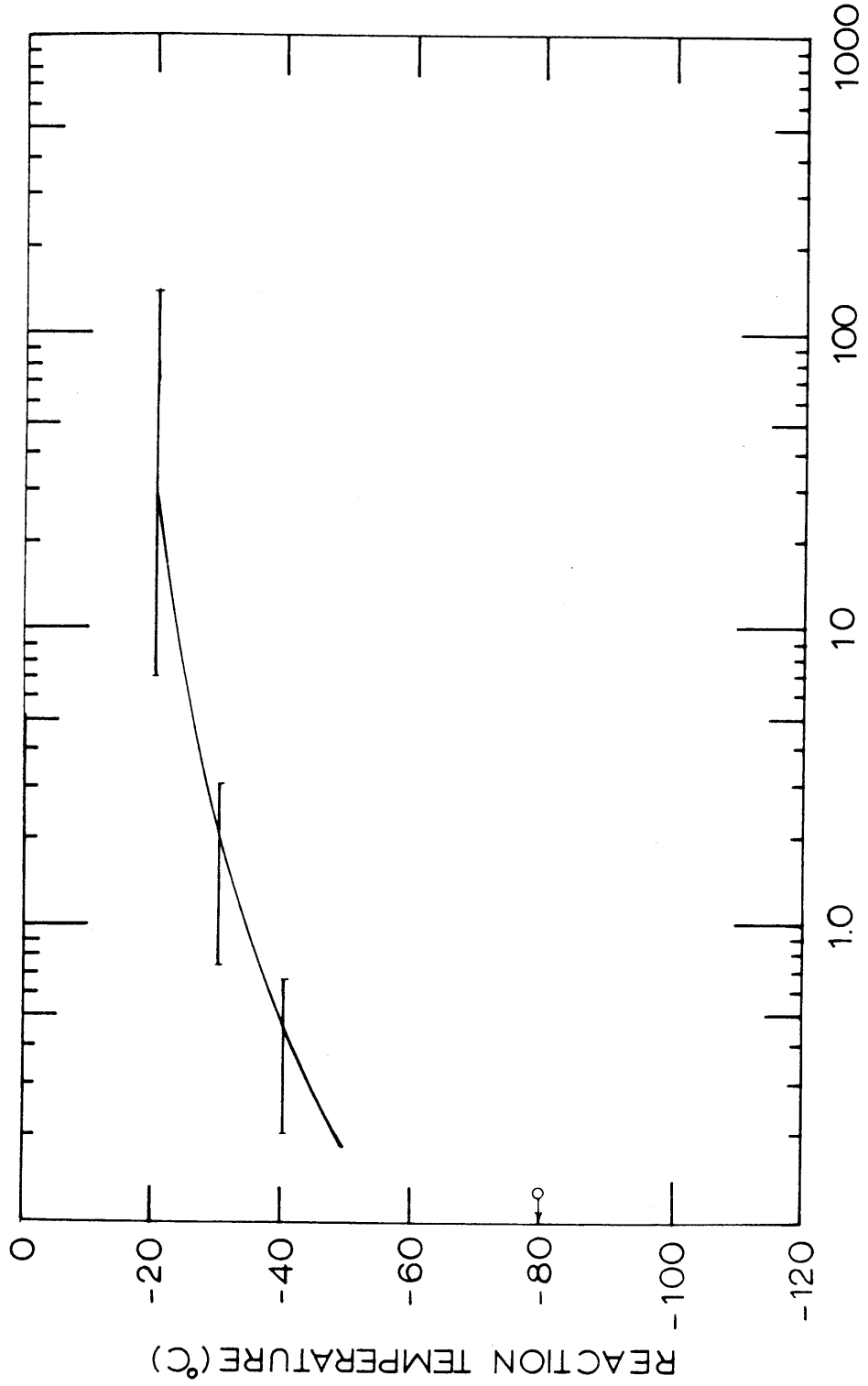

Figure 11. Incubation Period as a Function of Reaction Temperature for the 25 Ni 2Mn Alloy.

too short to be determined. Otherwise the curve is similar to that shown in Fig. 10.

Fig. 12 presents the initial nucleation rate as a function of reaction temperature for both the alloys, calculated as outlined in the previous section. For each reaction temperature, the average incubation period was used to calculate the nucleation rate. For the 24Ni3Mn alloy, the nucleation rate was highest at -125°C and decreased rapidly with increasing or decreasing reaction temperature. For the 25Ni2Mn alloy, the initial nucleation rate continually increased with decreasing temperature down to -50°C, which was the lowest temperature at which the isothermal transformation could be studied without having some martensite present before reaching the reaction temperature.

5.2 Discussion of Results

These results indicate that in properly chosen alloys martensite can form by a completely isothermal process over a wide range of temperature (-196° to -20°C).* The general C-shape of the transformation temperature-incubation period curve in Fig. 10 is similar in form to the findings of Shih et al.[16] and others[10,20].

*It is to be noted that the structure of the isothermally formed martensite throughout the temperature range of investigation was identified as body-centered cubic (b.c.c.). No ε-martensite (hexagonal close-packed) was observed in these studies.

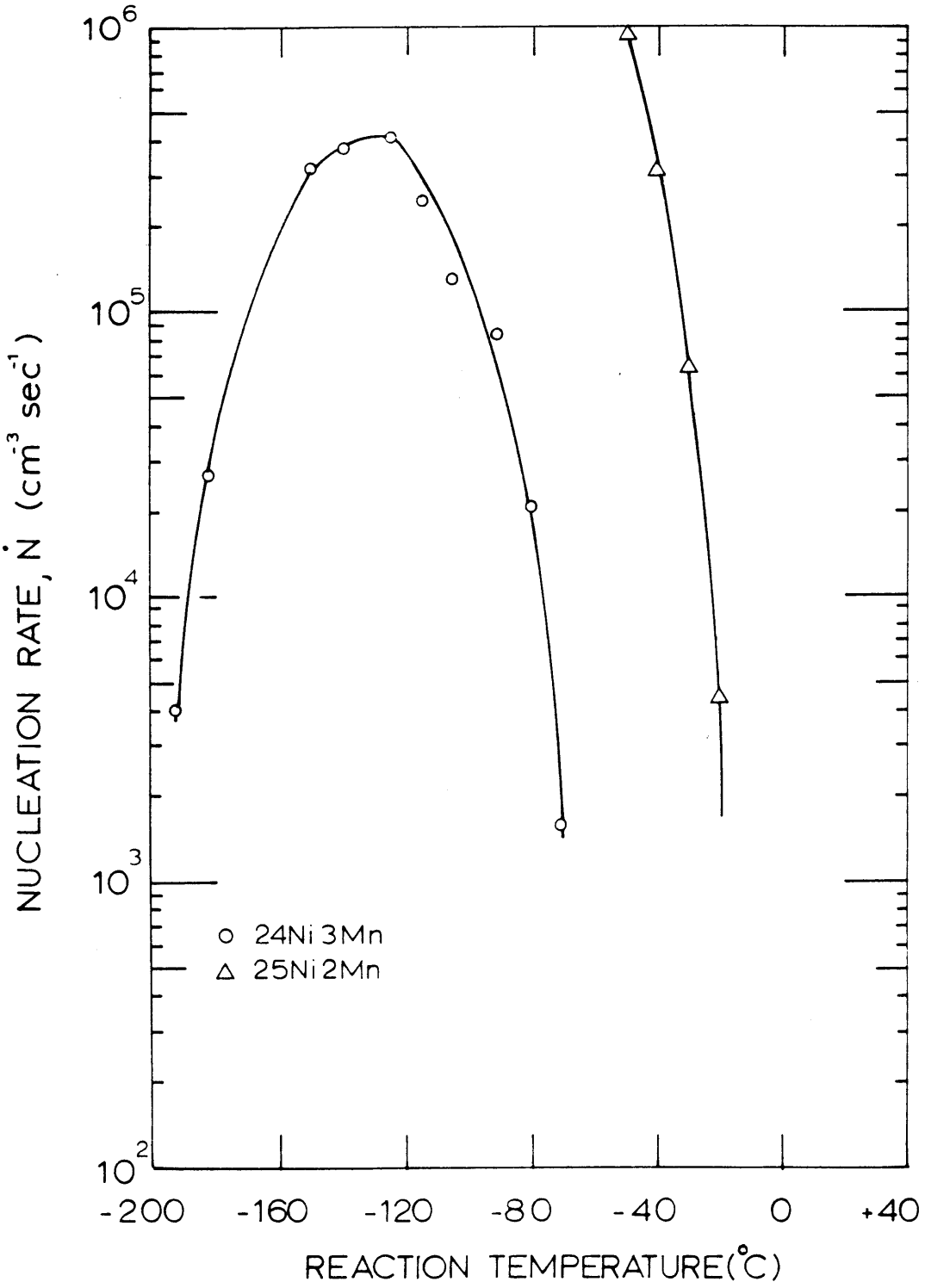

Figure 12. Nucleation Rate as a Function of Reaction Temperature for the Alloys of 24Ni3Mn and 25Ni2Mn.

The variation of the incubation period from one sample to another (indicated by horizontal lines at each reaction temperature) is probably caused by small differences in chemical composition, inasmuch as the transformation is critically dependent on the alloy content. Similar variations were also noted by previous investigators[16,21,22]. Shih et al. also found that alloys having almost identical nickel contents but slight variations in manganese exhibited marked differences in reaction kinetics. The temperature of maximum nucleation rate (shortest incubation period) was also found to be dependent on composition. Thus, the discrepancies in the literature among the reported results on the transformation kinetics of iron-nickel-manganese alloys having almost identical compositions may be explained on the basis of slight variations in compositions. This probably accounts for the difference of 15°C in the temperature for maximum nucleation rate that is found between the 24Ni3Mn (24.2 percent nickel-2.98 percent manganese) alloy of the present investigation and the 23.2 percent nickel - 3.62 percent manganese alloy of Shih et al., although thermodynamically they are virtually equivalent (shown in Section 7.2).

The nucleation rate of the 24Ni3Mn alloy in Fig. 12 is greater by a factor of about 100 than the rate found by Shih et al. for their alloy. This arises partly from the

difference in composition and partly from the higher average volume per martensitic plate estimated by them.

The 25Ni2Mn alloy does not disclose a complete C-curve, because it is shown in Section 7.2 that at any given temperature this alloy has higher driving force towards martensitic transformation than does the 24Ni3Mn alloy. Consequently, the nose of the C-curve occurs at a higher temperature, and because of the lower manganese content, the reaction rate is so fast that it is not possible to quench below the nose temperature without the formation of some martensite. Thus, the incubation period becomes too short to be detectable even at -60°C.

From the nucleation rates, the increment of free energy required to activate the most potent embryos, ΔW_a can be calculated from equation (9), (p. 16). To obtain a value of n_i Shih et al. arbitrarily assumed that there is one most potent embryo per grain of austenite, and arrived at a value of $n_i = 10^5$ per cm^3, which is to low[21]. An alternative approach is described here to arrive at a more reasonable value.

Cech and Turnbull[26] investigated the martensitic transformation in fine particles of an iron -30.2 percent nickel alloy and found that there was a wide change in M_s temperature in the range of sizes between 30 to 70 microns. Taking the

mean value of 50 microns and assuming one most potent embryo is enclosed in this volume of 10^{-7} cm^3, we have the number of most potent embryos n_i equal to 10^7 per cm^3. Moreover Raghavan and Entwisle[21] have also been able to match the calculated and experimental isothermal transformation curves of different grain sizes by taking a constant value of n_i equal to 10^7 per cm^3, basing their choice on the experimental evidence of Cech and Turnbull[26].

With $n_i = 10^7$ per cm^3 and $\nu = 10^{13}$ per second, the values of ΔW_a calculated from equation (9) are listed in Table II.

The values of ΔW_a for the 24Ni3Mn alloy are lower by 350 - 1250 cal/mole than those reported by Shih et al. This is a very small difference, especially if the differences in manganese content and the corrected volumes per martensitic plate are taken into account. The temperature dependence of activation energy is quite similar to the findings of Shih et al. and Machlin and Cohen[9].

It should be mentioned here that the ΔW_a values reported in this and other investigations correspond to 0.2 percent transformation and are calculated on the assumption that only the initial embryos are available for transformation. It will be shown in Sections 6 and 8 that this is not strictly true; at lower reaction temperatures, even within 0.2 percent transformation, an appreciable number of autocatalytic embryos

TABLE II

Activation Energies for Isothermal Martensitic Transformations in 24Ni3Mn and 25Ni2Mn Alloys

Alloy	Temperature °C	ΔW_a cal/mole
24Ni3Mn	-70	15,600
	-80	13,800
	-90	12,600
	-105	11,500
	-115	10,600
	-125	9,800
	-140	8,800
	-150	8,200
	-183	6,400
	-196	5,800
25Ni2Mn	-20	18,900
	-30	16,900
	-40	15,500
	-50	14,300

are produced and are available for transformation. The calculated activation energy based on equation (9) is slightly lower (by a maximum of only 400 cal/mole) than what is obtained if autocatalysis is taken into account. However, since the autocatalytic parameter is not known with enough accuracy over the whole temperature range of isothermal transformation, and the value of activation energy is also not appreciably affected by considering autocatalysis, the ΔW_a values corresponding to 0.2 percent transformation, calculated from equation (9), have been used for comparison with the theory.

In Section 7.3 (p.94) it will be shown that the measured values of activation energies match very well with the calculated values of activation energy using equation (11) (p. 20), based on the Kaufman and Cohen model.[1]

6. EFFECT OF GRAIN SIZE ON INCUBATION PERIOD AND NUCLEATION RATE

In Section 2, it was suggested that if the number of embryos was not a function of grain size then the effect of grain size on the incubation period should be merely that due to the size of the first-formed plates. In other words, the incubation period should be inversely proportional to the volume of the first-formed plates. This section reports experimental results to test this prediction.

6.1 Results

As mentioned earlier, different grain sizes were established in the test specimens by two different methods: (1) by varying the austenitizing temperature (one hour) of specimens having a constant amount of cold work and (2) by varying the previous thermal and mechanical history of specimens, but keeping the final austenitizing temperature constant. However, the range of grain sizes that could be studied was limited in either method. When the grain size was varied by changing the austenitizing temperature (procedure 1), the austenitizing temperature could not exceed 900°C for the reason discussed in Appendix A. Procedure (2) also produced a limited range of grain sizes because below certain amount of final cold work, the specimen did not fully recrystallize at the chosen austenitizing treatment.

Fig. 13 is a plot of the grain size as a function of austenitizing temperature for 23Ni3Mn, 24Ni3Mn, and 25Ni2Mn alloys. All three alloys showed very similar grain sizes versus temperature so that the data could be represented by a single curve. The vertical line at each grain size indicates the range of values obtained for the grain size in 3-4 different specimens.

6.1.1 Incubation Period versus Grain Size

Fig. 14 summarizes the incubation periods as a function of grain size for the 24Ni3Mn alloy reacted at -140°, -125°, -115° and -105°C. The incubation period shown at each grain size is the average of 3-4 different specimens. In each instance, the incubation period decreased with increasing grain size. For all grain sizes, the incubation period was shortest at -125°C, and the incubation period increased with increasing or decreasing reaction temperature.

Fig. 15 shows the incubation periods as a function of grain size for the 23Ni3Mn and 25Ni2Mn alloys reacted at -50°C and at -40°C respectively. The arrows pointing upwards indicate that the specimens did not exhibit any transformation within that time, and therefore the curves have been extended by dashed lines. Each point represents an average value for 3-4 different specimens. The behavior here was similar to that found for the samples of the 24Ni3Mn alloy. At comparable grain sizes the 23Ni3Mn alloy exhibited a much longer incubation

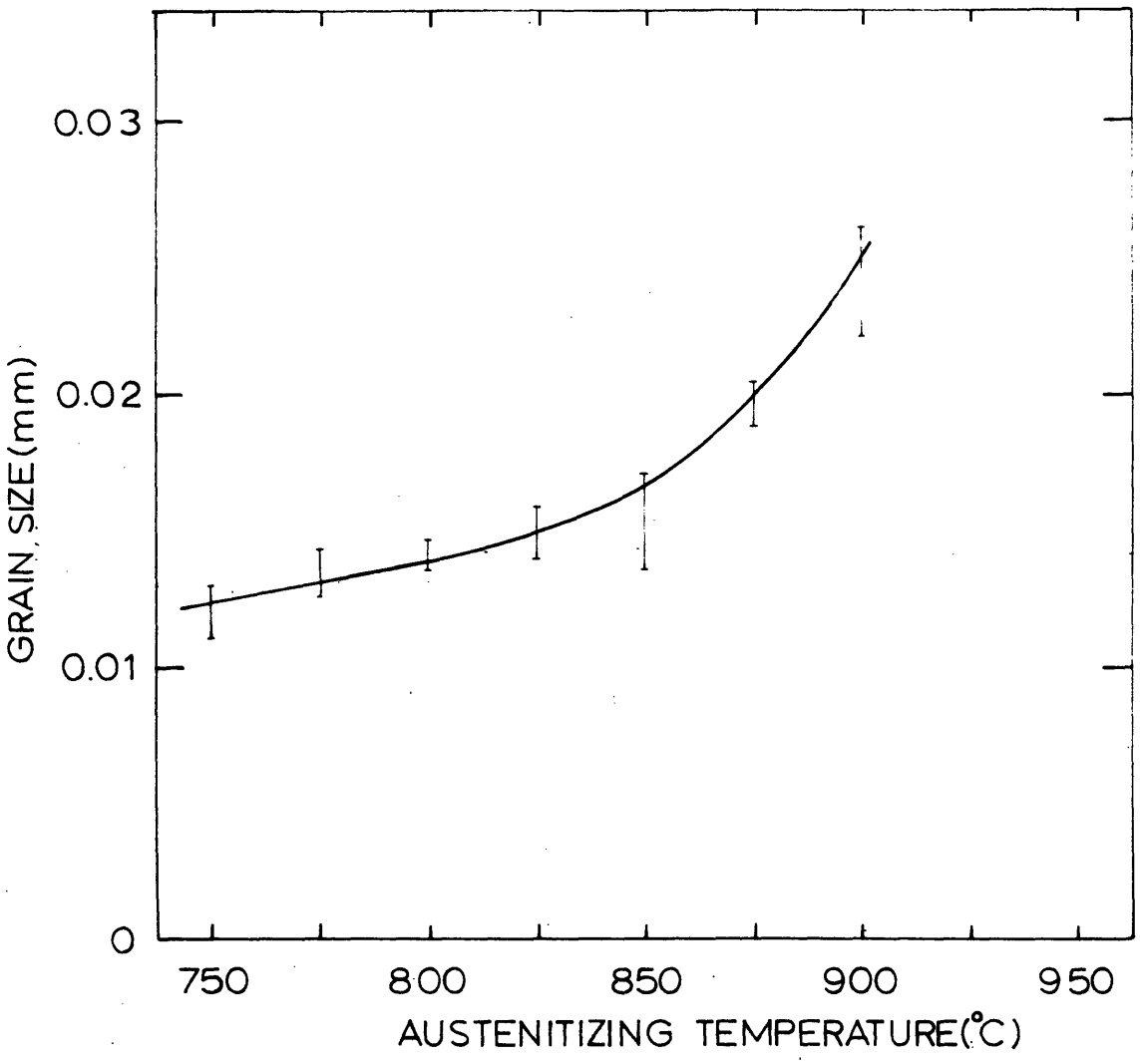

Figure 13. Grain Size as a Function of Austenitizing Temperature (1 hour) for 23Ni 3Mn, 24Ni 3Mn, and 25Ni 2Mn Alloys.

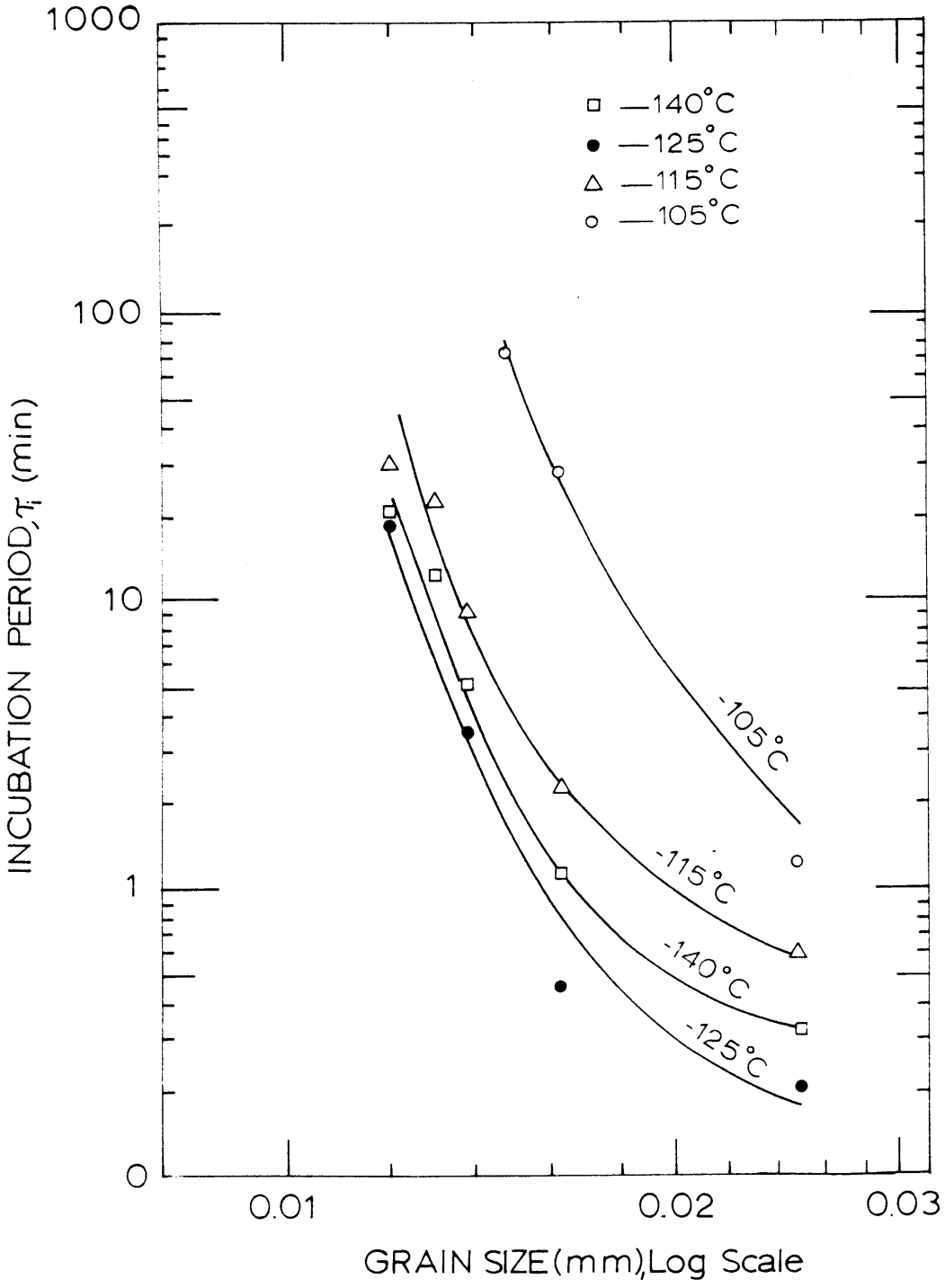

Figure 14. Incubation Period as a Function of Grain Size for the 24 Ni 3Mn Alloy, Reacted at the Indicated Temperatures.

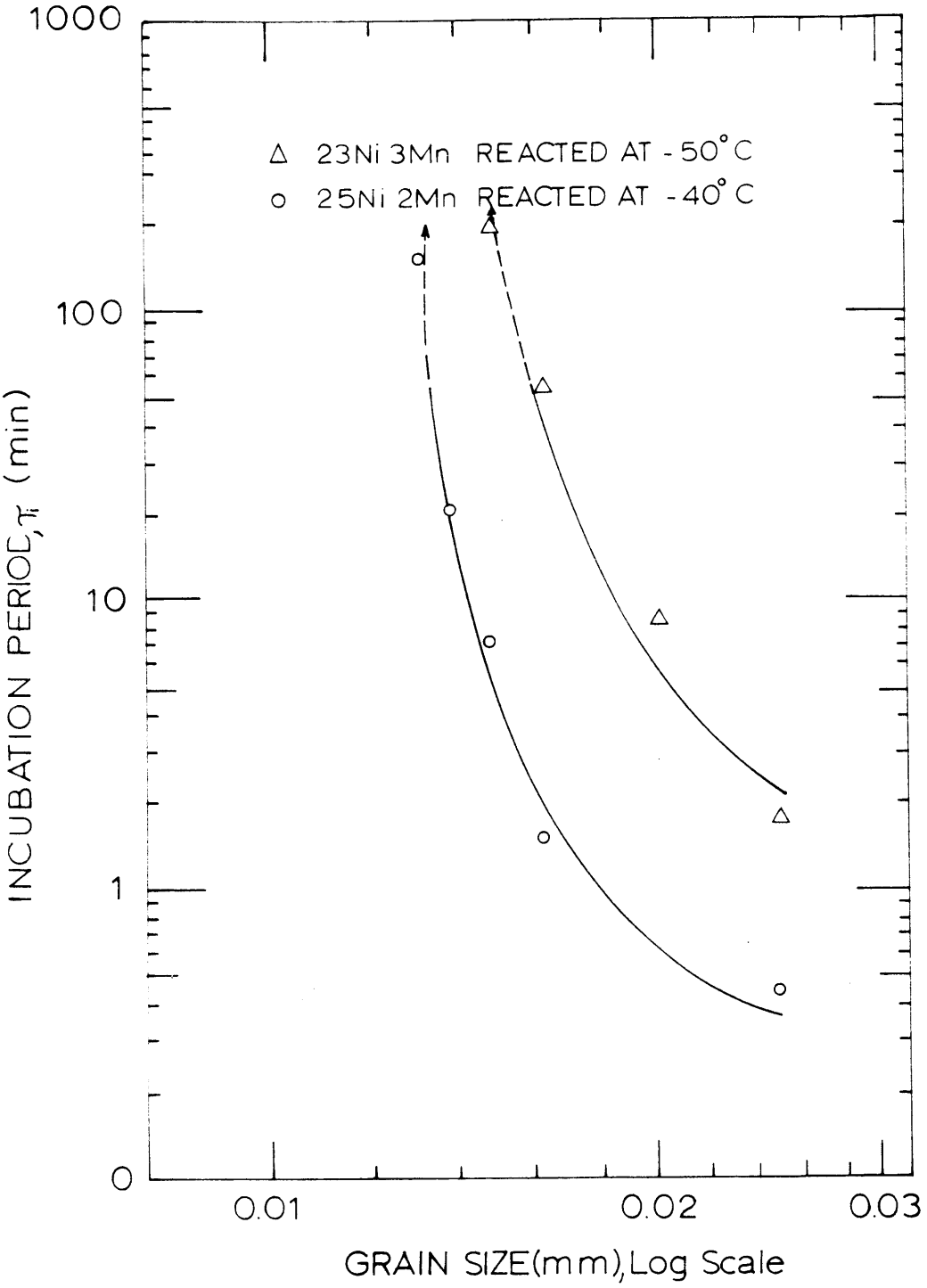

Figure 15. Incubation Period as a Function of Grain Size for the 23Ni 3Mn and 25Ni 2Mn Alloys Reacted at the Indicated Temperatures.

period at -50°C than the 25Ni2Mn alloy at -40°C.

The incubation periods of specimens whose grain size was varied by altering the previous thermal and mechanical history while keeping the final austenitizing temperature constant are listed in Table III. The 25Ni2MnA alloy was used for preparing these specimens. An austenitizing treatment of one-half hour at 800°C was used to establish the different grain sizes, and 4-6 specimens of each treatment were transformed at -20°C. Full details of prior thermal and mechanical history, amount of final cold work, the observed incubation periods, and the measured grain sizes are given in Table III.

6.1.2 Nucleation Rate versus Grain Size

The initial nucleation rates as a function of grain size for the 24Ni3Mn alloy reacted at -140°, -125°, -115° and -105°C are shown in Fig. 16. In each case, the nucleation rate increased with increasing grain size. For all austenitic grain sizes, the nucleation rate was highest at -125°C.

Fig. 17 is a plot of the initial nucleation rate as a function of grain size for samples of the 23Ni3Mn and 25Ni2Mn alloys reacted at the indicated temperatures. The arrows pointing downwards indicate that the nucleation rates were lower than represented by the corresponding points since the specimens of these grain sizes did not show 0.2 percent

Grain Size Effect in 25Ni2MnA Alloy

All specimens given the same treatment up to 0.125 inches in diameter. Final austenitizing treatment in all cases was 800°C for 30 minutes and reaction temperature was -20°C.

Serial No.	Specimen History	Final Reduction in area, percent	Average Grain Diameter, $\bar{d}$, mm	Incubation Period T_i sec.	Mean Incubation Period, sec.
1	0.125 in. dia., annealed at 800°C for 30 min., swaged to 0.0535 in. dia.	82	0.017	216 294 210 174	223
2	0.125 in. dia., annealed at 900°C for 15 min., swaged to 0.0765 in. dia., annealed at 950°C for 30 min., electropolished, swaged to 0.0535 in. dia.	48	0.022	48 84 210 150	123
3	0.125 in. dia., annealed at 900°C for 15 min., swaged to 0.0765 in. dia., annealed at 1100°C for 15 min., electropolished, swaged to 0.0535 in. dia.	46	0.035	36 21 7 9 6 21	18
4	0.125 in. dia., annealed at 900°C for 15 min., swaged to 0.0765 in. dia., annealed at 1200°C for 1 hour, electropolished, swaged to 0.0535 in. dia.	46	0.039	6 6 15 18 15 12	12

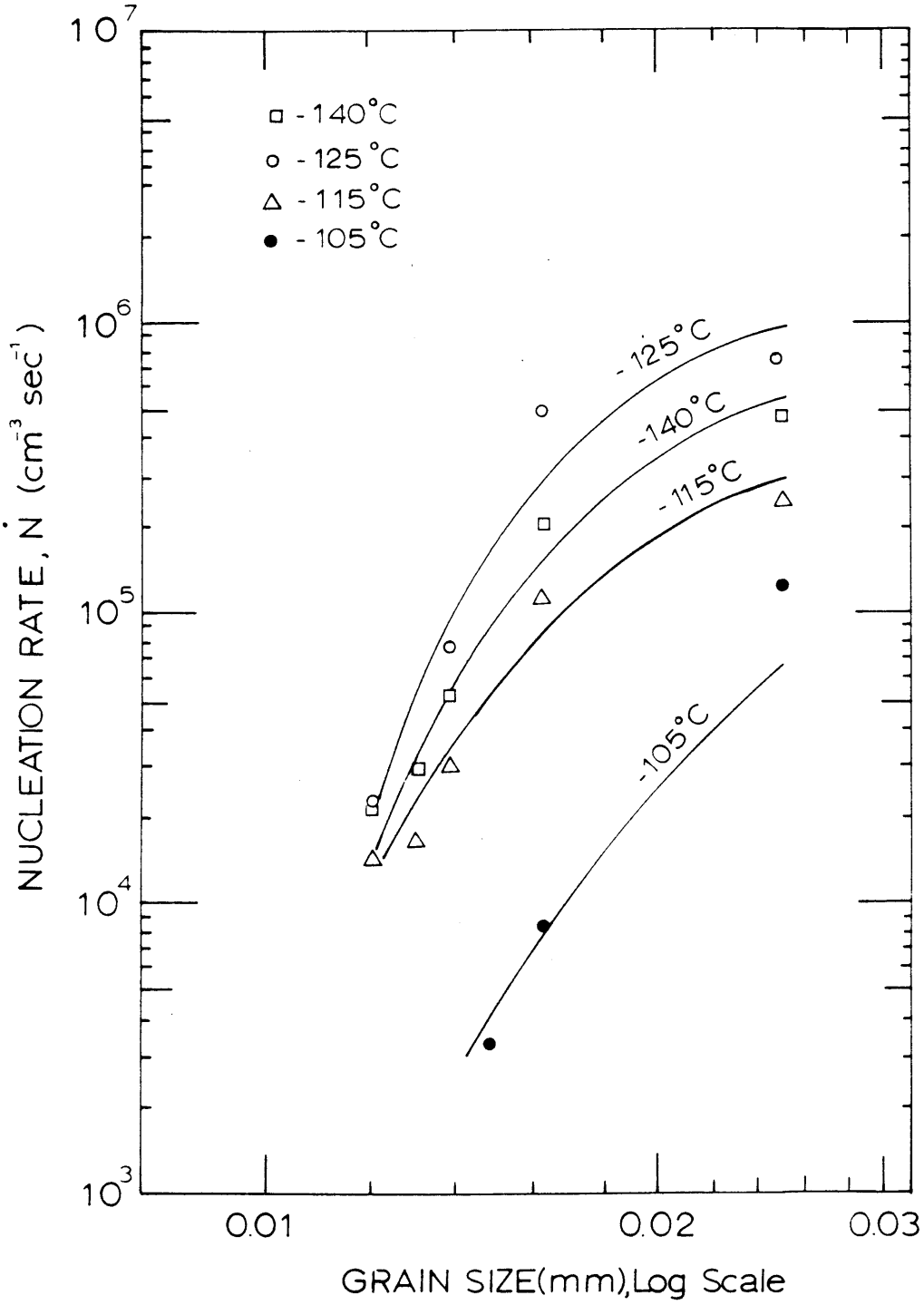

Figure 16. The Initial Nucleation Rate as a Function of Grain Size for the 24Ni3Mn Alloy Reacted at the Indicated Temperatures.

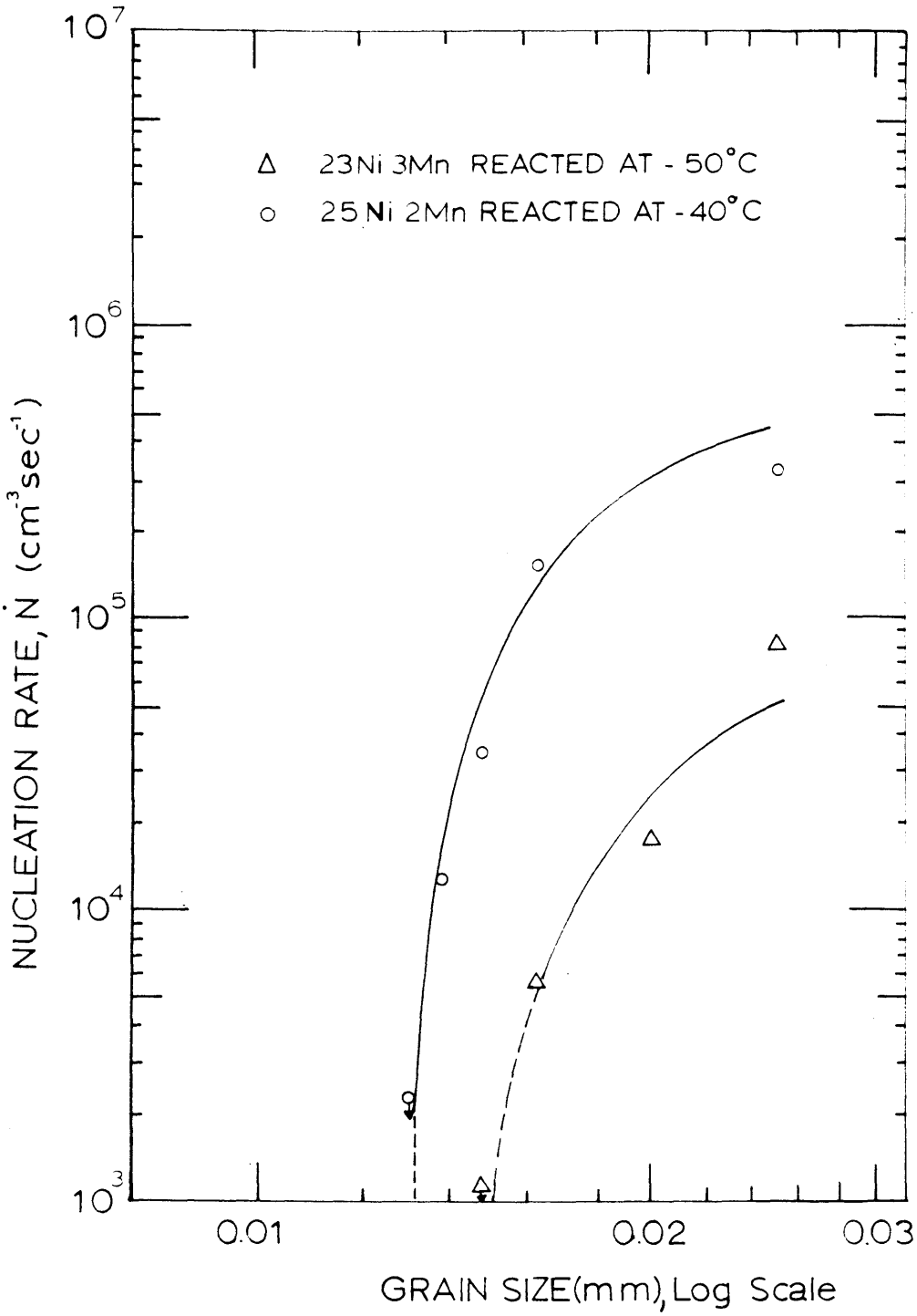

Figure 17. The Initial Nucleation Rate as a Function of Grain Size for 23Ni 3Mn and 25Ni 2Mn Alloys Reacted at the Indicated Temperatures.

transformation within the reacted time as indicated in Fig.15. The 23Ni3Mn alloy showed a much lower nucleation rate at -50°C than the 25Ni2Mn alloy reacted at -40°C.

6.2 Discussion of Results

The decrease of incubation period with increasing grain size shown in Figs. 14 and 15 can be interpreted with the aid of equation (8). Rearranging its terms:

$$\tau_i = \frac{0.002}{\dot{N}\,\bar{v}} \qquad (21)$$

τ_i is thus inversely proportional to the initial nucleation rate and to the average volume of first-formed plates. Fig. 5 indicates that the average volume of the initial martensitic plates increases with increasing grain size, and according to Figs. 16 and 17, the nucleation rate also increases with increasing grain size. Thus, the product $\dot{N}\bar{v}$ increases with increasing grain size, causing the decrease in incubation period.

In the 24Ni3Mn alloy, the shortest incubation period at -125°C (Fig. 14) and correspondingly the highest nucleation rate (Fig. 16) reflect the fact that -125°C corresponds to the nose of a C-curve. The incubation periods and nucleation rates as a function of reaction temperature at all grain sizes follow very closely the form of C-curve kinetics exhibited in Fig. 10.

The 23Ni3Mn alloy undergoes a slower rate of transformation at -50°C than does the 25Ni2Mn alloy at -40°C. This causes a longer incubation period and lower nucleation rate for the former than for the latter. In Section 7.2, it will be shown that these two alloys have the same thermodynamic driving force towards the martensitic transformation, and yet, there is a significant difference in kinetics. This is because of the difference in manganese content of the alloys. Similar results were discussed in Section 5.2; in alloys having comparable nickel contents, slight variations in the manganese content causes drastic changes in reaction kinetics. Further discussion of these effects will be found in Section 7.2.

Upon considering the interpretation of the increase in the nucleation rate at a particular reaction temperature with increasing grain size, it is not intuitatively obvious why $\dot{N}$ should increase with increasing grain size. However, the increase of $\dot{N}$ with increasing grain size is also evident from Fig. 18 where τ_i has been plotted against $(\bar{d})^{-3}$.

If, at a given reaction temperature, $\dot{N}$ would have remained independent of grain size, then from equation (21):

$$\tau_i \propto (\bar{v})^{-1} \qquad (22)$$

Thus a plot of τ_i against $(\bar{v})^{-1}$ should be a straight line.

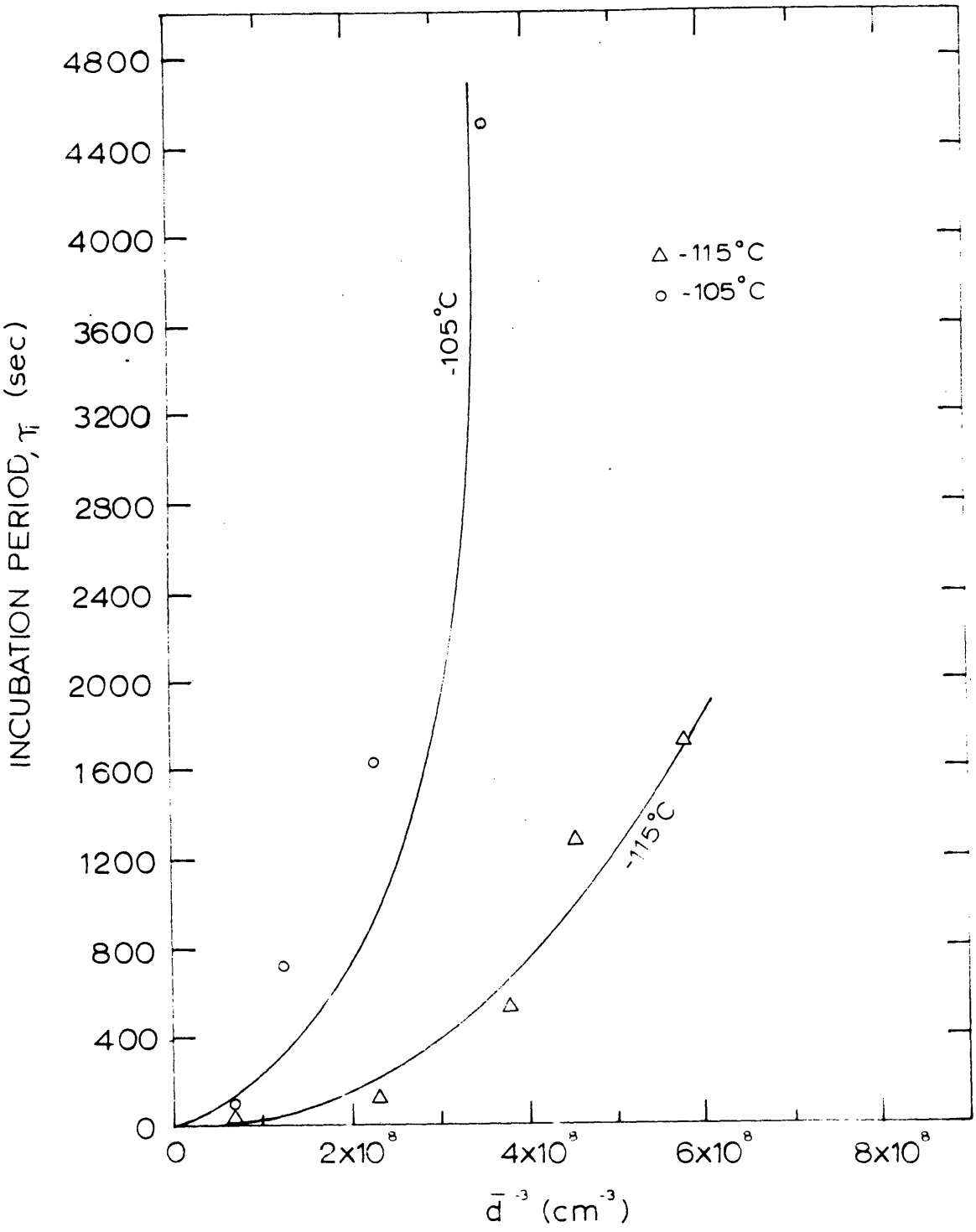

Figure 18. Incubation Period as a Function of $\bar{d}^{-3}$ for the 24Ni 3Mn Alloy Reacted at the Indicated Temperatures.

In Fig. 5 it is seen that, in a small grain size range, the average volume of a martensitic plate, calculated by the assumption that the plate diameter is limited by the austenitic grain or twin boundaries, is proportional to the volume obtained when variations in plate sizes are taken into account. So, within a limited grain size range

$$(\bar{v}) \simeq \alpha \ \bar{d}^{+3} \tag{23}$$

Thus a plot of τ_i against $\bar{d}^{-3}$ should be a straight line passing through the origin if $\dot{N}$ is independent of grain size. But Fig. 18 shows that the actual relationship is non-linear, indicating that $\dot{N}$ is not constant. However, τ_i should really be dependent on $\bar{v}^{-1}$, rather than on $\bar{d}^{-3}$. So to test the relationship of $\dot{N}$ on grain size rigorously, τ_i was plotted against $(\bar{v})^{-1}$ and the results are shown in Fig. 19. Even Fig. 19 shows that $\dot{N}$ is not independent of grain size; on the other hand $\dot{N}$ is increasing with the increase in grain size. In Figs. 18 and 19 only the results of the 24Ni3Mn alloy reacted at -115° and -105°C are shown for clarity. The other data disclose similar trends.

The increase in nucleation rate with increasing grain size can be explained with the help of equation (12), which is written below:

$$0.002 = n_i \ \bar{v} \ \tau_i \ \nu \exp \ (-\Delta W_a/RT) \tag{12}$$

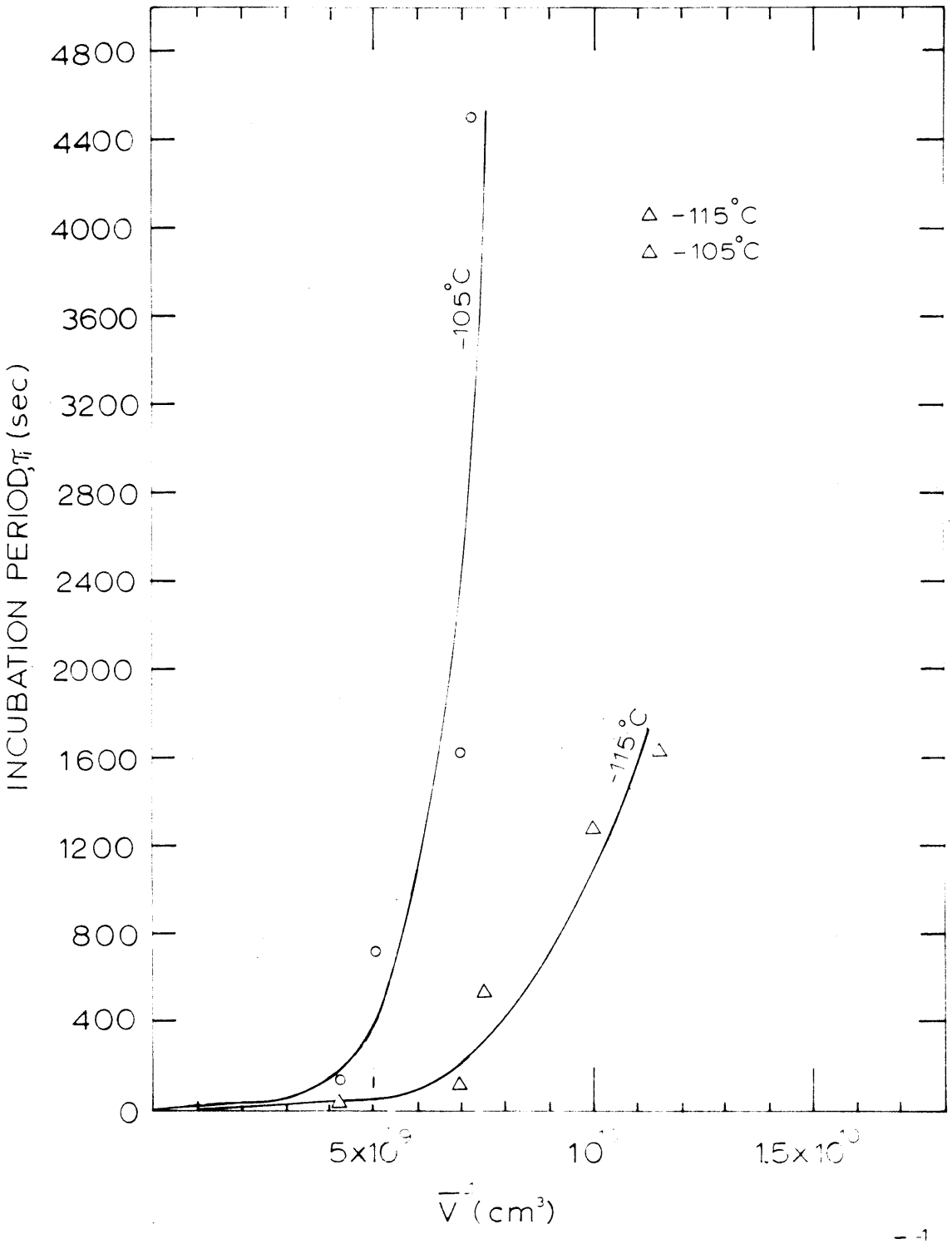

Figure 19. Incubation Period as a Function of $\bar{V}^{-1}$ for the 24Ni 3Mn Alloy Reacted at the Indicated Temperatures.

Then, for a particular alloy and at a particular reaction temperature

$$\tau_i \propto \frac{1}{n_i \bar{v}} \tag{24}$$

It was shown in Section 5.2 that a reasonable value for n_i is 10^7 per cm^3. Now if the grain size is so small that, for the corresponding $\bar{v}$, the number of plates required to form 0.2 percent martensite is equal to or more than n_i, then the incubation period tends to be longer than what is expected from the dependency on volume only because so many of the initial embryos have to be consumed. In Fig. 7, it is seen that the number of plates per unit volume required to form 0.2 percent martensite varies from 2.1×10^7 per cm^3 in specimens of grain size 0.012 mm to 8.4×10^6 per cm^3 in specimens of grain size 0.025 mm. The former number exceeds the initial number of embryos, and the incubation period is correspondingly longer for achieving the required 0.2 percent transformation. Thus, starting with specimens of small grain size, it is natural for the incubation period to decrease with increasing grain size at a rate faster than suggested by the relations $\tau_i \propto \bar{d}^{-3}$ or $\tau_i \propto \bar{v}^{-1}$

The above argument indicates that if the nucleation rate could be determined for a much smaller amount of transformation than 0.2 percent so that only a very small fraction of the

initial number of embryos would have to be activated throughout the grain-size range under investigation, then the nucleation rate might have remained constant as a function of grain size. Unfortunately, it is not possible to detect such small amounts of transformation. However, the true initial nucleation rate can be obtained according to the approach outlined below.

Raghavan and Entwisle[21] have shown that the autocatalytic effect of the martensitic transformation is present even during very early stages of the transformation. This autocatalytic factor can be incorporated into the kinetics in the following way. When a plate of martensite forms, the surrounding austenite is subjected both to elastic and plastic strain. It is assumed that in this stress and plastic strain field, new embryos are produced autocatalytically and that these are available for nucleating further transformation. Raghavan and Entwisle assumed that the number of autocatalytic embryos is proportional to the volume of transformation. This assumption has been validated in the present investigation, and the corresponding results are presented in Section 8.3.

Considering one cubic centimeter of material, at any time t, when the volume fraction of martensite is f, the total number of existing embryos n_t is given by:

$$n_t = (n_i + pf - N_v)\ (1-f) \qquad (25)$$

Where p is the number of autocatalytic embryos produced during the formation of 1 cm^3 of martensite, and N_v is the number of plates required to give the fraction of martensite f, i.e., the number of embryos that have been activated. If it is assumed that all embryos require the same activation energy (as confirmed in Section 8.3) for the formation of martensite plates, then

$$dN_v = n_t \nu \exp(-\Delta W_a/RT)dt \tag{26}$$

$$\text{so that } \dot{N} = \frac{1}{1-f}\frac{dN_v}{dt} = \frac{1}{1-f} n_t \nu \exp(-\Delta W_a/RT) \tag{27}$$

From equation (25):

$$\dot{N} = (n_i + pf - N_v) \nu \exp(-\Delta W_a/RT) \tag{28}$$

The nucleation rate can now be calculated for different grain sizes from equation (28), for a number of plates much smaller than the initial number of embryos. Table IV shows this calculation for the smallest and largest grain sizes at a reaction temperature of -115°C. The numerical value of p has been taken as 2×10^{10} and in Section 8.3 it is shown that this value of p best matches the calculated fraction transformed versus time curve (f-t) with the experimental transformation curve at -115°C. The value of p was found to remain constant at a given reaction temperature for different

TABLE IV

Calculation of Nucleation Rate as a Function of Number of Plates Formed in 24Ni3Mn Alloy for a Reaction Temperature of -115°C, Taking into Account Autocatalysis

Grain Size of 0.012 mm			Number of Plates Formed, N_V	Grain Size of 0.025 mm			Ratio of $\dot{N}$ of Grain Size of 0.025 mm to that of 0.012mm
f	n_t	$\dot{N}$		f	n_t	$\dot{N}$	
	cm^{-3}	$cm^{-3}sec^{-1}$	cm^{-3}		cm^{-3}	$cm^{-3}sec^{-1}$	
8.70×10^{-8}	1.00×10^{7}	2.46×10^{5}	10^{3}	2.35×10^{-7}	1.00×10^{7}	2.46×10^{5}	1.00
4.35×10^{-7}	1.00×10^{7}	2.46×10^{5}	5×10^{3}	1.17×10^{-6}	1.00×10^{7}	2.46×10^{5}	1.00
8.70×10^{-7}	1.00×10^{7}	2.46×10^{5}	10^{4}	2.35×10^{-6}	1.00×10^{7}	2.47×10^{5}	1.00
4.35×10^{-6}	1.00×10^{7}	2.47×10^{5}	5×10^{4}	1.17×10^{-5}	1.02×10^{7}	2.50×10^{5}	1.01
8.70×10^{-6}	1.00×10^{7}	2.47×10^{5}	10^{5}	2.35×10^{-5}	1.04×10^{7}	2.55×10^{5}	1.03
4.35×10^{-5}	1.04×10^{7}	2.55×10^{5}	5×10^{5}	1.17×10^{-4}	1.18×10^{7}	2.91×10^{5}	1.14
8.70×10^{-5}	1.07×10^{7}	2.64×10^{5}	10^{6}	2.35×10^{-4}	1.37×10^{7}	3.36×10^{5}	1.28
4.35×10^{-4}	1.37×10^{7}	3.37×10^{5}	5×10^{6}	1.17×10^{-3}	2.85×10^{7}	7.00×10^{5}	2.08
8.70×10^{-4}	1.74×10^{7}	4.27×10^{5}	10^{7}	2.35×10^{-3}	4.70×10^{7}	1.15×10^{6}	2.70
2.61×10^{-3}	3.22×10^{7}	7.91×10^{5}	3×10^{7}	7.05×10^{-3}	1.21×10^{8}	2.97×10^{6}	3.76

grain sizes by Raghavan and Entisle. ΔW_a was taken as 10,600 cal/mole for the transformation temperature of -115°C (Table II). To get n_t and $\dot{N}$ as a function of N_v it is also necessary to know f for the corresponding N_v. This relationship is a simple one, if $\bar{v}$ can be used as already determined at f = 0.002:

$$f = N_v \bar{v} \tag{29}$$

Since $\bar{v}$ has been evaluated as a function of grain size (Fig. 5), f can be calculated as a function of N_v for both grain sizes. The calculations are summarized in Table IV. The last column in Table IV shows the ratio of nucleation rates for these two grain sizes at various values of N_v.

It is seen from these calculations that, for a small number of plates formed, (up to 10^5 per cm^3), the volume fraction of martensite formed in specimens of either grain size is too small to create an appreciable number of autocatalytic embryos, thereby maintaining n_t almost equal to n_i. Then, $\dot{N}$ is almost the same in either grain size. However, for any given N_v greater than 10^5, the nucleation rate for the 0.025 mm grain size tends to be higher than for the 0.012 mm grain size because the volume fraction of martensite formed at the larger grain size is large enough to create an appreciable number of autocatalytic embryos and hence increase the nucleation rate. This deviation is not large until about

5×10^6 plates are formed per unit volume, beyond which the ratio of nucleation rates between the two grain sizes (last column in Table IV) deviates from unity.

In Table III, it is evident that the incubation period decreases with increasing grain size. Fig. 20 is a plot of the incubation periods against the corresponding grain sizes. The vertical line at each grain size level indicates the range of values of τ_i exhibited by 4 to 6 different specimens as listed in the Table III. The circles represent the mean values of the incubation times. It is obvious that the deviation from the straight-line relationship of τ_i versus $\bar{d}^{-3}$ is much less here, compared to the series where the grain size was varied by changing the austenitizing temperature. This is due to larger grain sizes obtained in specimens of Table III than what was obtained in specimens whose grain size was varied by changing the austenitizing temperature. Still, the range of τ_i values tends to fall below the straight line in the small grain-size range, and above the straight line in large grain-size range, because the number of activated embryos required to form 0.2 percent martensite is not small enough to maintain a constant nucleation rate. The actual number of embryos required to form 0.2 percent martensite in specimens of this series can be obtained from Fig. 5, and this is found to vary from 1.25×10^7 for the smallest grain size to 6.5×10^6 for the largest. These numbers are not in the

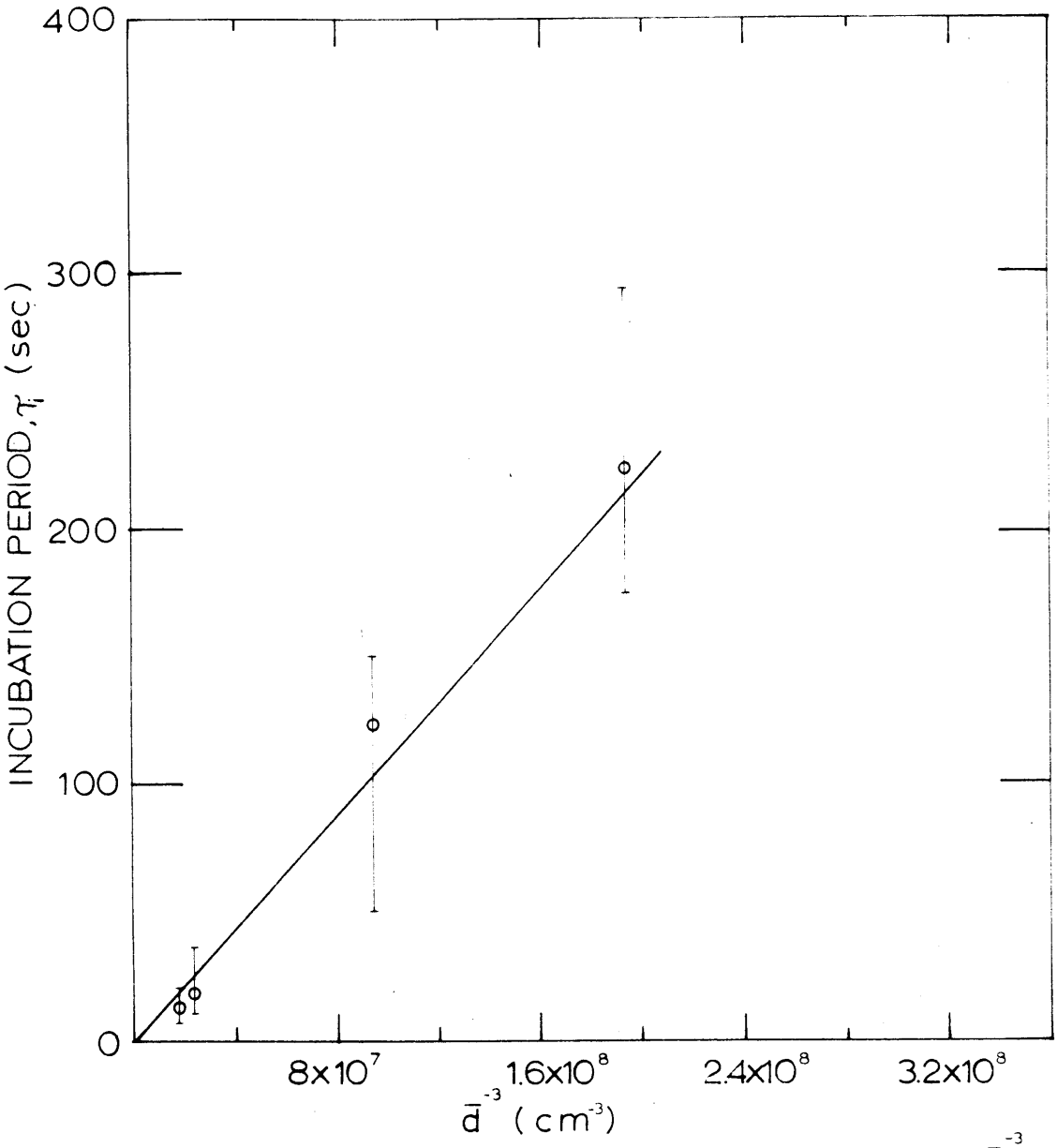

Figure 20. Incubation Period as a Function of $\bar{d}^{-3}$ for the 25Ni 2MnA Alloy Reacted at -20°C.

low range where a constant nucleation rate would prevail, and hence the observed deviation.

Incubation period determinations were also carried out in specimens with two step austenitizing treatments, and the results were compared with one-step austenitizing treatments. This is discussed below.

One specimen was austenitized at 900°C, cooled to room temperature, reaustenitized at 750°C, cooled to room temperature, and then transformed at -125°C. Another specimen was austenitized at 900°C, cooled to room temperature, and then transformed at -125°C. Both the specimens had the same grain size and showed the same incubation period, which was much shorter than the incubation periods of specimens austenitized at 750°C. Similar results were obtained at other reaction temperatures. This as well as the discussion presented before indicate that the different austenitizing treatments have no effect on the embryo distribution.

From the preceding discussion, it can be concluded that the true initial nucleation rate (not the apparent initial nucleation rate at f = 0.002) remains independent of the grain size. However, the apparent nucleation rate increases as a

function of grain size, especially in low grain-size range, because the number of plates required to form a detectable amount of martensite increases with decreasing $\bar{v}$ and hence grain size. Thus, the effect of grain size on the incubation period arises merely due to the size of the first-formed plates.

An important insight can be gained from the above discussion about the effect of the grain boundaries on the nucleation of the martensitic transformation. Since the initial nucleation rate and n_i are independent of the grain size, the indications are that the grain boundaries do not act as prefered nucleation sites. This means that the number of most-potent embryos are distributed rather uniformly throughout the matrix. If grain boundaries were important, as preferred nucleation sites, then n_i should depend inversely on $\bar{d}$:

$$\dot{N} \propto \frac{1}{\bar{d}} \tag{30}$$

The reported results are completely different from this relationship and support the contention that grain boundaries do not predominate as preferred nucleation sites.

7. THERMODYNAMIC CALCULATIONS ON MARTENSITIC TRANSFORMATIONS

7.1 Introduction

The free-energy change accompanying the martensitic transformation in iron-nickel alloys was derived by Kaufman and Cohen[27]. Recently Imai and Izumiyama[28] have calculated the change in free energy accompanying the martensitic transformation in iron-manganese alloys by a method similar to that of Kaufman and Cohen. Combining the above two investigations, the change in free energy accompanying the martensitic transformation in iron-nickel manganese alloys can be calculated as follows:

$$\begin{aligned} -\Delta F^{\gamma\rightarrow\alpha} &= (1-x-y)(1202-2.63\times10^{-3}T^2+1.54\times10^{-6}T^3) \\ &\quad +y(-2390-2.723T+2.893\times10^{-6}T^3) \\ &\quad +x(-3700+7.09\times10^{-4}T^2+3.91\times10^{-7}T^3) \\ &\quad +y(1-x-y)[-889-0.192+x(1-\ell nT)] \\ &\quad +x(1-x-y)[3600+0.58T(1-\ell nT)] \text{ cal/mole.} \end{aligned} \qquad (31)$$

where α and γ refer to body-centered cubic ferrite and face-centered cubic austenite solid solutions respectively. x and y are the atomic fractions of nickel and manganese respectively and T is the absolute temperature in °K.

Having, thus obtained an expression for the free-energy change accompanying the martensitic transformation in ternary alloys, it is possible to find out what percentage of nickel is thermodynamically equivalent to 1 percent manganese, since this information often becomes necessary for comparing the transformation kinetics of iron-nickel-manganese alloys having different nickel and manganese contents.

In addition, one can then calculate the activation energy for isothermal martensitic transformation in ternary alloys using equation (11), and these theoretical values can be compared with the experimental quantities obtained in the present investigation.

7.2 The Free-Energy Change and Kinetics of Nucleation

Fig. 21 shows $\Delta F^{\gamma \rightarrow \alpha}$ versus temperature curves for the alloys under investigation as well as the 23.2 percent nickel-3.62 percent manganese alloy of Shih et al.[16]. This shows that $\Delta F^{\gamma \rightarrow \alpha}$ of the 24Ni3Mn alloy is the same as for the alloy of Shih et al. Similarly the 23Ni3Mn and 25Ni2Mn alloys have the same values of $\Delta F^{\gamma \rightarrow \alpha}$.

It was reported in Section 5.1 that the temperature for maximum nucleation rate (temperature corresponding to the nose of the C-curve) was 15°C higher in the 24Ni3Mn alloy than the alloy of

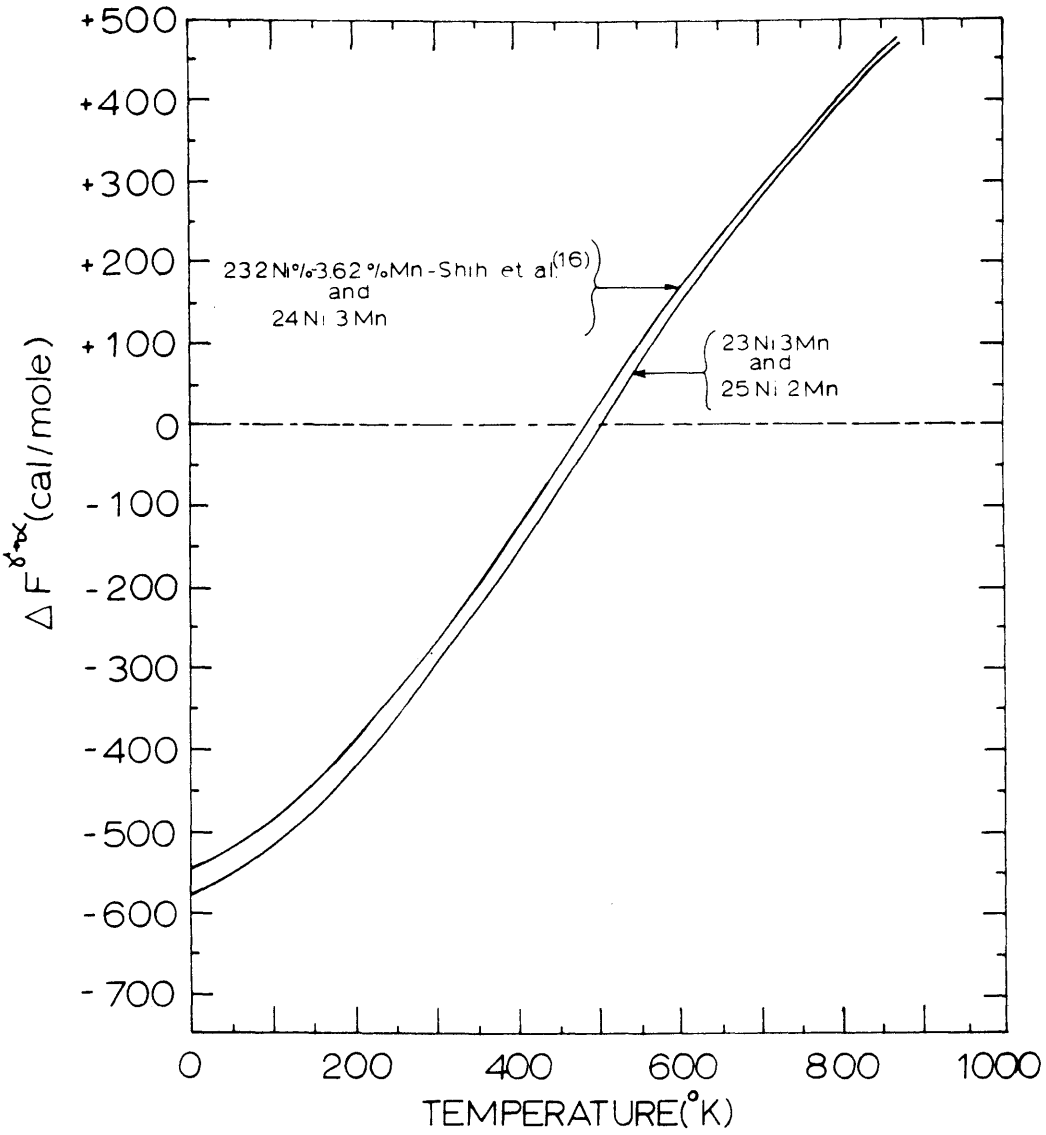

Figure 21. The Change in Free Energy Accompanying Martensitic Transformation in Iron-Nickel-Manganese Alloys as a Function of Temperature from Equation (31).

Shih et al. Moreover, at all reaction temperatures, the alloy of Shih et al. exhibited longer incubation periods and lower nucleation rates than did the 24Ni3Mn alloy. In addition, the 23Ni3Mn alloy at -50°C showed a slower transformation rate than the 25Ni2Mn alloy at -40°C (Fig. 17) despite the higher driving force ($|\Delta F^{\gamma \rightarrow \alpha}|$) for the transformation in the former alloy at -50°C.

It was noted that all of these alloys exhibit a completely isothermal mode of transformation within the temperature range of investigation so that the differences in kinetics cannot be interpreted in terms of thermal versus athermal changes. The transformation does not become athermal unless the manganese is substantially replaced by nickel.[30] Thus, all these results are in agreement with the finding of Shih et al. that alloys of nearly equal driving force can exhibit marked differences in kinetic behavior due to slight differences in their manganese contents.

Slight variations in the carbon content of the specimens were also found to cause wide changes in the reaction rate. This was noted when the specimens were austenitized at temperatures of 950°C and higher (Appendix A). For example, a specimen austenitized at 1050°C for 1 hour with as-received nickel leads, and then transformed at -70°C, showed an incubation period of 50 min. Another specimen, given the same austenitizing treatment with decarburized nickel leads, and

then transformed at -70°C, showed an incubation period of only 0.3 min. The specimen austenitized with the as-received nickel leads picked up only about 0.010 percent carbon from the leads by diffusion through the atmosphere of the tube; this difference in carbon content does not have any appreciable effect on the driving force for the transformation.*

Consequently, these results suggest that carbon and manganese play a much more pronounced role in decreasing the potency of embryos than can be expected from driving-force considerations alone.

From the equality of $\Delta F^{\gamma \rightarrow \alpha}$ values for the alloys of varying nickel and manganese contents reported in Fig. 21, the thermodynamic equivalency between manganese and nickel can be easily computed. The result is:

1 atomic percent manganese ≡ 1.6 atomic percent nickel

This thermodynamic equivalency between nickel and manganese can be used to ascertain the compositions of binary alloys of iron-nickel having the same driving force as those of iron-nickel-manganese alloys. Fig. 22 is such an example,

---

* From the derivation given by Bell and Owen[29] it can be shown that driving force is changed only by 5 cal/mole due to an increment of 0.010 percent carbon, which is much too small to account for the observed change in the rate of transformation.

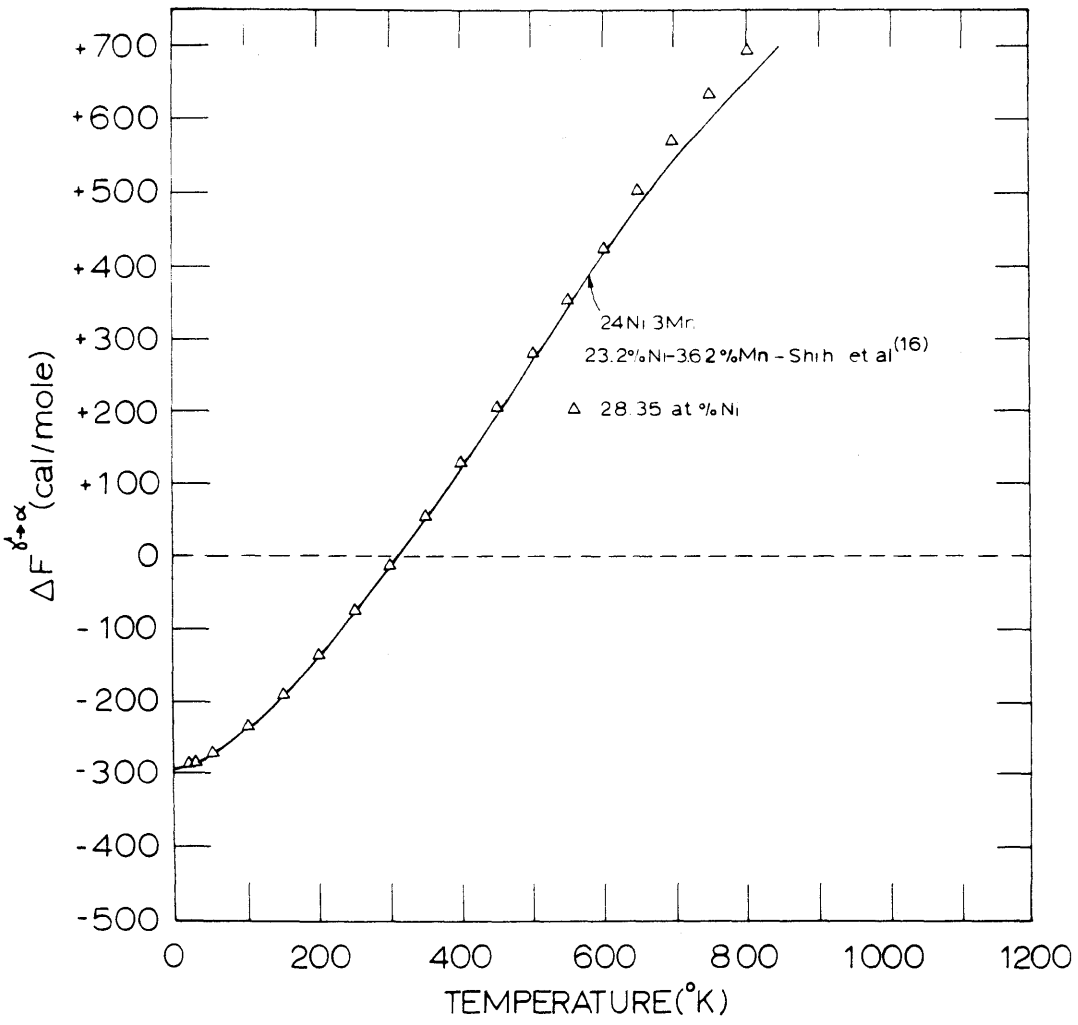

Figure 22. The Free Energy Change Accompanying the Martensitic Transformation in Iron-Nickel-Manganese and Iron-Nickel Alloys as a Function of Temperature from Equation (31).

where it can be seen that, in the temperature range of martensitic transformation, the 24Ni3Mn and 23.2 percent nickel - 3.62 percent manganese (alloy of Shih et al.) alloys have the same driving force ($\Delta F^{\gamma \rightarrow \alpha}$) as does an iron - 28.35 atomic percent nickel alloy. However, when manganese is completely replaced by nickel a wide change in the kinetic behavior is observed, even though the thermodynamic equivalency of 1 atomic percent manganese ≡ 1.6 atomic percent nickel is maintained. For example the 24Ni3Mn and 23.2 percent nickel - 3.62 percent manganese alloys show a completely isothermal mode of transformation at least down to liquid nitrogen temperature without any athermal martensite being present, whereas a thermodynamically equivalent iron - 28.35 atomic percent nickel alloy has an athermal M_s temperature around -2 to -3°C[27]. The cause of this vast change in kinetics when manganese is completely replaced by nickel is the change in the mode of transformation from isothermal to a burst transformation. It has recently been reported by Brook and Entwisle[30] that nickel is particularly effective in promoting transformation on $\{259\}_\gamma$. On the other hand, manganese favors transformation on $\{225\}_\gamma$ and they suggested that burst transformation does not occur in this habit plane because of greater restrictions imposed on plate growth. In addition, $\{259\}_\gamma$ habit plane favors a cooperative mechanism of martensite formation compared with the $\{225\}_\gamma$. Consequently manganese tends to favor the isothermal mode when it is added to iron-nickel alloys.

The driving force corresponding to the isothermal martensitic transformation in the alloys under study can be obtained from Fig. 21. In the 24Ni3Mn alloy the driving force varies from 505 cal/mode at -196°C to 380 cal/mode at -70°C. In the 23Ni3Mn and 25Ni2Mn alloys, it varies from 395 cal/mode at -50°C to 355 cal/mode at -20°C. These values compare very well with those found by Imai and Izumiyama[28] for a number of iron-nickel-chromium and iron-nickel-manganese alloys.

7.3 Activation Energy

The activation energy for the isothermal martensitic transformation ΔW_e^{ℓ} based on the Kaufman and Cohen[1] model was calculated from equation (11) for different sizes of of the most-potent embryos, r_e, keeping the value of σ within acceptable limits[14,17] and the value of A constant at 2.1×10^{10} dynes/cm^2. This value was obtained independently by Fisher et al.[14] and Knapp and Dehlinger[17] despite quite different methods of approach. Excellent agreement between the theoretical (ΔW_e^{ℓ}) and experimental (ΔW_a) activation energies was obtained for r_e = 188A° when σ = 120 ergs/cm^2 and A = 2.1×10^{10} dynes/cm^2 . The results for the 24Ni3Mn alloy are given in Fig. 23. Only the results for 24Ni3Mn alloy are presented since the activation energies could be measured over a wider range of temperature in this alloy than in the others. The temperature dependence as well as the magnitude of ΔW_e^{ℓ} is almost identical with that of ΔW_a.

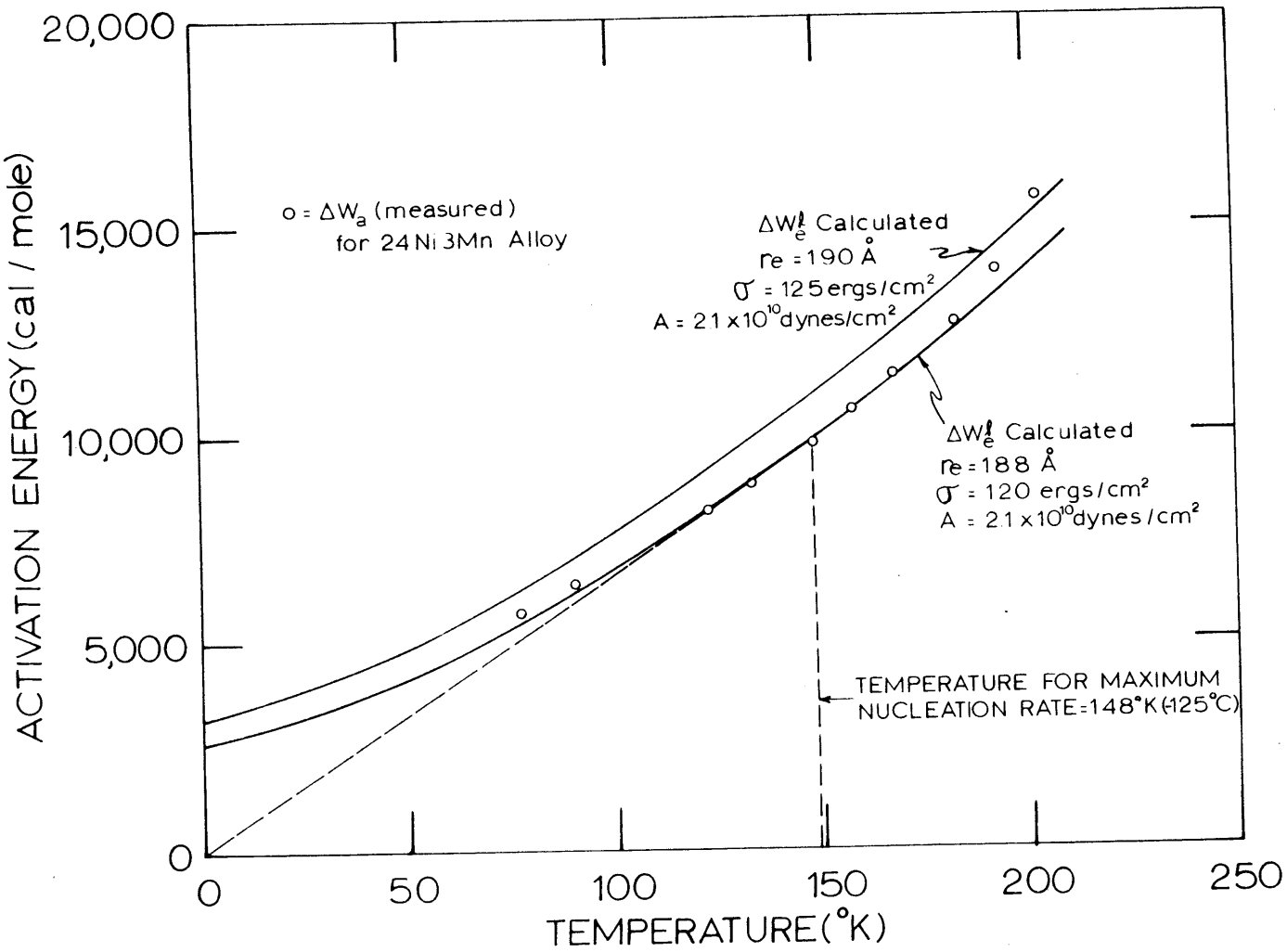

Figure 23. Calculated and Measured Values of Activation Energy as a Function of Temperature for Isothermal Nucleation of Martensite in 24 Ni 3Mn Alloy

The temperature for the maximum nucleation rate, given by the temperature at which $\Delta W_e^{\ell}/T = d\Delta W_e^{\ell}/dT$, also corresponds exactly to the experimentally determined temperature of -125°C. In Fig. 23, ΔW_e^{ℓ} calculated for r_e = 190A°, taking σ = 125 ergs/cm^2 and the A same as before, is also shown to indicate the dependency of ΔW_e^{ℓ} on the pertinent parameters.

Calculation of ΔW_e^{ℓ} for the 23.2 percent nickel - 3.62 percent manganese alloy of Shih et al.[16] was also undertaken because it became possible to compare more realistically the theoretical and measured values of activation energies, since the driving force could now be computed for the ternary alloy system. The results are given in Fig. 24. Very close agreement was obtained for r_e = 195A° and σ = 125 ergs/cm^2. The temperature of maximum nucleation rate also coincides very well with their experimentally observed temperature of -140°C. These values of r_e and σ differ somewhat from the values (r_e = 180A°, σ = 160 ergs/cm^2) obtained by Kaufman and Cohen[1] because these authors had to assume that the iron-nickel-manganese alloy of Shih et al. was equivalent in composition to an iron -25 atomic percent nickel alloy for calculating $\Delta F^{\gamma\rightarrow\alpha}$. It has been shown in Section 7.2 (Fig. 22) that the $\Delta F^{\gamma\rightarrow\alpha}$ value for the alloy of Shih et al. is actually equivalent to an iron - 28.35 atomic percent nickel alloy. To compensate for this discrepancy, σ had to be increased in the Kaufman-Cohen treatment to match the calculated values of ΔW_e^{ℓ} with the experimental values of ΔW_a.

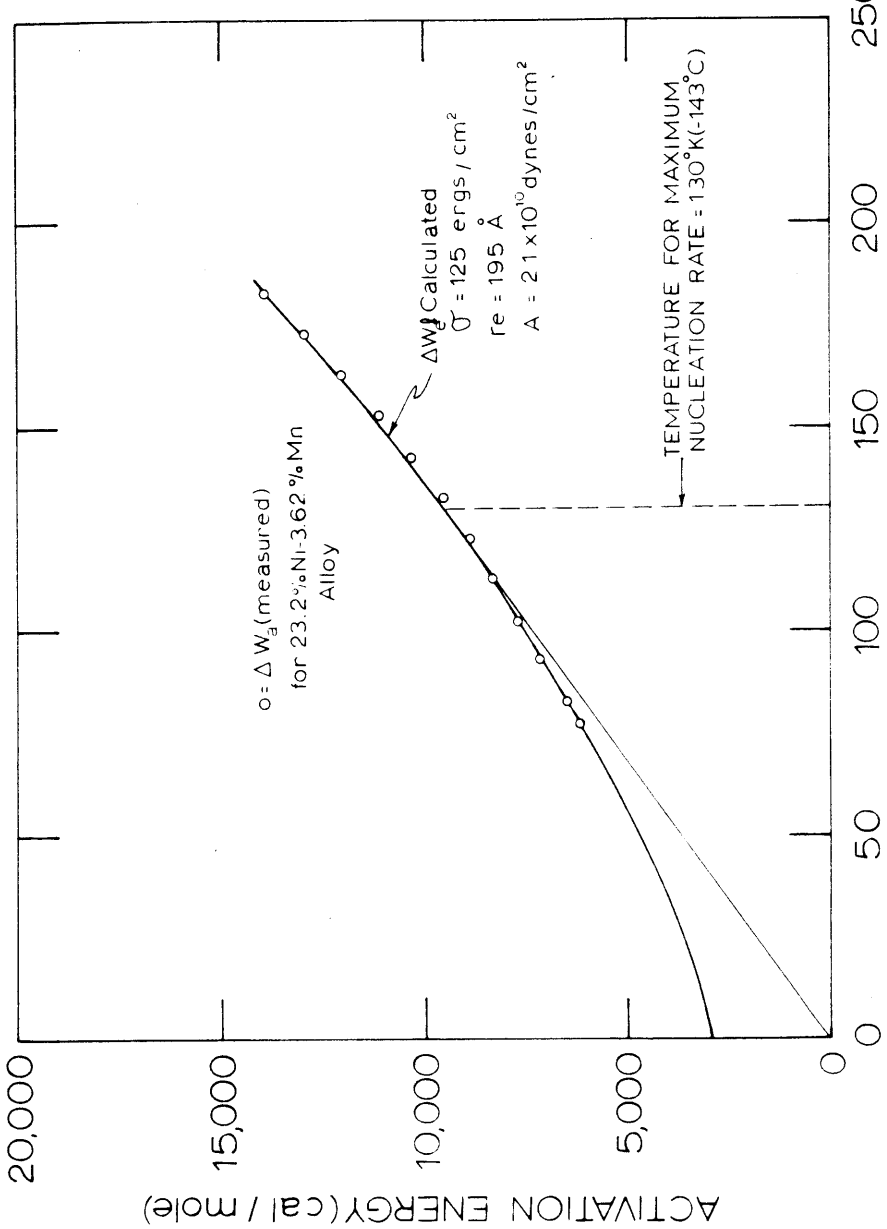

Figure 24. Calculated and Measured Values of Activation Energy as a Function of Temperature for Isothermal Nucleation of Martensite in 23.2%Ni-3.62%Mn Alloy of Shih et al.[16]

Additional support for this interpretation of the results comes from the data shown in Fig. 25. In this Fig. the activation energy values of isothermal martensite transformations reported by several investigators[16,20] have been plotted against th corresponding $\Delta F^{\gamma \to \alpha}$ values. According to the model, ΔW_a should be linearly dependent on $\Delta F^{\gamma \to \alpha}$ if r_e remains constant, and this is found to be the case. The points may be also considered to fall within a narrow band; in that case, the values of r_e and σ, calculated from the measured slopes and intercepts, are found to lie in the following ranges:

$$\sigma = 120 - 130 \text{ ergs/cm}^2; \; r_e = 180 - 200\text{A}^\circ$$

A similar plot was attempted before by Entwisel[20], however, the $\Delta F^{\gamma \to \alpha}$ values were then not known for the iron-nickel-manganese alloys. Also the magnitude of n_i was uncertain. From the range of r_e obtained from Fig. 25, it is evident that in iron-nickel-manganese alloys exhibiting a completely isothermal mode of transformation, the potency of the embryos is almost constant or lies within a narrow range. This concept can explain some important experimental observations which are discussed in the next two sections.

7.4 The Absence of Athermal Martensitic Transformation Below the Temperature Range of Isothermal Transformation

Entwisle[20] found that 22.42 percent nickel - 3.57 percent manganese and 23.30 percent nickel - 3.84 percent

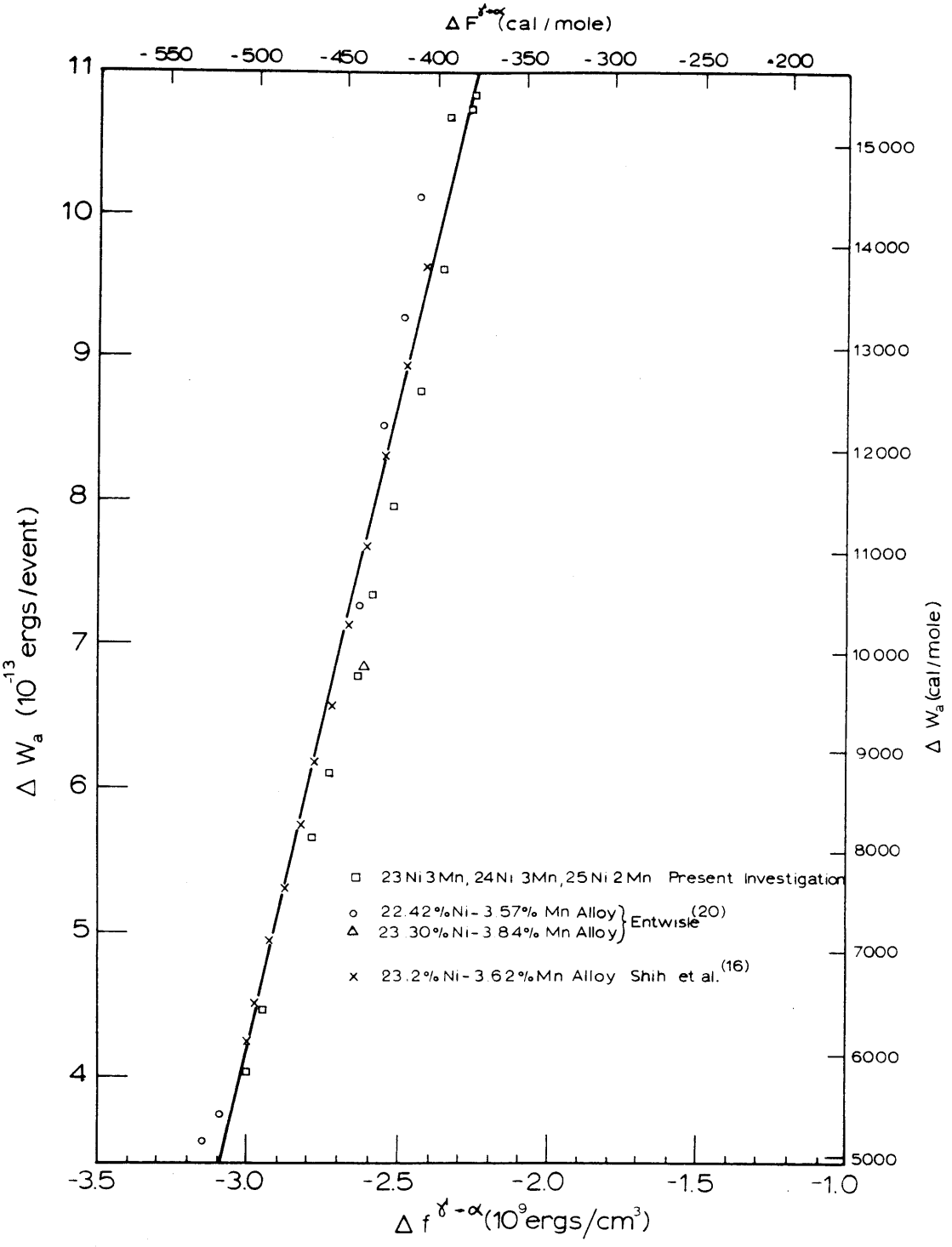

Figure 25. Measured Activation Energy for the Isothermal Martensitic Transformation in Iron-Nickel-Manganese Alloys as a Function of the Free Energy Change Accompanying the Transformation.

manganese alloys did not show any transformation when quenched and isothermally treated in liquid helium (4°K), whereas these alloys transformed isothermally in the temperature range of -196° to -78°C. Therefore, he concluded that there cannot be any athermal martensitic transformation below the range of temperature in which isothermal transformation occurs. This finding can be explained by the following considerations.

The time for 0.2 percent transformation τ_i is related to $\mathring{N}$ and $\bar{v}$ by the expression:

$$0.002 = \mathring{N}\bar{v}\tau_i \tag{8}$$

Using the value of $\bar{v}$ for 0.025 mm grain size from Fig. 5, rearranging the terms of above equation and taking logarithms of both sides:

$$\text{Log } \mathring{N}^{-1} = -6.93 + \text{Log } \tau_i \tag{32}$$

Taking logarithims of both sides of equation (9) (p. 16), and substituting numerical values of $n_i = 10^7$, and $\nu = 10^{13}$,

$$\text{Log } \mathring{N} = 20 - \frac{\Delta W_a}{4.576T} \tag{33}$$

Adding equations (32) and (33) and rearranging the terms,

$$\text{Log } \tau_i = \frac{\Delta W_a}{4.576T} - 13.07 \tag{34}$$

Now ΔW_a can be substituted by ΔW_e^{ℓ}, and this can be calculated for different values of r_e, using equation (11). Thus, the

time for 0.2 percent transformation can be obtained as a function of temperature for embryos of different radii present in an alloy. The results are given in Fig. 26 for the 24Ni3Mn alloy taking σ = 125 ergs/cm^2 and A = 2.1 x 10^{10} dynes/cm^2. The values of r_e used in the calculations are indicated for each curve. Similar calculations were made by Kaufman[31] for iron - 25 atomic percent nickel and iron - 30 atomic percent nickel alloys. However, he took σ = 160 ergs/cm^2 for the reason discussed before. It can be seen from Fig. 26 that, if the alloy contains embryos of radii no greater than about 210Å, it would exhibit isothermal transformation over a wide range of temperature but would not transform athermally even on quenching to liquid helium. If only embryos of much lower potency are present, the alloy would not show any isothermal transformation in a reasonable time at any temperature. If, on the other hand, embryos of higher potency (greater than 225A°) are present, the alloy would show athermal transformation, and the M_s temperature will be governed by the most-potent embryos.

7.5 Attempts at Direct Observation of Embryos

The discussion in the preceding paragraphs also illuminates the problem of the direct observation of embryos in thin foils of austenite by transmission electron microscopy. According to the foregoing calculations, the embryos should be large enough to detect. However, despite painstaking

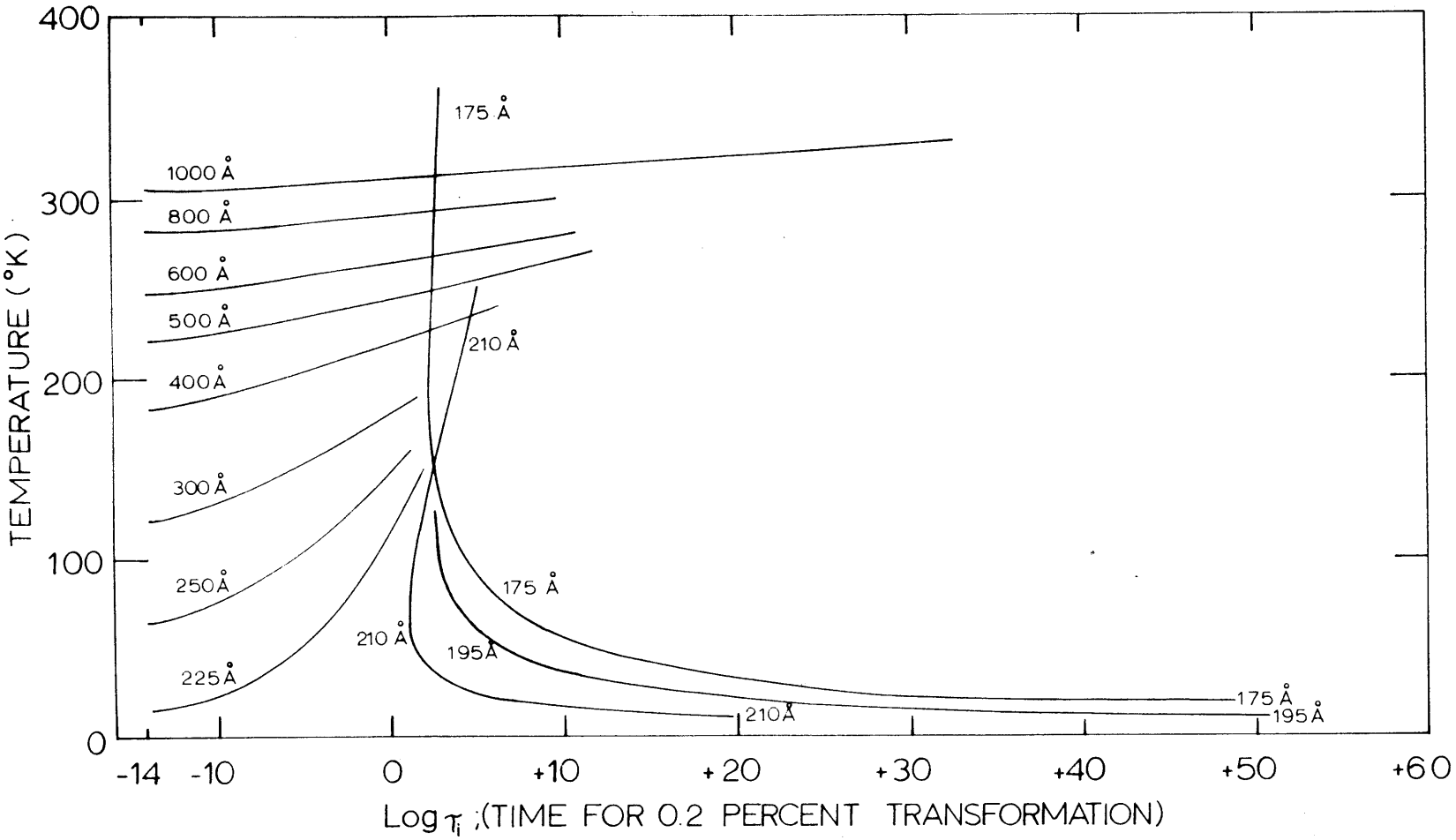

Figure 26. Calculated Time for 0.2 Percent Transformation as a Function of Reaction Temperature for Indicated Embryo Radii in 24 Ni 3Mn Alloy.

observations on a number of foils, it was not possible to identify any structural defect which could act as an embryo. Earlier attempts [32,33,34] along this line have also failed to reveal the martensitic embryos.

The failure to observe the martensitic embryos can be rationalized as follows. It has been shown before that a reasonable value for the density of pre-existing embryos is only 10^7 per cm^3 and it has been shown in Sections 7.3 and 7.4 that their radius should be about 180 - 200A°. Both these factors lead to a vanishingly small probability of observing such embryos in thin foils of austenite. This can be shown by the following order of magnitude calculation. If it is assumed that, to detect reliably an embryo of the aforementioned size ($\sim$ 200A°) in the image of an observed area of thin foil of austenite, the magnified embryo diameter should be around 0.2 cm, then a magnification of about 50,000x has to be used. This limits the area of the thin foil of austenite under observation to around $(2\text{-}3) \times 10^{-8}$ cm^2, depending on the size of electron microscope. Taking the average thickness of thin foil as 2000A°, the volume of the foil under examination is $(4\text{-}6) \times 10^{-13}$ cm^3. Since there are only 10^7 initial potent embryos per cm^3 of the foil within the volume under observation, the probability of finding an embryo is only $(4\text{-}6) \times 10^{-6}$. This shows that one will have to observe approximately 10^5 or 10^5 different areas of a thin

foil of austenite to detect one embryo. Even if one could happen to see an embryo in this extensive search, it would not be a reproducible observation and hence would in all probability miss attention.

In the above approximation, it has been assumed that to detect an embryo its magnified diameter should be around 0.2 cm in the image. Even if this size requirement is lowered to only 0.1 mm (resolution of human eye), the probability of finding an embryo in a particular area of the thin foil would still only be about 2 in a 1000 fields of observation. This analysis clearly shows that the direct observation of an embryo is very unlikely.

It should also be mentioned that studies of the dislocation structure in the deformed austenite surrounding martensitic plates, as well as in austenite with 3-5 percent tensile strain, did not reveal any extended dislocation nodes. This indicates that the stacking fault energy in the iron-nickel-manganese alloys under investigation was at least 50 ergs/cm^2; therefore, stacking faults are not likely to act as preferred nucleation sites for martensitic (b.c.c.) transformation in the iron-nickel-manganese alloys under investigation.

In connection with the transmission electron microscopy of austenite the fine structure of isothermally formed martensite was also investigated. Since these results have no bearing on the kinetics, no detailed investigation was

undertaken in this direction. However, typical results are given in Appendix B.

8. PROGRESS OF THE ISOTHERMAL MARTENSITIC TRANSFORMATION

The foregoing sections were concerned only with the early stages of transformation. In this section, an attempt is made to explain quantitatively the progress of the transformation and the shape of the isothermal transformation curve.

8.1 The Nature of the Transformation Curve

The nature of the isothermal transformation curve was first established by Shih et al.[16]. The isothermal transformation curve starts at a slow rate, then the rate increases rapidly with time and is nearly linear for a certain period, following which it begins to decrease.

The increase in the initial transformation rate with time can be accounted for in at least two ways:

(1) an autocatalytic effect in which the first-formed plates produce more embryos which increase the rate of subsequent transformation, or

(2) the slow growth of the martensitic plates over a considerable period of time.

The second alternative has recently been suggested by Magee[35] wherein he considered the propagation of the embryo interface to be the critical condition for the formation of martensitic plates. The resistance to the motion of the

interface was taken into account by Magee,[35] and it was shown that the net stress on the interface increases as the plate grows in size. This circumstance increases the velocity of propagation and was thought to explain the increasing rate of transformation in the isothermal transformation curve. However, the experimental evidence noted below does not support this description.

Bunshah and Mehl[5], Das Gupta and Lement[6] Machlin and Cohen[9] and Cech and Hollomon[10] have reported that isothermal transformation progresses mainly due to the formation of new plates, rather than to the progressive growth of the existing plates. In the present investigation as well, this finding has been verified experimentally (Section 8.3). Bunshah and Mehl[5] found that a martensitic plate grows to full size in about 10^{-7} seconds. Cech and Hollomon[10] noted that it takes less than $\frac{1}{24}$ second for the full growth of a martensitic plate. Recently, Yeo[36] has reported slow growth of martensitic plates in an iron - 28.8 percent nickel - 0.008 percent carbon alloy during isothermal martensitic transformation at room temperature. The martensitic plates grew to full size within about 1 second, but this (gradual growth) was later[37] found to be confined to surface martensite.

Magee[35] relied on the experimental findings of slow growth rates to support his contention that propagation of

the embryo interface is the rate-controlling factor. However, Raghavan[22] has correctly pointed out that, as long as the time of formation of a plate of full size is of the order of 1 second (the slowest reported growth rate) or much less (as reported by many others), a treatment of the progress of the transformation which is concerned with the shape of the transformation curves extending over several minutes or hours has no need to take the growth factor into account. Thus, the autocatalytic effect, whose existence is well established, is utilized here for the interpretation of the transformation curve.

A simple explanation for the decrease in the rate of transformation in the later stages is the partitioning of austenite into smaller and smaller pockets as the transformation progresses. Since the martensitic plate sizes are limited by the size of these pockets, the volume contribution per plate decreases as the transformation proceeds and causes a falling-off in the transformation rate. According to Magee's treatment, the decreasing transformation rate arises due to the velocity of interface being limited by the velocity of sound in the material. This argument is not supported by the experimental observations reported in the preceeding paragraph. So, partitioning of the austenite will be considered here to be responsible for decreasing the transformation rate.

8.2 Calculation of Fraction Transformed as a Function of Time, Taking into Account Partitioning of Austenite and the Autocatalytic Effect

To interpret quantitatively the progress of the isothermal transformation, both the autocatalytic factor and the partitioning of austenite should be considered. Raghavan and Entwisle[21] were the first to take both these effects into account for interpreting the shape of the isothermal transformation curve. They used the partitioning model of Fisher et al.[14] and of Fisher[11]. First, the treatment of Raghavan and Entwisle is outlined below and the amendments that seem necessary are then suggested in the discussion.

Autocatalysis may involve either the creation of new embryos or stimulation of less critical embryos already present. For the sake of simplicity, we assume that only the new embryos are created. The autocatalysis can be conveniently described in terms of a known quantity in one of three possible ways. The autocatalytic embryos n' generated may be proportional to (1) the number of martensitic plates formed, (2) the total surface area of the plates formed, or (3) the volume of martensite formed. All three approaches were tried by Raghavan[22] and he found that the third alternative was in better agreement with the experimental findings than either (1) or (2), and therefore he assumed that the autocatalytic

embryos n^{v} are proportional to the volume of transformation.

The rate of nucleation of plates was derived in the Section 6.3 according to the above assumption (equation (28) p. 79). In order to calculate the fraction transformed as a function of time, the volume contribution per martensite plate is needed as a function of the progress of transformation. This comes out of the partitioning treatment outlined below.

Considering 1 cubic centimeter of alloy let q cm^3 be the volume of an average grain of austenite, and let m be the fraction (assumed constant by Fisher[11]) of the volume of an austenite pocket that is transformed to martensite. After N_V plates have formed per unit volume of alloy, the austenite is cut up into pockets $q/(qN_V+1)$ cm^3 in size. The fraction transformed f can be related to N_V as:

$$\frac{df}{dN_V} = \frac{qm}{(qN_V+1)} \quad (1-f) \tag{35}$$

Integrating the above expression, and substituting the initial condition of f = 0 when N_V = 0, the following relation is obtained:

$$(qN_V+1) = (1-f)^{-\frac{1}{m}} \tag{36}$$

Substituting (36) in (35), we have:

$$\frac{df}{dN_v} = m\ q\ (1-f)^{\frac{1+m}{m}} \tag{37}$$

This equation expresses the volume of a plate as a function of the progress of transformation. Combining equations (28) and (37), setting (1-f) = u, and rearranging the terms:

$$\nu \exp\ (-\Delta W_a/RT)\ dt = -\frac{1}{m}\ \frac{du}{\left[1+qp+qn_i-qpu-u^{-\frac{1}{m}}\right] u^{1+\frac{1}{m}}} \tag{38}$$

where p is the autocatalytic parameter, defined as the number of autocatalytic embryos produced during the formation of 1 cm^3 of martensite. n_i is the initial number of embryos per cm^3 of the alloy and ΔW_a is the activation energy for the nucleation of initial as well as the autocatalytically produced embryos.

To obtain the volume fraction of martensite as a function of time, this expression can be integrated numerically, using a digital computer.

When computing the transformation curves, numerical values had to be assigned to the various parameters in equation (38). The grain volume q was measured directly. $\nu \exp\ (-\Delta W_a/RT)$ is a scaling factor, which does not alter the shape of the transformation curve. It can be left as a constant for any given transformation curve and its value can be determined by matching the experimental time of transformation with the calculated

time of transformation. It has also been checked independently by the nucleation measurements. n_i was taken equal to 10^7, as before. In the present investigation, m has been taken to represent the average semithickness-to-radius ratio of the martensitic plates. Raghavan and Entwisle did the same thing, but they did not systematically determine m as a function of fraction transformation. Their calculated fraction transformation versus time curve always fell below the experimental curve after 10 percent transformation, and they suggested that a better systematic evaluation of m might improve the fit between the experimental and calculated curves. Accordingly, m was determined in this investigation as a function of fraction transformation in 10 specimens of fixed grain size (0.025 mm), but having varying amounts of martensite present, between 0.2 percent and 40 percent. The accurate estimation of m is difficult, and is especially so when transformation occurs in clusters. m was found to increase with the fraction transformation because, as the transformation progressed, the smaller martensitic plates were relatively thicker than those formed earlier. From the experimental results, it was found that m as a linear function of fraction transformed would make a reasonable representation of the change of m, and this would also be convenient for computation purposes. Thus, in the relation $\frac{1}{m} = a + bu$, where u is the fraction untransformed, and a and b are constants, a and b were found to be -2 and 20, respectively. Obviously, this linear assumption is not valid up to 100 percent

transformation, and since no measurements were performed in specimens having more than 40 percent transformation, it should not be used in the calculation of the fraction transformed much beyond this range.

Thus, all the terms in equation (38) are known except the autocatalytic parameter p. Transformation curves were therefore calculated for different values of p. For a particular reaction temperature a value of p could be selected which would best match the shapes of the calculated and experimental transformation curves at the early stages (5-12 percent transformation). This value of p was accepted as the autocatalytic parameter for that particular reaction temperature. Then, the value of $\nu \exp(-\Delta W_a/RT)$ could be computed to yield a calculated time equal to the experimental time. From this the value of ΔW_a could be calculated, and compared to that obtained from the initial nucleation-rate measurements (listed in Table II).

8.3 Discussion of Calculated and Experimental Curves

All the results reported and discussed in this section were obtained for the 24Ni3Mn alloy at a fixed grain size of 0.025 mm, corresponding to a 1-hour austenitizing treatment at 900°C.

Figs. 27 and 28 show the experimental and predicted curves for the indicated reaction temperatures and values of p. Excellent agreement between the experimental results and

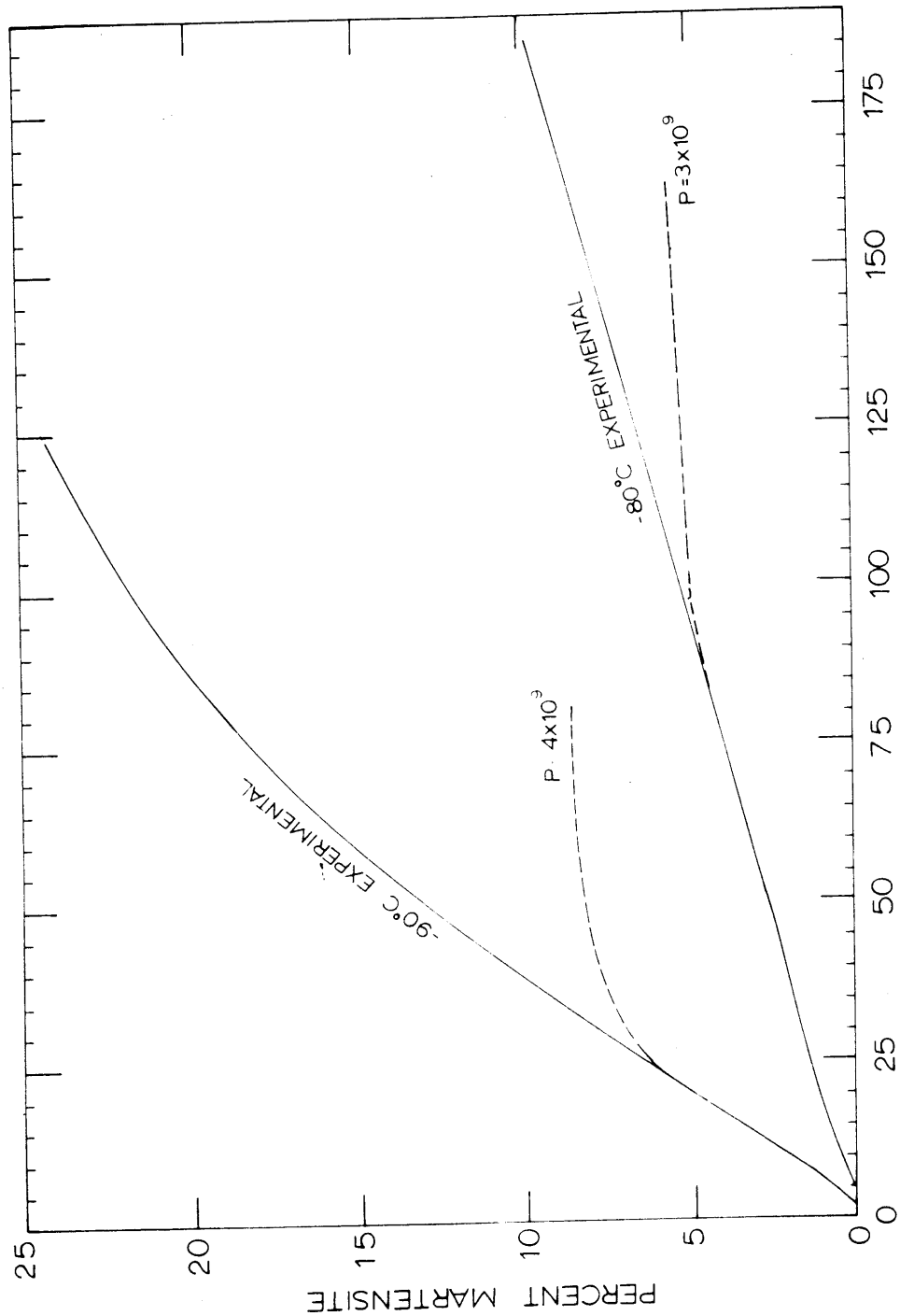

Figure 27. Comparison of Experimental and Calculated Transformation Curve for the 24Ni3Mn Alloy Reacted at the Indicated Temperatures. The Values of p used in the Calculations are Indicated for each Curve.

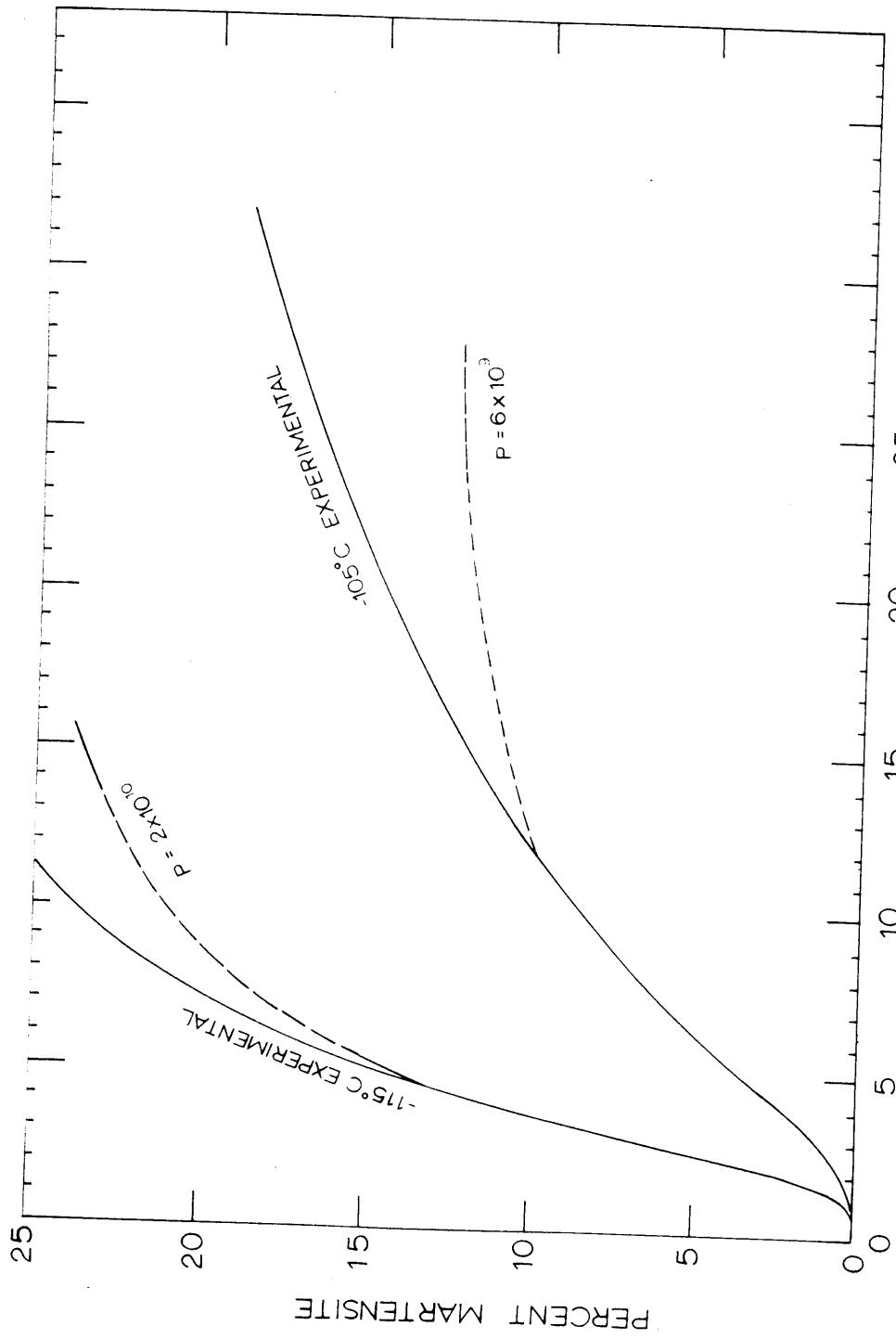

Figure 28. Comparison of Experimental and Calculated Transformation Curve for the 24Ni3Mn Alloy Reacted at the Indicated Temperatures. The Values of p used in the Calculations are Indicated for each Curve.

theoretical predictions is obtained up to 5-12 percent of transformation; thereafter, the calculated curve falls always below the experimental one and flattens out rapidly. It can be seen that the shape of the calculated curve is quite sensitive to the value of p. The value of p increases as the temperature of transformation decreases.

Raghavan and Entwisle found very good agreement between the calculated and experimental curves during the initial stages of transformation with specimens of different austenitic grain size reacted at a particular temperature, using a single value of autocatalytic parameter p and a single value of the factor $\nu \exp(-\Delta W_a/RT)$. They also found a systematic increase of p with lowering of the reaction temperature. In the present investigation, the agreement between the calculated and experimental curve has been obtained over a wider and different temperature range than that of Raghavan and Entwisle. The steady increase of the autocatalytic parameter with decreasing temperature of transformation is in agreement with the view that embryos will be more readily created as the driving force for transformation increases and as relaxation effects are reduced.

The values of ΔW_a obtained from the scaling factors $\nu \exp(-\Delta W_a/RT)$ at different reaction temperatures are listed in Table V. Comparison of these values with the ΔW_a values listed in Table II show that the values based on the

TABLE V

Calculation of Activation Energy for the 24Ni3Mn Alloy from the Progress of Transformation and from the Initial Nucleation Rate at 0.2 percent Transformation Taking Autocatalysis into Account within 0.2 percent Transformation

Reaction Temperature, 0°C	n_t at 0.2 percent Transformation, cm^{-3}	ΔW_a From the Progress of Transformation, cal/mole	ΔW_a Corresponding to 0.2 Percent Transformation Taking Autocatalysis into Account, cal/mole
-115	4.16×10^7	11,100	11,000
-105	1.36×10^7	11,800	11,600
-90	9.60×10^6	13,000	12,600
-80	7.60×10^6	14,100	13,800

transformation curves are only 300 to 500 cal/mole higher than those based on the nucleation measurements. However, as mentioned in Section 5.2, the values of ΔW_a based on nucleation measurements have been calculated on the assumption that only the initial embryos are available for transformation up to 0.2 percent. But it has been shown in Section 6.2 that even with less than 0.2 percent transformation an appreciable number of autocatalytic embryos are produced. The lower the reaction temperature, the greater is the number of autocatalytic embryos. This increases the deviation at lower reaction temperatures between the ΔW_a values listed in Tables II and V. Knowing the autocatalytic parameter as a function of reaction temperature, it is possible to calculate the total number of embryos, n_t, available at 0.2 percent transformation from equation (25) (p. 78) and then ΔW_a at 0.2 percent transformation can be calculated by taking the number of embryos equal to n_t instead of $n_i = 10^7$ per cm^3. The results of such calculations are shown in Table V for transformation temperatures at which the autocatalytic parameter is known at least within a factor of 2.

It is seen from Table V that at lower reaction temperatures, if the correction due to autocatalysis is taken into account, the ΔW_a values corresponding to 0.2 percent transformation are in close agreement with the ΔW_a values obtained from progress of transformation.

In Table V it can be seen that, at higher reaction temperatures (-90° to -80°C) where the autocatalytic parameter is small, the total number of embryos available for transformation at 0.2 percent consists mainly of the initial embryos. Hence, the measured ΔW_a corresponding to 0.2 percent transformation is the representative activation energy for the initial number of embryos. In this temperature range of -90° to -80°C, the ΔW_a calculated from progress of transformation is only 300 - 400 cal/mole higher than the activation energy for the initial embryos.

The above analysis shows that the activation energy for nucleation of autocatalytic embryos is only very slightly different, if at all, from that of the initial embryos. This justifies the use of a single average potency for the initial as well as the autocatalytic embryos for calculating the fraction transformed as a function of time.

Accordingly, the agreement between the calculated and experimental transformation curves, and the striking agreement found by Raghavan and Entwisle in the initial stages for a set of grain sizes at a given temperature, lend support to the model proposed.

In the present investigation, a selected value of p required by the model for the best fit between the calculated and experimental transformation curves was checked independently by the following way. A number of specimens were

transformed at -115°C, each one to a different fraction transformed, and N_v was determined in these specimens. Fig. 29 shows the plot of N_v as a function of time of transformation. This plot clearly reveals that the increase in the rate of transformation is due to formation of new plates, and not by the slow growth of the martensitic plates over a considerable period of time as suggested by Magee[35]. The slope of the curve in Fig. 29, corrected by the factor $1/(1-f)$, is the nucleation rate $\dot{N}$, so that $\dot{N}$ can now be determined as a function of the number of plates formed. Nucleation rates obtained in this way are shown in Table VI. Also, equation (27) provides a way of calculating the nucleation rate as a function of number of plates formed using different values of the autocatalytic parameter. At -115°C the best match (Fig. 28) between the experimental and calculated transformation curves was obtained for $p = 2 \times 10^{10}$. Therefore, nucleation rates were calculated from equation (27) using $p = 2 \times 10^{10}$ and the corresponding $\nu \exp(-\Delta W_a/RT)$ for the best match. Calculations were performed only up to $N_v = 5 \times 10^8$ to minimize the effects of partitioning, thus providing a way of checking the autocatalytic effect solely. It is seen in the Table VI that the nucleation rates calculated by these different methods vary only by a factor of 2-6. This is not a large discrepancy considering the uncertainties in N_v and p determinations. Both these quantities may easily have an uncertainty of a factor of 2.

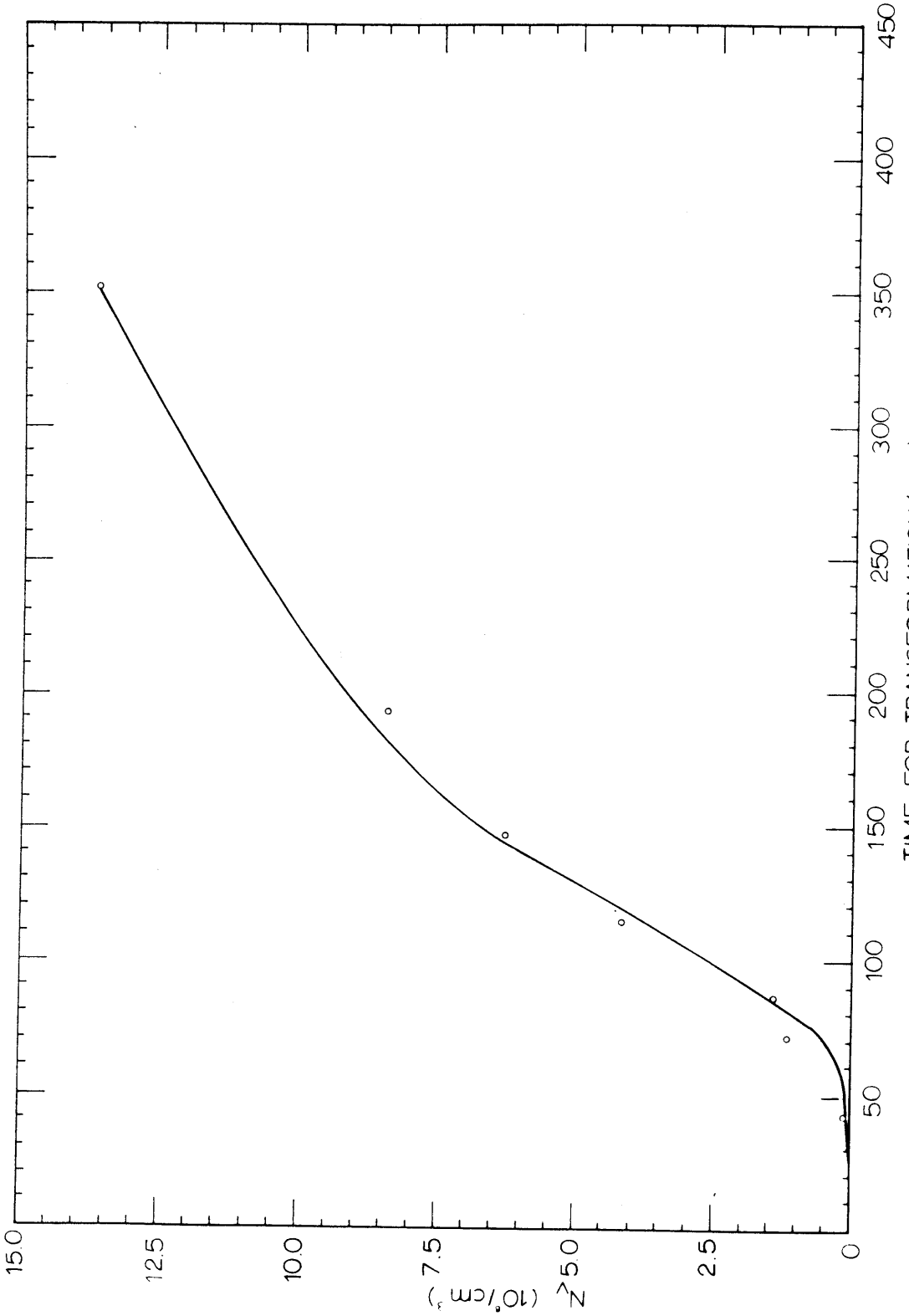

Figure 29. Number of Plates Formed per cm^3 of the Alloy 24Ni 3Mn, as a Function of Time of Transformation at -115°C.

TABLE VI

Calculation of Nucleation Rate as a Function of Number of Plates Formed from (1) the Measured Number of Plates as a Function of Time and (2) Equation (27), for the 24Ni3Mn Alloy Reacted at -115°C

Number of Plates Formed from Measurement, N_V, cm^{-3}	Nucleation Rate Measured, $\dot{N}$, $cm^{-3}sec^{-1}$	Nucleation Rate Calculated from Equation (27), $\dot{N}$, $cm^{-3}sec^{-1}$
10^7	3×10^5	2×10^5
3×10^7	2×10^6	5×10^5
5×10^7	5×10^6	8×10^5
10^8	7×10^6	2×10^6
5×10^8	10^7	7×10^6

Experimental scatter between the repeated experiments is the limiting factor in precise determination of either of these quantities. Thus, although close quantitative agreement is difficult to obtain, the semiquantitative agreement does suggest that the chosen autocatalytic factor is in the right range.

The discussion in the preceding paragraphs leads to the conclusion that, towards the later stages of transformation, the failure to match the calculated and experimental transformation curves is due to the inaccurate description of partitioning effects. In order to check this, the number of plates required to give different amounts of transformation was calculated, using equation (36). In one case, m was assumed to remain constant at $\frac{1}{m} = 18$, and in the other case the relation of $\frac{1}{m} = -2 + 20u$ was used. The results of both sets of calculations are given in Table VII. It is seen that for constant m, as was used by Fisher[11], the number of plates required reaches a very high number, even at 15-20 percent transformation. For the case of varying m, the required number of plates as a function of fraction transformed does not rise so rapidly. However, even here the volume contribution per plate becomes unreasonably low with the progress of the transformation. This is clearly revealed if the total number of embryos available as a function of fraction transformed is calculated from equation (25). By substituting N_V from equation (36), the value of n_t as a function of fraction transformed is given by:

TABLE VII

Number of Martensitic Plates per unit Volume, N_V, Required to Give Different Amounts of Transformation for A Grain Size of 0.025 mm ($q = 9.28 \times 10^{-9} cm^3$) and for Constant and Varying m, Calculated from Equation (36)

Fraction Transformed, f	N_V for $\frac{1}{m} = 18$, cm^{-3}	N_V for $\frac{1}{m} = -2+20(1-f)$, cm^{-3}
0.002	0.38×10^7	0.38×10^7
0.005	1.02×10^7	1.02×10^7
0.01	2.15×10^7	2.13×10^7
0.02	4.73×10^7	4.62×10^7
0.05	1.52×10^8	1.39×10^8
0.07	2.69×10^8	2.33×10^8
0.10	5.67×10^8	4.41×10^8
0.12	8.97×10^8	6.34×10^8
0.15	1.77×10^9	1.05×10^9
0.20	5.50×10^9	2.17×10^9
0.25	1.89×10^{10}	4.42×10^9
0.30	6.48×10^{10}	7.58×10^9
0.35	2.51×10^{11}	1.23×10^{10}
0.40	1.06×10^{12}	1.77×10^{10}

$$n_t = n_i + pf - \frac{1}{q}\{1-f)^{-\frac{1}{m}} - 1\} \qquad (39)$$

The results of this calculation of n_t as a function of fraction transformed are shown in Fig. 30, taking $\frac{1}{m} = -2+20u$ and $p = 2x10^{10}$, corresponding to a reaction temperature of -115°C. The total number of available embryos starts to decrease after 12-13 percent transformation while Fig. 28 shows that the calculated curve starts to deviate from the experimental curve at approximately the same fraction transformed. The limitation of the partitioning model is clearly indicated by the fact that beyond 20 percent transformation, n_t decreases very fast, and at 27 percent transformation n_t becomes negative. It is in this range that the calculated curve deviates widely from the experimental curve. The calculated number of embryos becomes negative because the volume contribution per plate is reduced so much (due to the assumed partitioning geometry) that the total number of plates required to give 27 percent transformation far exceeds the total available number of embryos.

It should be mentioned in this connection that equation (39) is not strictly correct, because it does not take into account the reduction in the number of embryos that are swept by martensitic plates when they are formed. This can be accounted for by setting up a differential equation as shown in Appendix C. n_t corrected for this sweeping effect is also

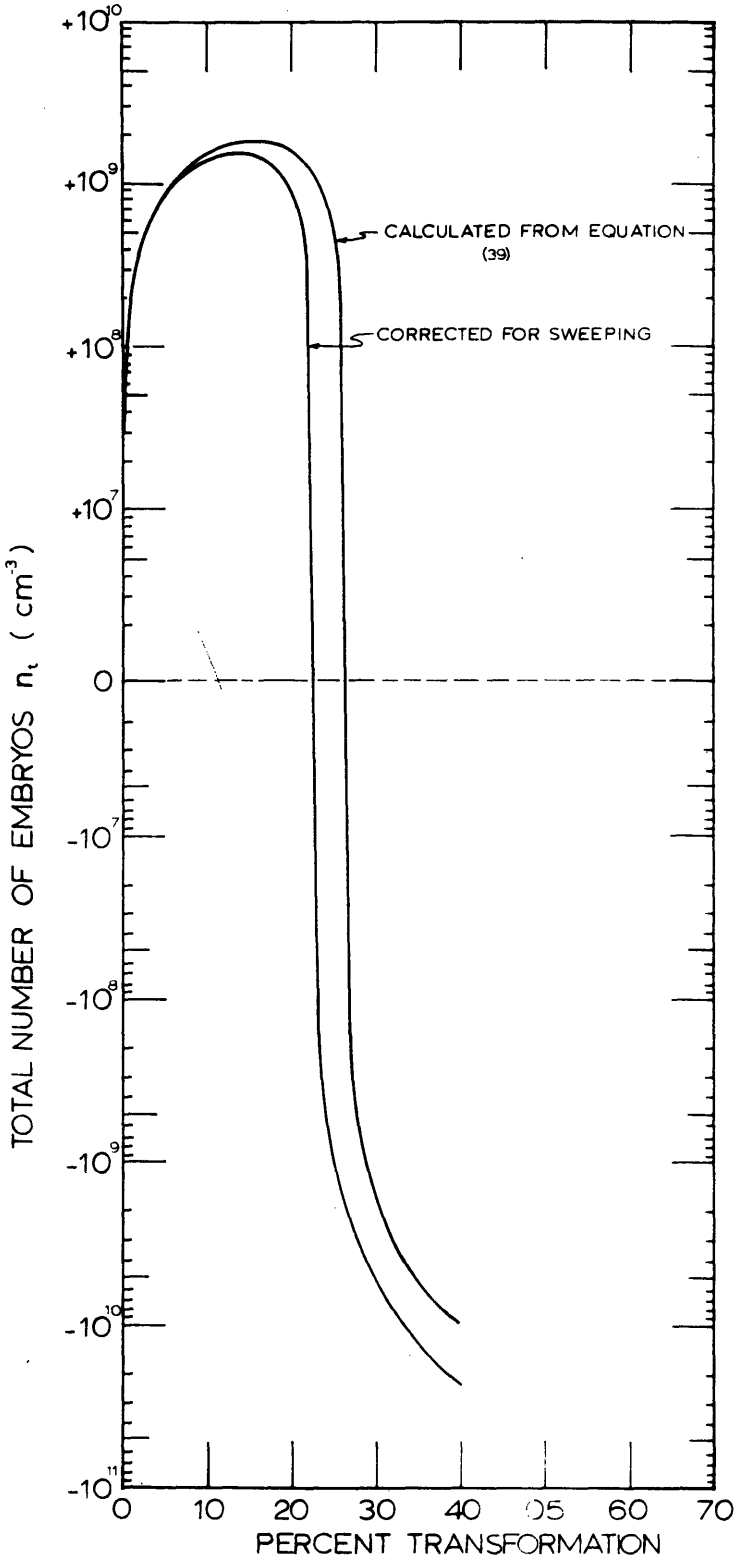

Figure 30. Total Number of Embryos as a Function of Fraction of Transformation, Considering Autocatalysis and Partitioning. Correction due to Embryos Being Swept up by the Formation of Martensitic Plates is also Included.

shown in Fig. 30 as a function of fraction transformed. It can be seen that up to about 8-10 percent transformation, n_t calculated in both ways is almost the same. However, after 10 percent transformation, the calculated curve, with the correction due to consumption of the embryos swept by the martensitic plate, decreases even more rapidly than the uncorrected curve. This indicates, again, that the partitioning model is at fault quantitatively.

Thus, the discussions in the preceding paragraphs point out that, for matching the calculated and experimental curves towards the later stages of transformation, a more realistic model of partitioning than that of Fisher et al.[14] is necessary. Raghavan[22] suggested that a realistic description of the way m changes with the progress of the transformation would give a better fit between the calculated and experimental curves, but the present investigation shows that this will not provide the necessary improvement. On the other hand, it seems that an accurate description of partitioning might eliminate the disparity.

9. CONCLUSIONS

(1) In suitably chosen iron-nickel-manganese alloys, martensite can form by a completely isothermal process over a wide range of temperatures at least -196°C to -20°C.

(2) The incubation period and nucleation rate as a function of reaction temperature at various austenitic grain sizes follow the general C-curve kinetics.

(3) The true initial nucleation rate (not the apparent initial nucleation rate at the smallest reliably detectable amount of martensite) is independent of grain size. The effect of grain size on the incubation period and the apparent initial nucleation rate arises primarily from the size of the first-formed plates.

(4) Grain boundaries do not act as preferred nucleation sites for the martensitic transformation in the alloys studied. On the other hand, the most-potent embryos seem to be distributed rather uniformly throughout the matrix.

(5) From the stand point of the driving force for martensitic transformations, 1 atomic percent manganese is thermodynamically equivalent to 1.6 atomic percent nickel.

(6) Alloys of equivalent thermodynamic driving force can exhibit marked differences in kinetics behavior due to slight differences in their manganese and carbon contents. This indicates that these elements play a very pronounced role in decreasing the potency of embryos over and above any influence on the driving force as such.

(7) The activation energies of the isothermal martensitic transformation in a number of iron-nickel-manganese alloys, as measured by several investigators, are in very good agreement with the theoretical activation energies, based on the model of Kaufman and Cohen[1].

(8) In iron-nickel-manganese alloys exhibiting a completely isothermal mode of transformation, the potency of the active embryos during the reactions is almost constant or lies within a narrow range. This concept accounts for the absence of athermal martensitic transformation below the temperature range of the isothermal transformation.

(9) The probability of observing pre-existing embryos (of the calculated size of 180-200A°) by transmission electron microscopy of the parent austenite is vanishingly small (1 part in 10^5 or 10^6) because of their low concentration (10^7 per cm^3).

(10) Stacking faults are not likely to act as preferred nucleation sites for martensitic (b.c.c.) transformation in the iron-nickel-manganese alloys under investigation.

(11) The increase in rate of the isothermal martensitic transformation as a function of time takes place due to formation of new plates (autocatalysis), and not to the slow growth of existing martensitic plates. The subsequent retardation arises from the partitioning of the austenite by the martensitic plates.

(12) By assuming that the initial and autocatalytic embryos have the same average potency, and that the number of autocatalytic embryos generated is proportional to the volume of martensite formed, the isothermal transformation curve can be explained quantitatively, at least up to several percent of transformation. The discrepancy between the calculated and experimental curves at the later stages of transformation seems to arise because of inaccuracies in the assumed geometry of partitioning.

(13) The activation energy as a function of temperature for the nucleation of autocatalytic embryos is very slightly higher, if at all, from that of the initial embryos.

10. SUGGESTIONS FOR FURTHER WORK

(1) Since it has been found that slight variations in carbon content cause pronounced changes in the reaction kinetics, it will be interesting to study the isothermal martensitic transformation in iron-nickel-manganese alloys having 0-0.025 weight percent carbon at constant nickel and manganese levels to investigate the role of carbon. Dislocation velocity measurements in this series of alloys should be undertaken to see if the observed changes in kinetics can be explained by the differences in dislocation velocity in austenite. This will further test Magee's[35] suggestion that the critical condition for the formation of martensite is the mechanical propagation of the dislocation interface. Similar experiments in alloys having constant levels of nickel and carbon, but with different manganese contents, will illuminate the role of manganese.

(2) Attempts should be undertaken to develop a realistic model of partitioning in an effort to match the calculated and experimental transformation curves in the later stages of transformation.

11. BIBLIOGRAPHY

1. L. Kaufman and M. Cohen, "Thermodynamics and Kinetics of Martensitic Transformations", Progress in Metal Physics, 7, Pergamon Press, (1958), p. 165.

2. R.P. Reed and J.F. Breedis, "Low Temperature Phase Transformations", Behavior of Materials at Cryogenic Temperatures, ASTM Special Technical Publication 387, American Soc. Testing Mats., (1966), p. 60.

3. G.V. Kurdjumov and O.P. Maksimova, "Kinetics of Austenite to Martensite Transformation at Low Temperatures", Doklady Akademii Nauk, SSSR, 61, No. 1, (1948), p. 83, H. Brutcher Translation No. 2187.

4. G.V. Kurdjumov and O.P. Maksimova "On the Energy of Formation of Martensite Nuclei", Doklady Akademii Nauk, SSSR, 73, (1950), p. 95.

5. R.F. Bunshah and R.F. Mehl, "Rate of Propagation of Martensite", Trans. AIME, 197, (1953), p. 1251.

6. S.C. Das Gupta and B.S. Lement, "Stabilization of the Austenite-Martensite Reaction in a High Chromium Steel", Trans. AIME, 197 (1953), p. 530.

7. S.A. Kulin and G.R. Speich, "Isothermal Martensite Formation in an Iron-Chromium-Nickel Alloy", Trans. AIME, 194, (1952), p. 258.

8. M. Cohen, E.S. Machlin and V.G. Paranjpe, "Thermodynamics of the Martensitic Transformation", Thermodynamics in Physical Metallurgy, ASM., (1950), p. 242.

9. E.S. Machlin and M. Cohen, "Isothermal Mode of the Martensitic Transformation", Trans. AIME, 194, (1952), p. 489.

10. R.E. Cech and J.H. Hollomon, "Rate of Formation of Isothermal Martensite in Iron-Nickel-Manganese Alloys", Trans. AIME, 197, (1953), p. 685.

11. J.C. Fisher, "Application of Nucleation Theory to Isothermal Martensite", Acta Met., 1, (1953), p. 32.

12. F.W. Jones and W.I. Pumphrey, "Free Energy and Metastable States in the Iron-Nickel and Iron-Manganese Systems", Journal of Iron and Steel Inst., 163, (1949), p. 121.

13. J.C. Fisher, "Martensite Nucleation in Substitutional Iron Alloys", Trans. AIME, 197, (1953), p. 918.

14. J.C. Fisher, J.H. Hollomon and D. Turnbull, "Kinetics of the Austenite Martensite Transformation", Trans. AIME, 185, (1949), p. 691.

15. L. Kaufman and M. Cohen, "The Mechanism of Phase Transformations in Metals", Institute of Metal Monograph and Report Series, No. 18, (1955), p. 187.

16. C.H. Shih, B.L. Averbach and M. Cohen, "Some Characteristics of the Isothermal Martensitic Transformation", Trans. AIME, 203, (1955), p. 183.

17. H. Knapp and U. Dehlinger, "Mechanik Und Kinetik Der Diffusionslosen Martensitbildung", Acta Met. 4, (1956), p. 289.

18. F.C. Frank, "Martensite", Acta Met., 1, (1953), p. 15.

19. J. Philibert and C. Crussard, "Kinetics of the Martensite Transformation in a Hyper Eutectoid Steel", Journal of Iron and Steel Inst., 180, (1955), p. 39.

20. A.R. Entwisle, "Isothermal Martensite in Iron-Nickel-Manganese Alloys", Unpublished Report of the work carried out in the Department of Metallurgy, M.I.T., (1960-1961).

21. V. Raghavan and A.R. Entwisle, "Isothermal Martensite Kinetics in Iron Alloys", Physical Properties of Martensite and Bainite, Iron and Steel Inst., Special Report No. 93, (1965), p. 30.

22. V. Raghavan, "Isothermal Formation of Martensite", Ph.D. Thesis, Department of Metallurgy, University of Sheffield, (1964).

23. B.S. Lement, B.L. Averbach and M. Cohen, "Microstructural Changes on Tempering Iron-Carbon Alloys", Trans. ASM, 46, (1954), p. 851.

24. R.L. Fullman, "Measurement of Particle Sizes in Opaque Bodies", Trans. AIME, 197, (1953), p. 447.

25. S.R. Pati and M. Cohen, "Measurement of Nucleation Rate of an Isothermal Martensitic Transformation", Acta Met., 14, (1966), p. 1001.

26. R.E. Cech and D. Turnbull, "Heterogeneous Nucleation of the Martensite Transformation", Trans. AIME, 206, (1956), p. 124.

27. L. Kaufman and M. Cohen, "The Martensitic Transformation in the Iron-Nickel System", Trans. AIME, 206, (1956), p. 1393.

28. Y. Imai and M. Izumiyama, "Relationship between the Solid Phase Equilibrium and the Isothermal Martensite Transformation in Iron-Nickel-Chromium and Iron-Nickel-Manganese Alloys", The 1188th Report of the Research Institute for Iron, Steel and Other Metals", Reported in Japan Institute of Metals, 27, (1963), p. 171.

29. T. Bell and W.S. Owen, "The Thermodynamics of the Martensite Transformation in Iron-Carbon and Iron-Nitrogen", to be published.

30. R. Brook and A.R. Entwisle, "Kinetics of Burst Transformation to Martensite", Journal of Iron and Steel Inst. 203, (1965), p. 905.

31. L. Kaufman, Manufacturing Laboratories Inc., unpublished work.

32. M.H. Richman, M. Cohen and H.G.F. Wilsdorf, "Experimental Evidence for Martensitic Embryos", Acta Met., 7, (1959), p. 819.

33. J. Graggero and D. Hull, "On the Nucleation of Martensite", Acta Met., 10, (1962), p. 995.

34. Z. Nishiyama and K. Shimizu, "Study of the Substructures of the Martensite in Iron-Nickel Alloy by Means of Transmission Electron Microscopy", Acta Met., 9, (1961), p. 980.

35. C.L. Magee, "Transformation Kinetics, Microplasticity and Aging of Martensite", Ph.D. Thesis Submitted to Carnegie Institute of Technology, (1966).

36. R.B.G. Yeo, "Growth of Martensite in an Iron - 28.8 percent Nickel Alloy", Trans. ASM, 57, No. 1,(1964), p. 48.

37. J.A. Klosterman, "Physical Properties of Martensite and Bainite", Iron Steel Inst. Special Report No. 93, (1965), p. 20.

APPENDIX A

COMPOSITIONAL VARIATIONS OCCURRING IN SPECIMENS AS A FUNCTION OF AUSTENITIZING TEMPERATURE

Two difficulties were noted in the procedure for altering the grain size by varying the austenitizing temperature, especially for austenitizing temperatures higher than 950°C.

The first problem arose because of manganese loss from the surface of the specimen at the higher austenitizing temperatures. The manganese-depleted layer on the surface caused premature initiation of martensite near the surface upon cooling to room temperature and below. The manganese-depleted layer could not be reproducibly removed even by extensive electropolishing of the austenitized specimen. The manganese depletion was finally avoided by electroplating 0.001 to 0.002 inches of pure nickel on the specimen before the austenitizing treatment.

The second difficulty was due to transfer of carbon from the nickel leads through the tube atmosphere to the specimen at austenitizing temperatures of 950°C and above. The amount of carbon picked up by the specimen could be determined from the analysis of carbon content before and after the austenitizing treatment, and this was approximately in balance with the amount of carbon lost by the leads. Though the nickel

leads initially contained only 0.03 to 0.04 percent carbon, a transfer of carbon still took place due to the lower activity of carbon in iron-nickel-manganese alloys than in nickel. The effect of this carbon pick-up was to make the specimen more resistant to transformation at the surface. This contamination increased with increasing austenitizing temperature. To determine the maximum austenitizing temperature up to which the contamination by carbon was negligible, decarburized nickel leads were spot welded to a set of specimens, and incubation periods were determined as a function of austenitizing temperature. The leads used in this series were decarburized by wet hydrogen treatments at 1200°C for 24 hours, and the amount of carbon left after decarburization was analyzed as 0.002 percent. At austenitizing temperatures up to 900°C, both sets of specimens (with decarburized and as-received leads) showed the same incubation period at the same reaction temperature. Also chemical analysis did not reveal any difference in carbon content between the two sets of specimens, austenitized for 1 hour at temperatures up to 900°C. This proved that for an austenitizing time of 1 hour the problem of carbon transfer from the nickel leads did not exist at temperatures of 900°C or below.

Thus, no compositional changes occur in the specimen up to 900°C either from the manganese loss or carbon pick-up. However, as an added protection from manganese loss, the specimens were plated with nickel even for austenitizing temperatures up to 900°C.

APPENDIX B

TRANSMISSION ELECTRON MICROSCOPIC OBSERVATIONS

Figs. 31 and 32 show the fine structure of isothermally formed martensite in the 24Ni3Mn alloy reacted at -105°C. The existence of twins within the martensitic plates are easily recognized even at the relatively low magnification of 31,000x. The twins within these plates appear to be thicker than what is generally observed in the fine structure of athermal martensite. Both slip and twinning is found to act as the modes of deformation for the heterogeneous shear. The plane of heterogeneous shear was identified as $\{211\}_{\alpha}$.

The orientation relations between austenite and martensite were quite close to the Kurdjumov-Sacks relation: $(111)_{\gamma}//(110)_{\alpha}$; $[\bar{1}01]_{\gamma}// [\bar{1}11]_{\alpha}$, or the Nishiyama relation: $(111)_{\gamma}// (110)_{\alpha}$; $[\bar{2}11]_{\gamma}// [\bar{1}10]_{\alpha}$. Due to inaccuracies in determining orientations from electron diffraction patterns, a choice could not be made between these two relationships.

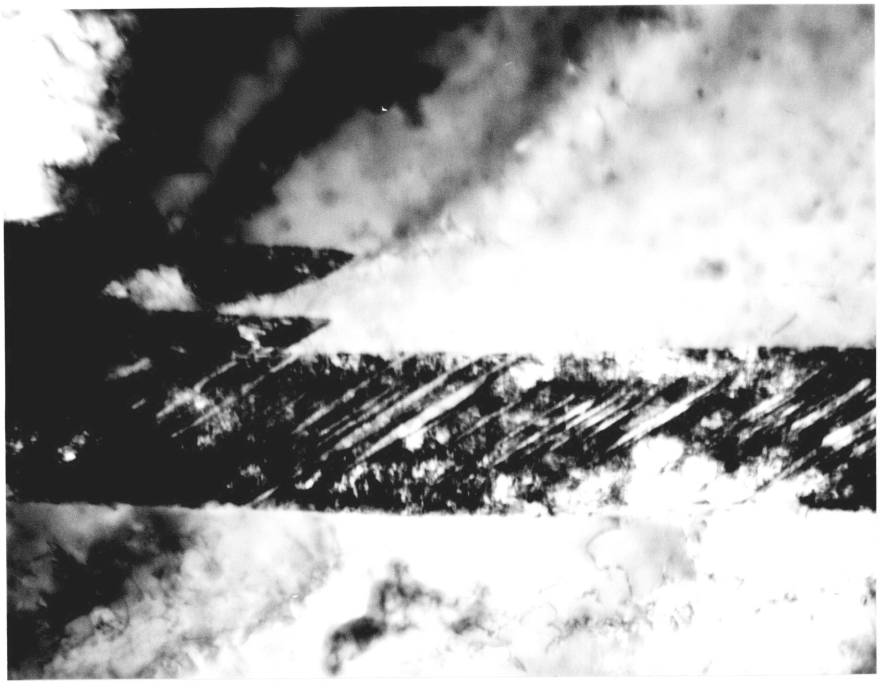

Figure 31. Fine structure of isothermally formed martensite in the 24Ni3Mn alloy, reacted at -105°C. 31,000X.

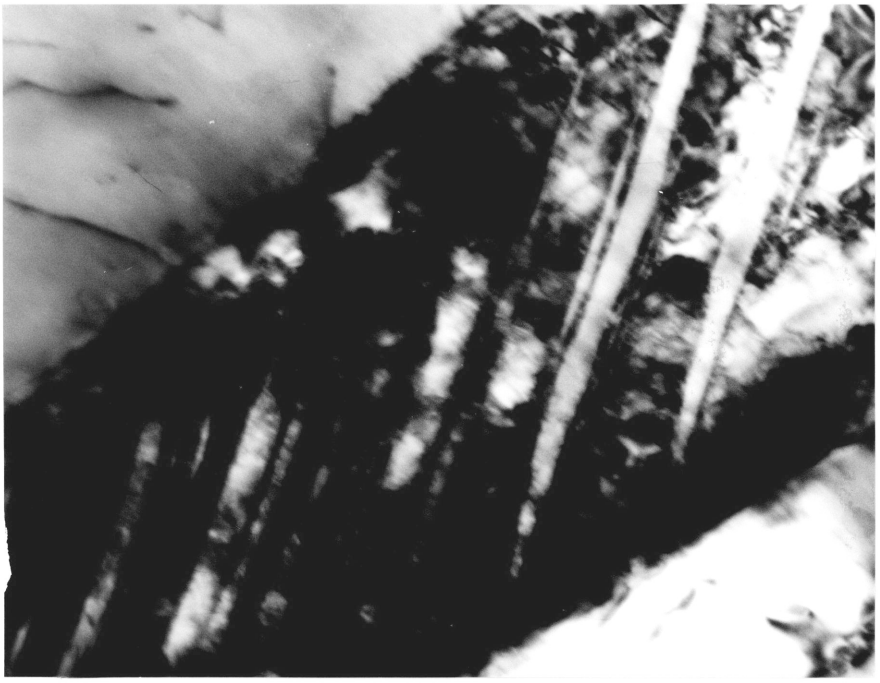

Figure 32. Fine structure of isothermal martensite in the 24Ni3Mn alloy, reacted at -105°C. 95,000X.

APPENDIX C

THE CALCULATION OF TOTAL NUMBER OF EMBRYOS INCLUDING THE CORRECTION DUE TO EMBRYOS BEING SWEPT UP BY THE MARTENSITIC PLATES

Equation (39) of the text (p.124) expresses the total number of embryos as a function of fraction transformed accounting for autocatalysis and partitioning of the austenite. However, as mentioned (p.124) this equation is not strictly correct since it does not take into consideration the number of embryos that are consumed during the growth of a martensitic plate initiated by some other embryo. This correction can be incorporated into the calculation of total number of embryos in the following way.

Considering 1 cm^3 of material, during an increment of time dt the volume of martensite formed is df and the corresponding number of plates is dN_v. The increment in the total number of embryos dn_t is then given by

$$dn_t = pdf - dN_v - n_t df$$

where p is the autocatalytic parameter and is the number of embryos generated by the formation of 1 cm^3 to martensite.

Expressing dN_v in terms of df from equation (37):

$$dn_t = \left[p - \frac{1}{mq(1-f)^{1+1/m}} - n_t \right] df$$

The above equation was integrated numerically with a digital computer to yield n_t as a function of f; by calculating dn_t at a succession of time, with df = 0.0001, starting with $n_t = n_i$ at f = 0 and replacing n_t each time by $n_t + dn_t$. The results are shown in Fig. 30 (p. 125).

BIOGRAPHICAL NOTE

The author was born on August 2, 1939 at Gopisagar, West-Bengal, India. He graduated from Manbazar High School in May 1955, and from Bankura Christian College in May 1957. He then enrolled in Bengal Engineering College, University of Calcutta, and received the B.E. (Met.) degree in May 1961. He was awarded the University Gold Medal on the result of the B.E. (Met.) examination and received substantial scholarships from the University of Calcutta and Bengal Engineering College. In September 1961 he joined the Indian Iron and Steel Company at Burnpur, India as an Officer Trainee.

In February 1963, the author entered the Graduate School of Massachusetts Institute of Technology and received the S.M. degree in Metallurgy in September 1964. From that time until the present, he has been enrolled in the Graduate School as a candidate for the degree of Doctor of Science in Metallurgy.